

1981

# Part I. Photoelectron Spectroscopic Studies of Amines, Alkenes, and Substituted Benzenes. Part II. Theoretical Studies of Quinones.

Melvin Dale Rozeboom

*Louisiana State University and Agricultural & Mechanical College*

Follow this and additional works at: [https://digitalcommons.lsu.edu/gradschool\\_disstheses](https://digitalcommons.lsu.edu/gradschool_disstheses)

---

## Recommended Citation

Rozeboom, Melvin Dale, "Part I. Photoelectron Spectroscopic Studies of Amines, Alkenes, and Substituted Benzenes. Part II. Theoretical Studies of Quinones." (1981). *LSU Historical Dissertations and Theses*. 3698.  
[https://digitalcommons.lsu.edu/gradschool\\_disstheses/3698](https://digitalcommons.lsu.edu/gradschool_disstheses/3698)

This Dissertation is brought to you for free and open access by the Graduate School at LSU Digital Commons. It has been accepted for inclusion in LSU Historical Dissertations and Theses by an authorized administrator of LSU Digital Commons. For more information, please contact [gradetd@lsu.edu](mailto:gradetd@lsu.edu).

## INFORMATION TO USERS

This was produced from a copy of a document sent to us for microfilming. While the most advanced technological means to photograph and reproduce this document have been used, the quality is heavily dependent upon the quality of the material submitted.

The following explanation of techniques is provided to help you understand markings or notations which may appear on this reproduction.

1. The sign or "target" for pages apparently lacking from the document photographed is "Missing Page(s)". If it was possible to obtain the missing page(s) or section, they are spliced into the film along with adjacent pages. This may have necessitated cutting through an image and duplicating adjacent pages to assure you of complete continuity.
2. When an image on the film is obliterated with a round black mark it is an indication that the film inspector noticed either blurred copy because of movement during exposure, or duplicate copy. Unless we meant to delete copyrighted materials that should not have been filmed, you will find a good image of the page in the adjacent frame. If copyrighted materials were deleted you will find a target note listing the pages in the adjacent frame.
3. When a map, drawing or chart, etc., is part of the material being photographed the photographer has followed a definite method in "sectioning" the material. It is customary to begin filming at the upper left hand corner of a large sheet and to continue from left to right in equal sections with small overlaps. If necessary, sectioning is continued again--beginning below the first row and continuing on until complete.
4. For any illustrations that cannot be reproduced satisfactorily by xerography, photographic prints can be purchased at additional cost and tipped into your xerographic copy. Requests can be made to our Dissertations Customer Services Department.
5. Some pages in any document may have indistinct print. In all cases we have filmed the best available copy.

University  
Microfilms  
International

300 N. ZEEB RD., ANN ARBOR, MI 48106

8207837

**Rozeboom, Melvin Dale**

PART I. PHOTOELECTRON SPECTROSCOPIC STUDIES OF AMINES,  
ALKENES, AND SUBSTITUTED BENZENES. PART II. THEORETICAL  
STUDIES OF QUINONES

*The Louisiana State University and Agricultural and Mechanical Col.*    PH.D. 1981

**University  
Microfilms  
International** 300 N. Zeeb Road, Ann Arbor, MI 48106

PART I. PHOTOELECTRON SPECTROSCOPIC STUDIES OF AMINES,  
ALKENES, AND SUBSTITUTED BENZENES

PART II. THEORETICAL STUDIES OF QUINONES

A Dissertation

Submitted to the Graduate Faculty of the  
Louisiana State University and  
Agricultural and Mechanical College  
in partial fulfillment of the  
requirements for the degree of

Doctor of Philosophy

in

The Department of Chemistry

by

Melvin Dale Rozeboom  
B.A., Central College, 1973  
M.S., South Dakota State University, 1977

December, 1981

## ACKNOWLEDGMENT

The author would like to recognize and thank Dr. Kendall N. Houk for his unflagging support and encouragement. He deeply appreciates the personally fine example Dr. Houk provided while Dr. Houk was at Louisiana State University, and after Dr. Houk relocated his career to the University of Pittsburgh. The author also acknowledges the assistance given by Dr. George R. Newkome in Dr. Houk's absence.

The author also acknowledges the discussions and assistance of the postdoctoral associates and the other graduate students in Dr. Houk's research group in the years spent at Louisiana State University.

For all of the years of support and understanding that his family, particularly his wife Caryn, has given, the author is exceedingly grateful. Special thanks are also offered to Caryn for her work in typing various parts of this dissertation.

Financial support was provided by Louisiana State University, the National Science Foundation, and the National Institutes of Health throughout the span of this research in the form of teaching and research assistantships.

## FORWARD

This dissertation is divided into two parts:

I. Photoelectron spectroscopic studies of a variety of compounds, with different goals for each study. The spectra of nearly fifty amines have been recorded for different reasons, such as the mechanism by which radical cations are stabilized, conformational analysis, and drug activity. Eight exocyclic alkenes were studied to correlate the  $\pi$  IPs with reactivities and regioselectivities in 1,3-dipolar cycloadditions with para-nitrobenzenesulfonyl azide. Thirteen benzene derivatives were studied in an attempt to correlate IPs with photochemical reactivities.

II. Theoretical studies of quinones, to evaluate the potential stability of a little known class of compounds, the quinones of azulene. Substituted benzoquinones and naphthoquinones were studied to explain their regioselectivities toward attack by nucleophiles using frontier molecular orbital theory.

## TABLE OF CONTENTS

	<u>PAGE</u>
ACKNOWLEDGMENT.....	11
FORWARD.....	111
LIST OF TABLES.....	v11
LIST OF FIGURES.....	1x
LIST OF ABBREVIATIONS.....	xi1
ABSTRACT.....	xi11

### PART I. PHOTOELECTRON SPECTROSCOPIC STUDIES OF AMINES, ALKENES, AND SUBSTITUTED BENZENES

CHAPTER I	INTRODUCTION.....	1
	References.....	3
CHAPTER II	METHYL-SUBSTITUTED PIPERIDINES, OXANES, AND 4- <u>tert</u> -BUTYLCYCLOHEXANONES	
	Introduction.....	4
	Methyl-substituted Piperidines.....	6
	Methyl-substituted Oxanes and 1,3-Dioxanes.....	22
	Methyl-substituted 4- <u>tert</u> -Butyl-cyclohexanones.....	36
	Summary.....	41
	References.....	45
CHAPTER III	<u>N</u> -ARYLAZACYCLOALKANES	
	Introduction.....	50
	<u>N</u> -Arylaziridines.....	55

# TABLE OF CONTENTS (CONT.)

	<u>PAGE</u>
<u>N</u> -Arylazetidines.....	62
<u>N</u> -Arylpyrrolidines.....	66
<u>N</u> -Arylpiperidines.....	69
Determination of Conformations.....	73
Proton Affinities.....	76
Conclusions.....	80
References.....	81
 CHAPTER IV      PHENCYCLIDINES	
Introduction.....	83
Photoelectron Spectra.....	86
Discussion.....	97
References.....	99
 CHAPTER V      EXOCYCLIC ALKENES	
Introduction.....	101
Photoelectron Spectra.....	107
Discussion.....	112
References.....	117
 CHAPTER VI      CUMENES AND CYCLOPROPYLBENZENES	
Introduction.....	119
Photoelectron Spectra.....	122
Discussion.....	131
References.....	136



# TABLE OF CONTENTS (CONT.)

	<u>PAGE</u>
CHAPTER VII    EXPERIMENTAL.....	138
PART II. THEORETICAL STUDIES OF QUINONES	
CHAPTER VIII    QUINONES.....	
Introduction.....	140
The Quinones of Azulene.....	142
Azuloquinone Summary.....	162
Substituent Effects on Benzoquinone Molecular Orbitals.....	163
Substituent Effects on Naptho- quinone Molecular Orbitals.....	175
Molecular Orbitals and Regio- selectivity.....	183
References.....	188
VITA.....	193

# LIST OF TABLES

<u>TABLES</u>	<u>PAGE</u>
PART I.	
1. Ionization Potentials of Methyl-Substituted Piperidines.....	9
2. Ionization Potentials of Methyl-Substituted <u>N</u> -Methylpiperidines.....	10
3. STO-3G Orbital Energies and Proton Affinities for Methyl-Substituted Piperidines.....	15
4. STO-3G Orbital Energies and Proton Affinities for Methyl-Substituted <u>N</u> -Methylpiperidines.....	16
5. Ionization Potentials of Oxanes (Tetrahydropyrans).....	29
6. Ionization Potentials of 1,3-Dioxanes.....	30
7. STO-3G Orbital Energies for Oxanes (Tetrahydropyrans).....	35
8. Ionization Potentials of 4- <u>tert</u> -Butyl-cyclohexanones.....	39
9. STO-3G Orbital Energies for Cyclohexanones.....	43
10. Ionization Potentials (eV) of Azacycloalkanes..	57
11. Conformations of <u>N</u> -Arylazacycloalkanes.....	75
12. Experimental and Calculated Proton Accepting Properties of Azacycloalkanes.....	78
13. Ionization Potentials of Phencyclidine (PCP) and Analogs.....	90
14. Ionization Potentials of Endocyclic Alkenes and Exocyclic Alkenes.....	109
15. Ionization Potentials of Substituted Benzenes..	124

# LIST OF TABLES (CONT.)

<u>TABLES</u>	<u>PAGE</u>
PART II.	
1. Results of Calculations on the Benzoquinones...	149
2. Results of Calculations on the Naphthoquinones.	150
3. Results of Calculations on the Azuloquinones...	152
4. Calculated LUMO Coefficients of the Azuloquinones in Figure 3 (MINDO/3).....	158
5. Frontier $\pi$ Molecular Orbitals (STO-3G) of Benzoquinone and 2-Substituted Benzoquinones...	170
6. Frontier $\pi$ Molecular Orbitals (STO-3G) of Naphthoquinone and Substituted Naphthoquinones.	178

# LIST OF FIGURES

<u>FIGURES</u>	<u>PAGE</u>
PART I.	
1. Photoelectron Spectra of Piperidine, <u>N</u> -Pethylpiperidine, <u>cis</u> -1,2,6-Trimethylpiperidine and 1,2,2,6,6-Pentamethylpiperidine.....	8
2. Orbital Contour Plots of Piperidine with an Axial and Equatorial Lone Pair.....	17
3. Orbital Contour Plots of the HOMO and SHOMO of Oxane.....	24
4. Photoelectron Spectra of 2-Methyloxane, 4-Methyloxane, <u>cis</u> -2,4-Dimethyloxane, and <u>trans</u> -2,6-Dimethyloxane.....	27
5. Photoelectron Spectra of <u>cis</u> -2,4-Dimethyl-1,3-dioxane, <u>cis</u> -4,6-Dimethyl-1,3-dioxane, and 2,2,4,6-Tetramethyl-1,3-dioxane.....	28
6. Photoelectron Spectra of Cyclohexanone and 4- <u>tert</u> -Butylcyclohexanone.....	38
7. Orbital Contour Plots of the HOMO and SHOMO of Cyclohexanone.....	42
8. The Three Highest Occupied Molecular Orbitals of <u>N</u> -arylazacycloalkanes.....	53
9. Photoelectron Spectra of <u>N</u> -Phenylaziridine and <u>N</u> -(2,6-Xylyl)aziridine.....	56
10. Photoelectron Spectra of <u>N</u> -Phenylazetidine, <u>N</u> -(2-Tolyl)azetidine and <u>N</u> -(2,6-Xylyl)azetidine	63
11. Photoelectron Spectra of <u>N</u> -Phenylpyrrolidine, <u>N</u> -(2-Tolyl)pyrrolidine, and <u>N</u> -(2,6-Xylyl)-pyrrolidine.....	67
12. Photoelectron Spectra of <u>N</u> -Phenylpiperidine, <u>N</u> -(2-Tolyl)piperidine, and <u>N</u> -(2,6-Xylyl)piperidine.....	70

# LIST OF FIGURES (CONT.)

<u>FIGURES</u>	<u>PAGE</u>
13. STO-3G Orbital Energies as a Function of Rotational Angle.....	72
14. STO-3G Orbital Coefficients of <u>N,N</u> -Dimethylaniline in Perpendicular and Coplanar Conformations.....	73
15. The Similarities Between Acetylcholine and PCP.	84
16. Photoelectron Spectra of 1-Phenylcyclohexylamine, <u>N</u> -(1-Phenylcyclohexyl)methylamine, <u>N</u> -(1-Phenylcyclohexyl)ethylamine, <u>N,N</u> -(1-Phenylcyclohexyl)dimethylamine, <u>N</u> -(1-Phenylcyclohexyl)piperidine, and <u>N</u> -(1-Phenylcyclohexyl)morpholine.....	87
17. Photoelectron Spectra of <u>N</u> -[1-(3-Aminophenyl)-cyclohexyl]piperidine, <u>N</u> -[1-(3-Nitrophenyl)-cyclohexyl]piperidine, <u>N</u> -[1-(2-Thienyl)cyclohexyl]piperidine, and <u>N</u> -(1-Cyanocyclohexyl)piperidine.....	88
18. Photoelectron Spectrum of Ketamine.....	89
19. Sustmann's Classification Scheme for 1,3-Dipolar Cycloadditions.....	103
20. Photoelectron Spectra of Ethylidenecyclohexane and Isopropylidenecyclohexane.....	108
21. Photoelectron Spectra of Cumene, Cyclopropylbenzene, and Benzobicyclo[3.1.0]hexane.....	123
22. Plot of $\text{Ph}_g$ IP of Substituted Benzenes vs $\text{Ph}_g$ IP of Substituted Cumenes and Cyclopropylbenzenes.....	133

# LIST OF FIGURES (CONT.)

<u>FIGURES</u>	<u>PAGE</u>
PART II.	
1. Naphthalene and the Naphthoquinones (NQs).....	143
2. Azulene and the Azuloquinones (AQs).....	144
3. ORTEP Plots of the Quinones Predicted to be Nonplanar.....	146
4. Summary of Sites of Attack by Nucleophiles on Substituted Benzoquinones.....	165
5. Summary of Sites of Attack by Nucleophiles on Substituted Naphthoquinones.....	166
6. Some STO-3G $\pi$ Molecular Orbitals and Energies of Benzoquinone.....	168
7. Orbital Mixing in Benzoquinone Caused by a Donor Substituent.....	173
8. Some STO-3G $\pi$ Molecular Orbitals and Energies of 1,4-Naphthoquinone.....	176
9. Geometries, LUMO Coefficients, and $\pi$ and Total Charges of 2-Methoxybenzoquinone.....	184

### LIST OF ABBREVIATIONS

Ac	Acetyl group $C_2H_3O$
Ar	Aromatic ring (with substituents)
FMO	Frontier Molecular Orbital
HOMO	Highest Occupied MO
IP	Ionization Potential
LUMO	Lowest Unoccupied MO
MO	Molecular Orbital
PES	Photoelectron Spectroscopy
SHOMO	Second Highest Occupied MO
SLUMO	Second Lowest Unoccupied MO
THOMO	Third Highest Occupied MO
TLUMO	Third Lowest Unoccupied MO

## ABSTRACT

Methyl-substituted piperidines, oxanes, 1,3-dioxanes, and cyclohexanones were studied by photoelectron spectroscopy (pes) to determine the mechanism by which alkyl groups stabilize radical cations. Hyperconjugation was found to be the dominant mechanism, while inductive effects and charge-induced polarization were indicated to be less effective.

N-Arylazacycloalkanes were studied by pes to correlate solution basicities with ionization potentials (IPs). Conformational analysis of these compounds indicated that aryl-substituted aziridines are coplanar (conjugating) in all cases studied, while ortho substituent(s) may cause rotation and loss of conjugation between the lone pair and the phenyl ring as the amine ring size is increased. N-Phenylpiperidine was indicated to be non-coplanar, despite the lack of ortho substituents.

Pes studies of phencyclidine and a number of its analogs demonstrate that the amine lone pair IP changes predictably, depending on the nature and location of the substituent. The phencyclidine analogs which have the lowest IPs are the most reactive in rat behavioral studies and binding studies.

Some exocyclic alkenes were studied by pes to try to correlate the IP with the observed reactivity and regioselectivity in 1,3-dipolar cycloadditions. Cumenes and cyclopropylbenzenes were studied in an attempt to correlate IPs with photochemical



reactivity studies. Both of these sets of compounds also showed normal substituent effects on the IPs as substituents were added.

Three different classes of quinones were studied by semi-empirical and ab initio methods to predict their stabilities and reactivities. The MINDO/3 results are genuine predictions of the thermodynamic stabilities and reactivities of the little known quinones of azulene. 1,5- and 1,7-azuloquinone are predicted to be the most stable and the least susceptible to nucleophilic attack. Benzoquinones and naphthoquinones were studied for comparison to the azuloquinones. STO-3G studies of substituted benzoquinones and naphthoquinones using frontier molecular orbital theory correctly indicate the preferred site(s) of reaction with nucleophiles.

PART I. PHOTOELECTRON SPECTROSCOPIC STUDIES OF AMINES,  
ALKENES, AND SUBSTITUTED BENZENES

## CHAPTER I. INTRODUCTION

Irradiation of a substance causes ejection of electrons having binding energies less than the energy of radiation. The excess kinetic energy imparted to the electron reveals the binding energy. This is the photoelectric effect. The kinetic energy of the electrons ejected is dependent on the energy of incoming irradiation,  $h\nu$ , and the binding energy,  $E_i$ , more commonly known as the ionization potential ( $IP_i$ ). Conservation of energy in the process requires that  $h\nu = IP + E_k$  where  $E_k$  is the kinetic energy of the ejected electron. The kinetic energy imparted to the ion is assumed to be negligible, due to the large mass disparity between the electron and the ion.

In photoelectron spectroscopy (pes),<sup>1-5</sup> monochromatic ultraviolet radiation is used for excitation and only valence electrons are ionized. The spectroscopic analysis is based upon the kinetic energies of the electrons and the relative count rates at each energy, as opposed to an analysis of positive ions or photons, either absorbed or emitted. Ionization energies and band intensities of these ejected electrons are measured in order to probe the electronic structures of organic compounds.

Ionization potentials may be equated to the negatives of molecular orbital energies via Koopmans' theorem,<sup>6</sup> thus providing a measurement of the energies of the high-lying filled molecular orbitals. Ionization potentials may be compared to orbital energies obtained from semi-empirical or ab initio molecular orbital calculations. This comparison may provide some assistance

in making assignments in difficult cases, or the calculations may be used to support assignments. Calculations on the possible molecular conformations and isomers may provide insight into the mechanism of substituent effects on the ionization potentials (IPs) of interest in the study.

This work is a report on several studies by photoelectron spectroscopy: 1) the mechanism of radical cation stabilization by alkyl groups in methyl-substituted piperidines, oxanes, 1,3-dioxanes, and cyclohexanones (Chapter II); 2) conformational analyses of a series of N-arylazacycloalkanes (Chapter III); 3) some miscellaneous studies: a) correlation of ionization potentials with drug activities in a series of phencyclidines (Chapter IV); b) correlation of ionization potentials with the observed regioselectivities in the reaction between a series of exocyclic alkenes with a 1,3-dipole (Chapter V); and c) determination of the conformations and ground state electronic characteristics of cyclopropylbenzenes (Chapter VI). The experimental details are provided in Chapter VII.

REFERENCES

1. Heilbronner, E.; Maier, J. P. Electron Spectroscopy Brundle, C. R.; Baker, A. D., eds., Academic, London, 1977, 205.
2. Turner, D. W.; Baker, C.; Baker, A. D.; Brundle, C. R. Molecular Photoelectron Spectroscopy Wiley-Interscience, New York, 1970.
3. Rabalais, J. W. Principles of Ultraviolet Photoelectron Spectroscopy Wiley, New York, 1977.
4. Carlson, T. A. Photoelectron and Auger Spectroscopy Plenum, New York, 1975.
5. Eland, J. H. D. Photoelectron Spectroscopy Butterworths, London, 1974.
6. Koopmans, T. Physica (Utrecht) 1934, 1, 104.

CHAPTER II. METHYL-SUBSTITUTED PIPERIDINES, OXANES,  
AND 4-tert-BUTYLCYCLOHEXANONES

## INTRODUCTION

The mechanism by which alkyl groups stabilize charged species is a venerable subject of continuing interest. Based on relative gas-phase acidity and basicity data collected over the past decade, it is apparent that alkyl groups stabilize both cations and anions. Different mechanisms have been proposed to account for individual results, with polarizability being invoked most often, because of its applicability to both anions and cations.

The polarizability mechanism<sup>1-6</sup> involves an induced dipole in the substituent, brought about by the presence of the charged center. This resultant dipole disperses the charge electrostatically, stabilizing the ion. A change in the direction of the induced dipole is the only necessary alteration to adapt this mechanism to account for anion stabilization. Larger groups are more polarizable than smaller alkyl substituents, in agreement with the data, and the stabilization has been found to vary with  $r^{-4}$ , where  $r$  is the separation distance.

The dependence upon distance for a stabilizing influence is somewhat analogous to the inductive effect.<sup>7-10</sup> Ingold<sup>8</sup> has distinguished two different cases where the inductive effect of the methyl group is considered. From a study of absorption data and dipole moments, methyl groups are seen to be weakly electron withdrawing in saturated alkanes. In most other classes of compounds, however, methyl groups are electron donating,



particularly when electronegative groups are also present.

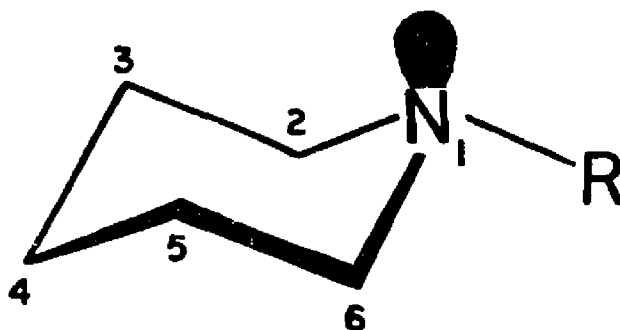
Both inductive effects and polarization tend to work together in stabilizing cations, but their respective magnitudes are different. In gas-phase proton transfer equilibria, the polarizability effects of hydrocarbon substituents completely dominate any inductive effects, usually being 3-7 times larger.<sup>11</sup>

Another possible mechanism, particularly for stabilizing cations, is hyperconjugation,<sup>12-13</sup> in which electrons are donated, or delocalized, from a  $\sigma$ -bonding electron pair to an electron deficient center. Evidence for hyperconjugation<sup>12-24</sup> has come from solvolysis studies,  $\beta$  isotope effects, and stereochemical studies. Schmidt and Schweig<sup>24</sup> have studied and separated the inductive and hyperconjugative effects occurring in alkyl halides using photoelectron spectroscopy.

In hopes of quantifying, or at least qualitatively understanding, the mechanism by which alkyl groups stabilize cations, we have studied the photoelectron spectra of three separate series of methyl-substituted compounds: piperidines, oxanes (tetrahydropyrans) and 1,3-dioxanes, and 4-~~tert~~-butyl-cyclohexanones. The results obtained for the piperidines and the oxanes have been particularly illuminating with regard to the mechanism of cation stabilization. These two series have one or more readily assignable low-energy ionization bands which are adequately separated from the rest of the spectrum. The 1,3-dioxanes are less useful due to the presence of a second

oxygen atom with a second set of non-bonding orbitals. This makes it necessary to consider all possible combinations of lone-pair orbitals which make up the molecular orbitals, and leads to less certainty in the assignment of the low energy ionizations. The 4-tert-butylcyclohexanone results proved to be of less value, due to the small substituent effects observed in the resolvable oxygen lone-pair ionizations. The  $\pi_{C=O}$  band is not well-resolved or readily identified in the compounds studied. Each series will be discussed independently, followed by a combined summary at the end of this chapter.

#### METHYL-SUBSTITUTED PIPERIDINES



The highest occupied molecular orbital (HOMO) of piperidine is the nitrogen lone pair orbital. The ionization band of the HOMO is well separated from the  $\sigma$  onset in the photoelectron spectrum. It is a broad band which is typical for nearly all aliphatic amines. The broadness of this band is indicative of considerable molecular reorganization upon ionization, since

neutral amines are pyramidal, but the radical cations are planar.<sup>25-28</sup>

The photoelectron spectra of piperidine and the four possible monomethyl-substituted derivatives were studied previously by Katrib,<sup>29</sup> who found that the methyl group exerts a decreased influence on the lone pair ionization potential as it is substituted on the ring carbons farther from the nitrogen. Except for the relatively large increase in IP observed when the methyl substituent is moved from the nitrogen to the alpha carbon, the differences at various carbon positions were quite small ( $\leq 0.11$  eV), but in the proper sequence for an inductive effect.

We have re-examined the photoelectron spectra of these and other polymethyl substituted piperidine derivatives. Figure 1 shows the low energy regions of several representative spectra and Tables 1 and 2 list the observed ionization potentials and IP changes, relative to the parent N-H and N-methylpiperidines studied here, including those studied by Katrib.

All the piperidines, and a number of acyclic secondary amines,<sup>30</sup> show a  $0.34 \pm 0.07$  eV decrease in IP upon N-methylation. Substitutions at carbon result in smaller IP decreases, relative to the parent, similar in magnitude to the decreases observed earlier.<sup>30</sup> However, we do not find a systematic distinction between a single 2-, 3-, or 4-methyl substituent; each decreases the amine IP by  $\leq 0.09$  eV.

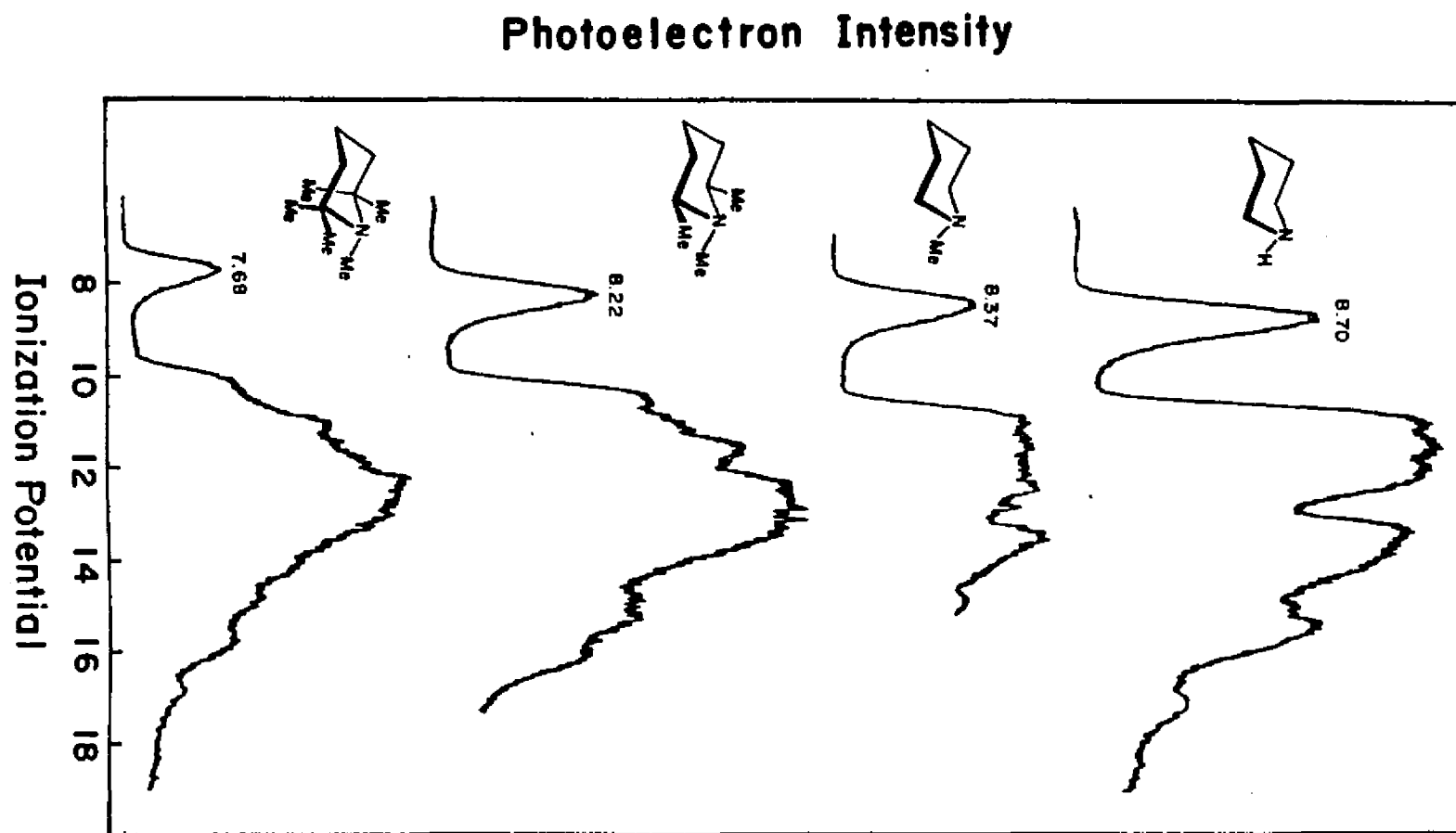


Figure 1. Photoelectron Spectra of Piperidine, N-Methylpiperidine, cis-1,2,6-Trimethylpiperidine, and 1,2,2,6,6-Pentamethylpiperidine.

Table 1. Ionization Potentials of Methyl-Substituted Piperidines.

Piperidine Substituent(s)	IP( $n_N$ ), eV <sup>a</sup>	$\Delta$ IP <sup>b</sup>
---	8.70 (8.69 <sup>c</sup> )	---
2-Me (eq)	8.63 (8.58 <sup>c</sup> )	-0.07
3-Me (eq)	8.63 (8.66 <sup>c</sup> )	-0.07
4-Me (eq)	8.61 (8.66 <sup>c</sup> )	-0.09
3,3-di-Me (eq, ax)	8.60	-0.10
<u>cis</u> -2,6-di-Me (eq, eq)	8.53	-0.17
2,2,6,6-tetra-Me (eq, ax, eq, ax)	(8.04 <sup>d</sup> )	-0.66
=====		

(a)  $\pm$  0.05 eV; previously reported values are enclosed in parentheses.

(b) Change in IP, relative to piperidine.

(c) Reference 62.

(d) Reference 63.

Table 2. Ionization Potentials of Methyl-Substituted N-Methylpiperidines.

<u>N</u> -Methylpiperidine Substituent(s)	IP( $n_N$ ), eV <sup>a</sup>	$\Delta$ IP <sup>b</sup>
---	8.37 (8.39 <sup>c</sup> )	---
2-Me (eq)	8.23	-0.14
3-Me (eq)	8.35	-0.02
4-Me (eq)	8.33	-0.04
4,4-di-Me (eq, ax)	8.29	-0.08
<u>cis</u> -3,5-di-Me (eq, eq)	8.23	-0.14
<u>trans</u> -3,5-di-Me (eq, ax)	8.26	-0.11
<u>cis</u> -2,6-di-Me (eq, eq)	8.22	-0.15
2,2,6,6-tetra-Me (eq, ax, eq, ax)	8.04	-0.69

=====

(a)  $\pm$  0.05 eV; previously reported values are enclosed in parentheses.

(b) Change in IP, relative to N-methylpiperidine.

(c) Reference 62.

In the monomethylpiperidines, the C-methyl substituents occupy equatorial positions in the chair conformation.<sup>31</sup> Addition of a second equatorial methyl group to 2-methylpiperidine to form cis-2,6-dimethylpiperidine results in a further decrease in the amine lone pair IP by 0.10 eV. This trend is similar in the N-methyl analog. The addition of a third methyl group to 1,3-dimethylpiperidine in the equatorial position to give cis-1,3,5-trimethylpiperidine causes a 0.12 eV decrease in the IP.

The substitution of an axial methyl substituent in 3-methylpiperidine, 1,3-dimethylpiperidine, and 1,4-dimethylpiperidine to give 3,3-dimethylpiperidine, trans-1,3,5-trimethylpiperidine, and 1,4,4-trimethylpiperidine, respectively, decreases the amine lone-pair IP by 0.03-0.10 eV. Assuming that these substituent effects are additive (within the  $\pm 0.05$  eV experimental limits), 2-, 3-, or 4-equatorial and 3- or 4-axial methyl substituents lower the IP of piperidine or the N-methyl analog by  $0.07 \pm 0.07$  eV per methyl group.

In contrast, axial 2- and 6-methyl substituents cause a very large decrease in the lone pair IP. The addition of two methyl groups to the axial positions of cis-2,6-dimethylpiperidine to form 2,2,6,6-tetramethylpiperidine lowers the IP by an additional 0.49 eV. Similarly, a 0.54 eV decrease is observed when two additional methyl groups are added to cis-1,2,6-trimethylpiperidine to form 1,2,2,6,6-pentamethylpiperidine. Each of these 2-axial methyl substituents lowers the amine IP by  $0.26 \pm 0.02$  eV,

indicating a unique influence on the amine lone pair by methyl substituents in those positions.

The nearly identical influence of C-methyl substituents on amine IPs in the piperidines and the N-methyl piperidines implies that the conformations at nitrogen are identical in these two series. The extent of conformational preference in both piperidine and N-methylpiperidine has been debated for many years, particularly for piperidine. Gas-phase and non-polar solvent studies have been interpreted to indicate a 60-70% preference for an axial lone-pair in piperidine at 25°, <sup>32</sup> while NMR data in methanol interpretations suggest a slight preference for an equatorial lone-pair. <sup>33</sup> For N-methylpiperidine, the axial lone-pair preference ranges from 75-99%. <sup>34-36</sup>

A STO-3G <sup>37</sup> calculation was performed on piperidine, based on the crystal structure of piperidine hydrogen sulfide. <sup>38</sup> Calculations on possible mono-methyl derivatives of piperidine, including axial and equatorial substitutions, were carried out by the replacement of the appropriate hydrogen by a methyl group having standard bond lengths and angles. All the possible mono-methyl derivatives of N-methylpiperidine were also calculated in the same manner. The geometries were not allowed to relax in the calculations, which may have resulted in some unrealistic 1,3-diaxial interactions which would have been reduced if geometrical relaxations were allowed.



The calculations indicate that the axial lone pair is favored in all cases. The preference ranges from 1.0-1.9 kcal/mole for the piperidines, and from 5.4-10.8 kcal/mole for the N-methyl-piperidines, with the exception of the 3-axial-methyl conformers which apparently have a highly destabilizing 1,3-diaxial interaction between the methyl group and the axial nitrogen substituent (either hydrogen or methyl). The smallest preference is found for the axial-2-methyl species, while the 3- and 4-equatorial-methyl derivatives determine the maximum range.

MM2 calculations<sup>39-40</sup> on many of these same conformers also indicate an axial lone-pair preference, although the range is greater, ranging from 0.24-1.62 kcal/mole for the piperidines and 2.50 kcal/mole for N-methylpiperidine. STO-3G calculations indicate that the smallest difference is observed for the axial and equatorial lone-pair conformers of axial-2-methylpiperidine. The largest preference is indicated for equatorial-3-methylpiperidine. [The equatorial lone-pair conformers of 4-methylpiperidine were not calculated, but it is expected that the MM2 calculated preference trends will continue to be consistent with the STO-3G results (vide supra)]. All conformers which have an axial methyl substituent were found to be less stable than their equatorial methyl counterparts, probably a result of 1,3-diaxial interactions.

Only minimal geometry changes are observed in these MM2 calculations, even with axial methyl substituents.<sup>40</sup> The axial-2-

hydrogens are distorted 5-6° from a "perfect" 180° dihedral angle with the nitrogen lone-pair in piperidine and various derivatives. Replacement of this hydrogen by a methyl group increases the distortion by 5-7°, to a value of 10-13°. This distortion is probably not large enough to cause a significant decrease in overlap and admixing of the lone-pair orbital and the substituent CC bond.

The experimental order in the ionization potentials is reproduced by the STO-3G calculations on piperidines having an axial lone-pair, but not by calculations on the equatorial lone-pair conformers. Even though the calculated values do not correlate exactly with the experimental IPs, the trends observed in the calculated results should be a reflection of the experimental trends. An axial lone-pair IP is calculated to be lower than that of an equatorial lone-pair and is noticeably influenced by an axial-2-methyl substituent. An equatorial lone-pair is essentially unaffected by methylation at any carbon position of the ring (Tables 3 and 4).

Contour plots<sup>41</sup> of the STO-3G lone pair orbitals, shown in Figure 2, indicate the mechanism by which the methyl group can stabilize the cation upon ionization. The equatorial lone-pair is admixed with the two vicinal anti-periplanar CC bonds of the ring which have an appropriate symmetry for good overlap. With the exception of the CC bond to an equatorial 4-methyl substituent, none of the possible substituent bonds overlap appreciably with

Table 3. STO-3G Orbital Energies and Proton Affinities for Methyl-substituted Piperidines

Piperidine Substituent	Equatorial NH (Axial $n_N$ )			Axial NH (Equatorial $n_N$ )	
	$-\epsilon$ (eV)	$\Delta\epsilon^a$	PA <sup>b</sup> (kcal/mole)	$-\epsilon$ (eV)	$\Delta\epsilon^a$
---	8.02	---	278.5	7.67	---
eq-2-Me	8.01	-0.01	280.3	7.65	-0.02
ax-2-Me	7.86	-0.16	281.3	7.64	-0.03
eq-3-Me	7.99	-0.03	279.7	7.60	-0.07
ax-3-Me	8.00	-0.02	276.5	7.66	-0.01
eq-4-Me	8.00	-0.02	279.2	7.65	-0.02
ax-4-Me	7.91	-0.11	279.4	7.65	-0.02

(a) Relative to piperidine.

(b) Experimental proton affinity is 225.4 kcal/mole for piperidine, reference 30.

Table 4. STO-3G Orbital Energies and Proton Affinities for Methyl-Substituted N-Methylpiperidines

<u>N</u> -Methylpiperidine Substituent	Equatorial NH (Axial $n_N$ )			Axial NH (Equatorial $n_N$ )	
	$-\epsilon$ (eV)	$\Delta\epsilon^a$	PA <sup>b</sup> (kcal/mole)	$-\epsilon$ (eV)	$\Delta\epsilon^a$
---	7.78	---	280.9	7.41	---
eq-2-Me	7.76	-0.02	282.4	7.38	-0.03
ax-2-Me	7.60	-0.18	283.4	7.37	-0.04
eq-3-Me	7.75	-0.03	282.0	7.35	-0.06
ax-3-Me	7.75	-0.03	278.7	--- <sup>c</sup>	--- <sup>c</sup>
eq-4-Me	7.76	-0.02	281.6	7.39	-0.02
ax-4-Me	7.69	-0.09	281.8	7.38	-0.03

(a) Relative to N-methylpiperidine.

(b) Experimental proton affinity is 228.8 kcal/mole for N-methylpiperidine, reference 30.

(c) Using standard geometries, the 1,3-diaxial Me-Me interaction is unrealistically large for this calculation to be meaningful.

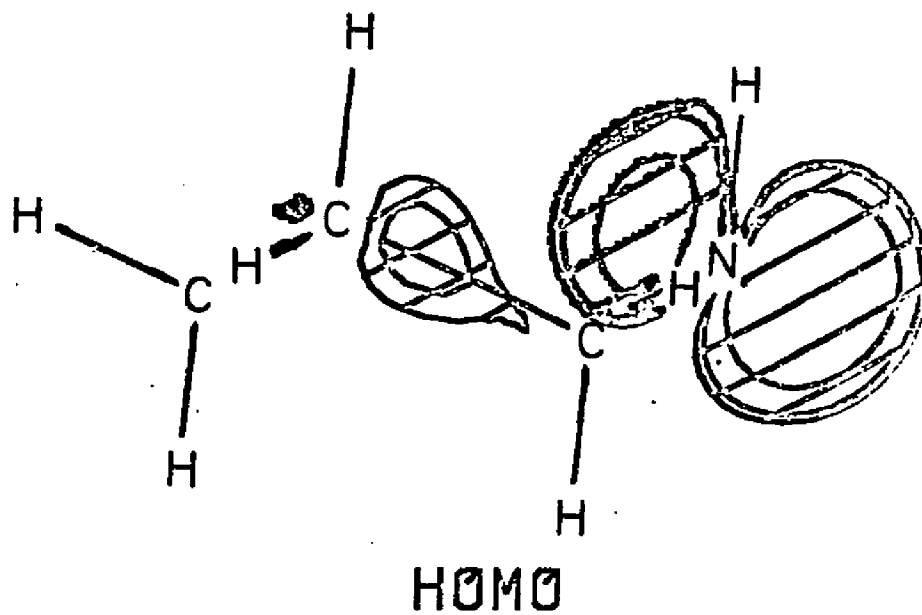
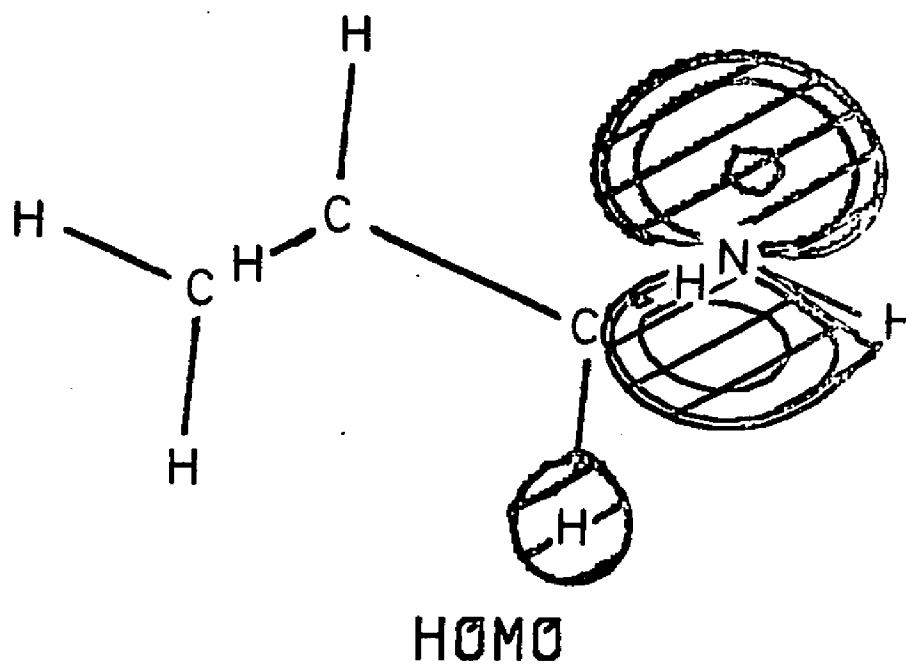


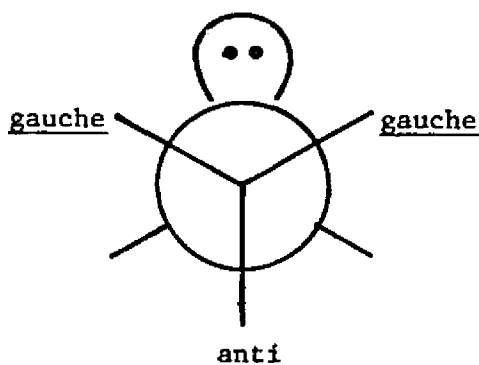
Figure 2. Orbital Contour Plots of Piperidine with an Axial and Equatorial Lone-Pair.<sup>41</sup>

the equatorial lone-pair (and the ring CC bonds). The equatorial 4-methyl group is spatially distant from the lone-pair; thus the extent of overlap through the ring is minimized.

The axial lone-pair overlaps with the CC bond of an axial-2-methyl substituent;<sup>42</sup> thus, the latter can influence the IP of an axial lone-pair. This suggests that the stabilization of the amine radical cation by alkyl groups occurs by a hyperconjugative mechanism, but only the axial lone-pair conformer is affected by the substituents.

Thus, theory reproduces the experimental conclusion that an axial-2-methyl substituent lowers the amine lone-pair IP by a much greater amount than methyl groups in other positions on the ring. An interpretation of the orbital contour diagrams suggests that the hyperconjugative mechanism is the predominant means for stabilization of the radical cation.

The slight preference for an axial lone-pair in piperidine is analogous to the conformational preference in some primary amines.<sup>40</sup> An anti orientation between the lone-pair and the hydrogen on the  $\alpha$  carbon of isopropylamine is preferred according to calculations<sup>40</sup> and experiment.<sup>43</sup> For ethylamine, however, calculations<sup>40,44</sup> favor a gauche orientation between the amine lone-pair and the CC bond, i.e. an anti hydrogen, while inconclusive experimental data have suggested an anti CC bond. In methylamine, the hydrogen anti to the lone pair is seen to be a longer, weaker CH bond, both experimentally and computationally.<sup>45</sup>



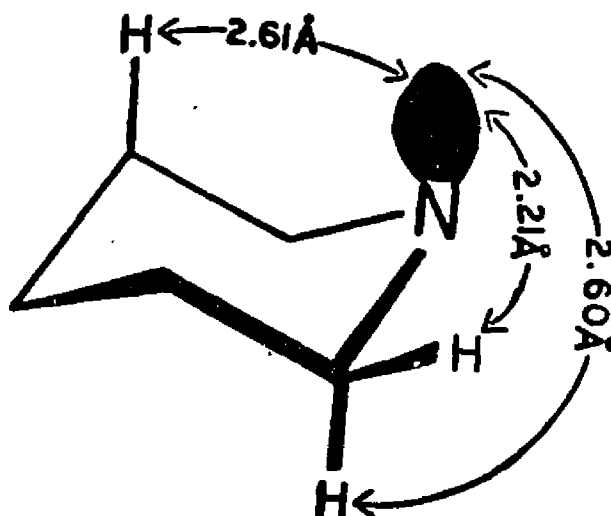
Based on bond strengths and pes data,<sup>46-48</sup> a  $\sigma_{CC}$  orbital lies higher in energy than a  $\sigma_{CH}$  orbital. According to the methylamine results referred to above, and in general, the  $\sigma_{CH}^*$  orbital is lower in energy than the  $\sigma_{CC}^*$  orbital, i.e. the same order in both the occupied and vacant orbitals. (The longer bond length was said to be due to electron donation into the vacant  $\sigma_{CH}^*$  orbital.<sup>45</sup>)

The differences between the energies of filled CC and CH orbitals are not expected to be large. The vacant CC and CH orbitals should also be close in energy. The conformational preference in piperidine is only slightly in favor of an axial lone-pair. Methylation of the nitrogen should not cause an appreciable electronic preference for an equatorial substituent. However, the axial methyl conformer possesses a strong 1,3-diaxial-interaction which results in a strong preference for an equatorial substituent.

The only mechanism which account for the large experimental IP changes which result when 2-axial methyl substituents are

added is hyperconjugation. Inductive effects should be dependent on the number of intervening bonds between lone pair and substituent, but without any stereochemical dependence. The dramatic difference between the effects shown for an axial vs. equatorial 2-methyl group invalidates the possibility that inductive effects are the predominant mechanism for stabilizing radical cations.

If polarizability (charge, induced dipole) is the dominant mechanism, the largest effect should be observed when the methyl group is closest to the lone-pair. The distances shown below were obtained from the MM2 calculations, and indicate that an axial-3-methyl group is actually as close to the lone-pair as an axial-2-methyl group and should therefore be more effective by the polarizability mechanism.



A much larger effect should have been observed for the axial methyl group in 3,3-dimethylpiperidine and trans-1,3,5-trimethyl-



piperidine if polarizability influenced the IP. Even though the IP decrease due to the axial methyl group in the trans trimethyl isomer is larger than that observed for the addition of the initial equatorial methyl group, the decrease is actually less than that observed for the added equatorial methyl group in cis-1,3,5-trimethylpiperidine (Table 2). A polarizability mechanism would have predicted that this trend would be reversed and enhanced.

The stereochemical dependence found experimentally and the calculated IPs also reflect that a  $\sigma_{CC}$  orbital is a more potent hyperconjugative donor than is a  $\sigma_{CH}$  orbital. If the converse was true, then the lone-pair IP decrease should have been less when the axial-2-methyl substituents were added than the decreases observed due to the equatorial-2-methyl substituents.

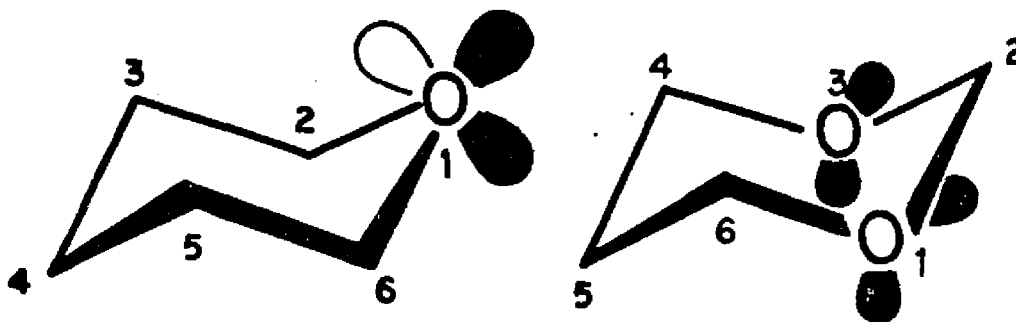
Finally, we contrast the dominance of hyperconjugation in influencing IPs with the polarizability model which has been so successful in rationalizing the magnitudes of proton affinities.<sup>1-6</sup> Proton affinities (PAs) are defined below:

$$PA = E_{BH^+} - (E_B + E_{H^+})$$

where  $E_{BH^+}$  is the total energy of the protonated base,  $E_B$  is the total energy of the free, non-protonated base, and  $E_{H^+}$  is the energy of the proton (=0).

Although the PAs calculated by STO-3G (Tables 3 and 4) for the axial lone-pair piperidines are 52-53 kcal/mole too high,<sup>30</sup> relative values should be reasonable at this level of calculation. While the PAs of axial-2-methylpiperidine and its N-methyl analog are ~1 kcal/mole larger than the PAs of the equatorial-2-methyl conformers, there is an additional methyl-H(N<sup>+</sup>) gauche interaction in the equatorial compounds which counteracts the expected greater stabilization from the polarizability mechanism. The PAs of the axial-3-methyl compounds show a destabilization effect which is opposite to that expected. However, this result may simply be a consequence of the ring rigidity in the calculations and would probably disappear if the ring were allowed to relax.

#### METHYL SUBSTITUTED OXANES AND 1,3-DIOXANES

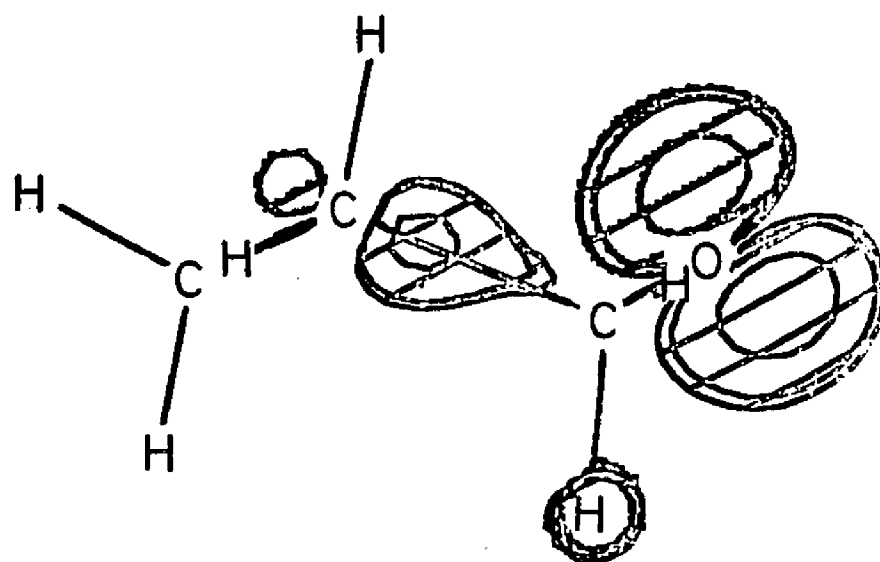


Oxane (tetrahydropyran) has two readily identifiable IPs in the low-energy region of its photoelectron spectrum. The HOMO is essentially a p orbital, while the second highest occupied

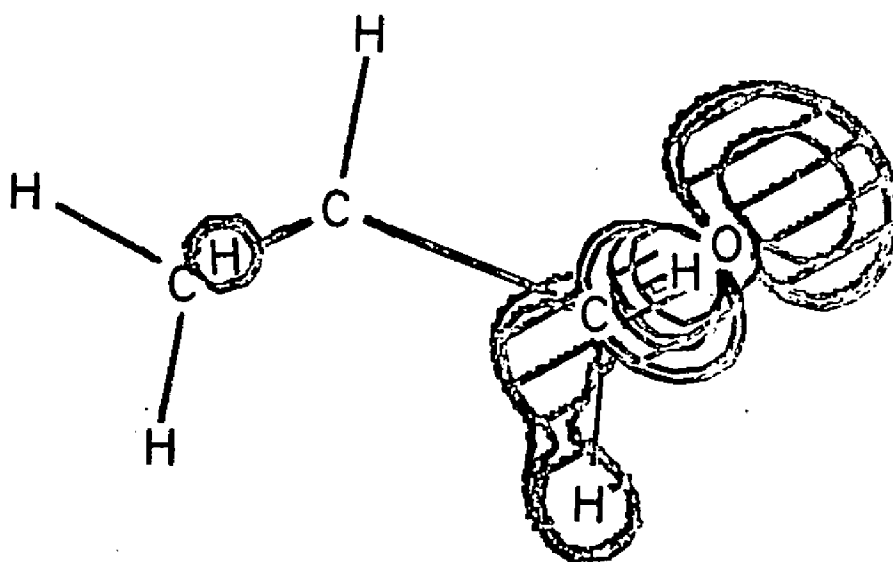
molecular orbital (SHOMO) is a hybrid in-plane lone-pair orbital which is also partially CO bonding.<sup>50-52</sup> These orbitals are similar in appearance to those of water and acyclic ethers.<sup>48</sup> Although oxane has a carbon skeleton which exerts an unsymmetrical perturbation on these orbitals, they mix to a minimal extent. Kobayashi<sup>51</sup> has referred to these orbitals as "equatorial" and "axial" lone-pairs, even though they are tilted from the "normal" directions in a six-membered ring. The tilt is barely in evidence in the STO-3G calculated orbital density diagrams shown in Figure 3.

The plots indicate that the HOMO is mixed most heavily with the vicinal CC bonding orbitals of the ring carbons, similar to those seen for the piperidine conformer with an equatorial lone-pair. The SHOMO is heavily admixed with the  $\alpha$ -axial CH bonding orbital in the parent molecule, which becomes the CC bonding orbital of an axial-2-methyl substituent, reminiscent of the piperidine conformer with an axial lone-pair. In this respect, these two orbitals stereoelectronically resemble "equatorial" and "axial" lone-pairs.

1,3-Dioxane, having two heteroatoms, each with two lone-pairs, has a total of four non-bonding molecular orbitals. Kobayashi proposed that the ionization order for the parent 1,3-dioxane to be  $n_{eq}^-$ ,  $n_{ax}^+$ ,  $\sigma$ ,  $n_{ax}^-$ ,  $\sigma$ , and  $n_{eq}^+$ , where (+) and (-)

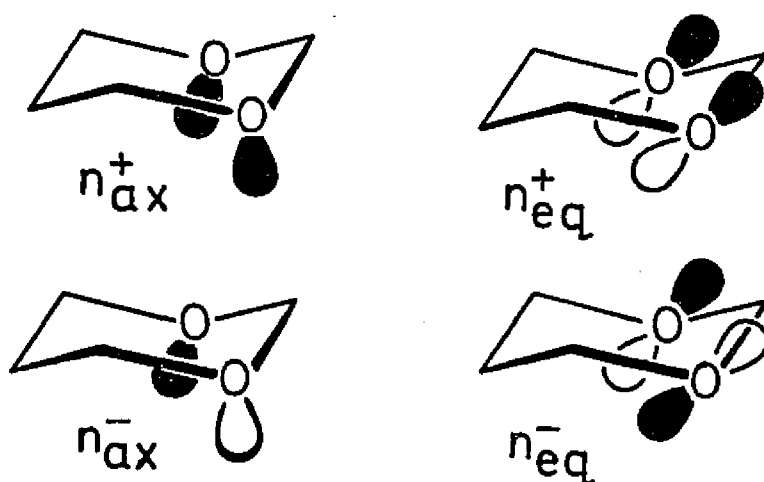


HOMO



SHOMO

Figure 3. Orbital Contour Plots of the HOMO and SHOMO of Oxane.



refer to bonding and antibonding combinations, respectively, of the axial (ax) and equatorial (eq) lone-pairs. Using a simple perturbation approach, the lone-pair antibonding (-) combinations are expected to show only minimal changes in their IPs when substituents are added at C-2 or C-5, i.e. on the nodal plane of these orbitals. Substituents at C-4 and/or C-6 should show a larger effect than at C-2, but the effect is expected to be smaller than for oxane, since the coefficients at each oxygen are  $1/\sqrt{2}$  those in oxane. The lone-pair bonding combinations (+) are expected to show a larger influence due to substituents which can interact with the lone-pairs of both oxygen atoms, especially at the 2-position. C-5 Substituents should also interact with the (+) combination, but the possible overlap is diminished because of the distance of separation. Substituents at the 4- or 6-position can hyperconjugate with only one of the oxygens and therefore will have less influence on the IP than from the 2-position.

Of the two bonding combinations, the shape of the  $n_{eq}^+$  orbital indicates that its strongest interaction should occur with the vicinal CC bonds of the ring, i.e., the CC bonds on either side of C5, but not with any of the CC bonds to substituents. The  $n_{ax}^+$  orbital can interact with bonds to axial substituents, most favorably with that of the 2-axial position. This is still a lesser perturbation of the lone-pair combination, compared to the interaction of the two lone-pairs and is expected to be less than the perturbation an axial-2-methyl group causes in the piperidines and oxanes. Even though the magnitude is likely to be less, the mechanism is identical.

We have examined the photoelectron spectra of some methyl-substituted oxanes (Figure 4) and a few 1,3-dioxanes (Figure 5). The IPs are assembled in Tables 5 and 6, respectively. A methyl substituent on 1,3-dioxane prefers the equatorial position, opposite to the preference of an electronegative hydroxy or methoxy group. These same electronegative substituents also show a preference for the axial position of oxane.<sup>53</sup> By analogy, a methyl group is expected to prefer an equatorial position in the oxanes, as in the piperidines and 1,3-dioxanes (vide infra).

The addition of a 2-methyl substituent to oxane decreases  $IP_1$  (equatorial lone-pair) by 0.11 eV, while  $IP_2$  (axial lone-pair) decreases by 0.05 eV. A 4-methyl substituent decreases the IPs by 0.03 and 0.11 eV, respectively, relative to oxane. In cis-2,4-dimethyloxane, the respective IPs are decreased by 0.15 and

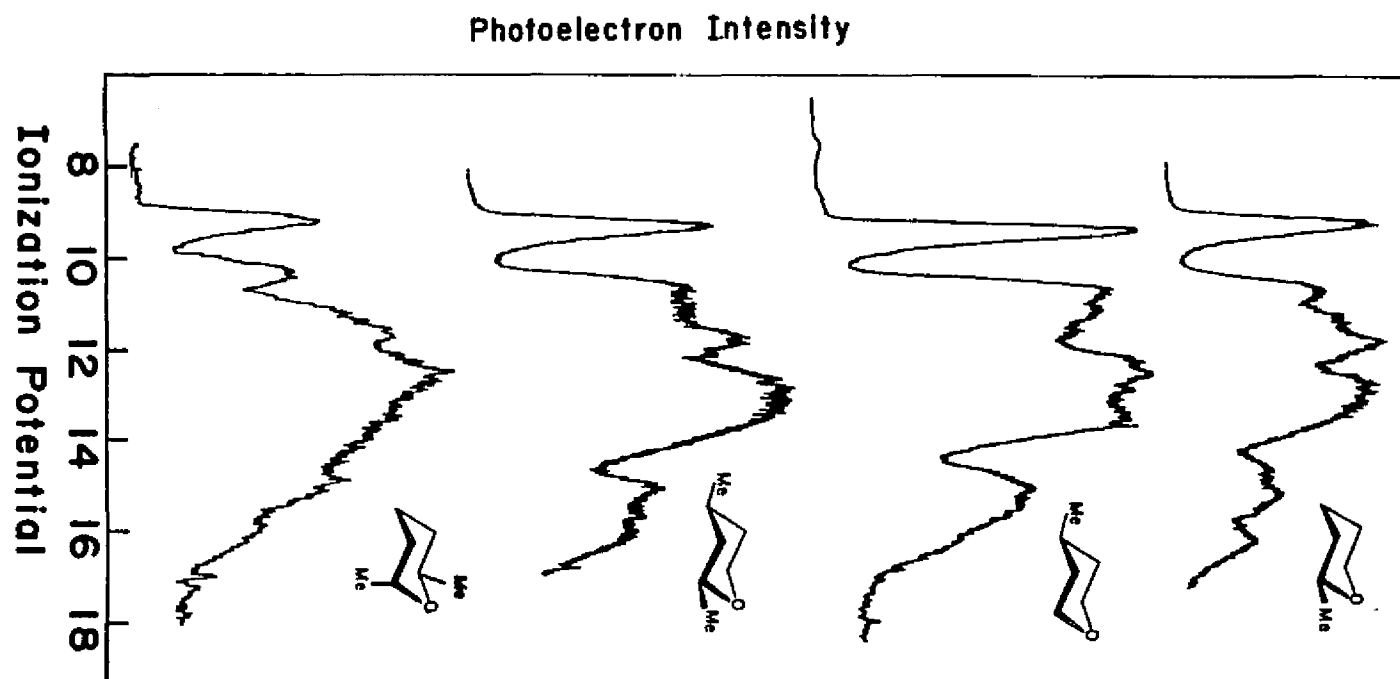


Figure 4. Photoelectron Spectra of 2-Methyloxane, 4-Methyloxane, cis-2,4-Dimethyloxane, and trans-2,6-Dimethyloxane.

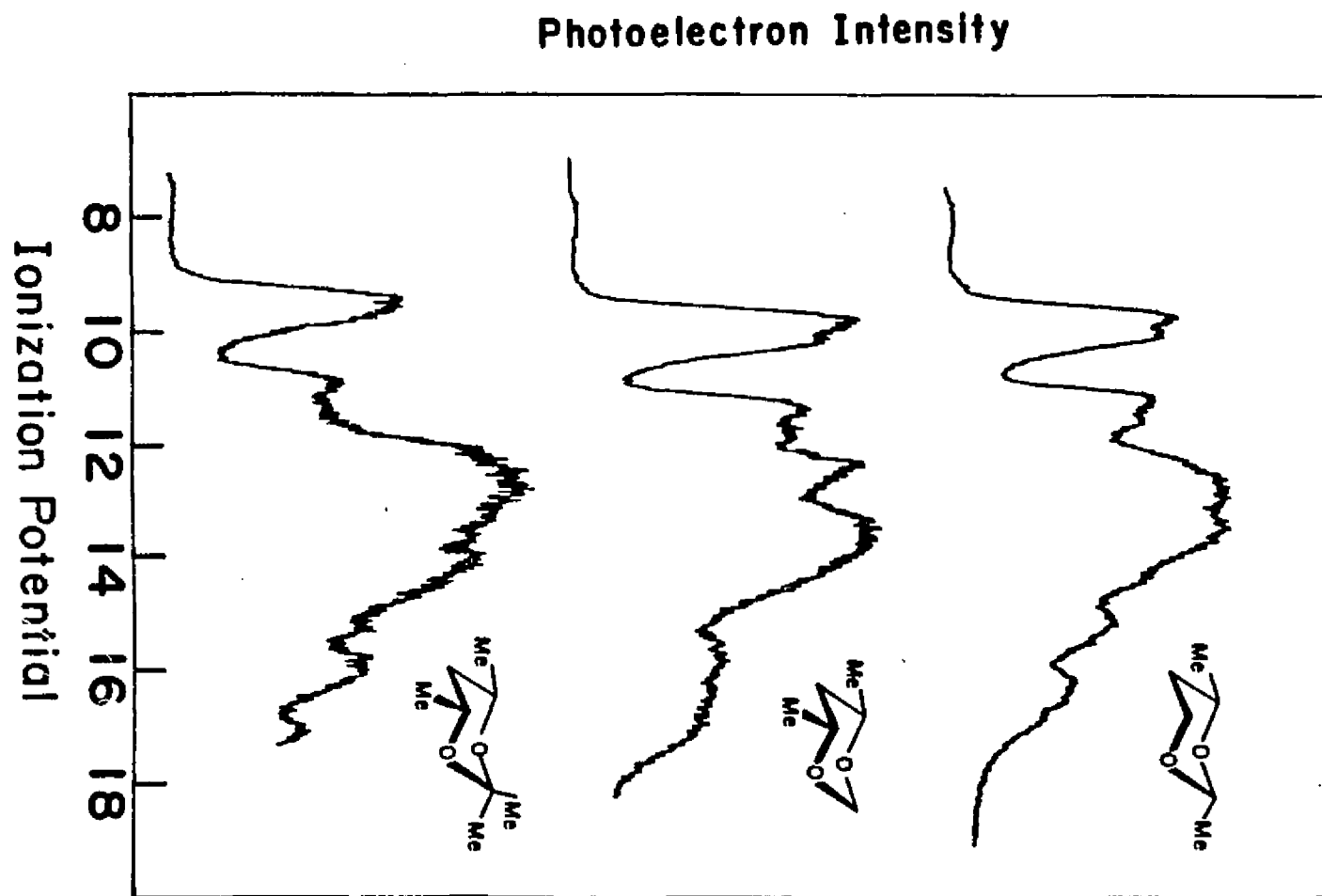


Figure 5. Photoelectron Spectra of cis-2,4-Dimethyl-1,3-dioxane, cis-4,6-Dimethyl-1,3-dioxane, and 2,2,4,6-Tetramethyl-1,3-dioxane.



Table 5. Ionization Potentials of Oxanes (Tetrahydropyrans)

<u>Oxane Substituent(s)</u>	<u>IP<sub>1</sub>, eV<sup>a</sup></u>	<u>IP<sub>2</sub>, eV<sup>a</sup></u>	<u>ΔIP<sub>1</sub></u>	<u>ΔIP<sub>2</sub></u>
---	(9.48 <sup>c</sup> )	(10.90 <sup>c</sup> )	---	---
2-Me (eq)	9.37	10.85	-0.11	-0.05
4-Me (eq)	9.45	10.79	-0.03	-0.11
<u>cis</u> -2,4-di-Me (eq, eq)	9.33	10.64	-0.15	-0.26
<u>trans</u> -2,6-di-Me (eq, ax)	9.26	10.37	-0.22	-0.53

=====

(a)  $\pm 0.05$  eV; previously reported values are enclosed in parentheses.

(b) Changes in IPs, relative to the parent species.

(c) Reference 51.

Table 6. Ionization Potentials of 1,3-Dioxanes

<u>1,3-Dioxane Substituent(s)</u>	<u>IP<sub>1</sub>, eV<sup>a</sup></u>	<u>IP<sub>2</sub>, eV<sup>a</sup></u>	<u>IP<sub>3</sub>, eV<sup>a</sup></u>	<u>IP<sub>4</sub>, eV<sup>a</sup></u>
---	(10.12 <sup>c</sup> )	(10.38 <sup>c</sup> )	(11.66 <sup>c</sup> )	(12.07 <sup>c</sup> )
<u>cis</u> -2,4-di-Me	9.83	10.15	11.35	11.75
<u>cis</u> -4,6-di-Me	9.82	10.14	11.29	11.61
2,2,4,6-tetra-Me	9.49	9.75	10.92	11.31

=====

(a)  $\pm 0.05$  eV; previously reported values are enclosed in parentheses.

(b) Changes in IPs, relative to the 1,3-dioxane.

(c) Reference 51.

0.26 eV, in reasonable agreement with the values which would be predicted, assuming that the substituent effects on the IPs are additive, although the decrease for  $IP_2$  is slightly greater than would be calculated. The addition of an axial methyl group to 2-methyloxane to give trans-2,6-dimethyloxane causes  $IP_1$  to decrease 0.22 eV, exactly double that observed for the first methyl group.  $IP_2$  decreases 0.53 eV, an effect much larger than anticipated assuming the additivity of substituent effects. Even after consideration of the limited number of samples, the measurement limitations, and other factors, it appears that this axial methyl group is responsible for a decrease of 0.2-0.3 eV in the second IP.

It is rather intriguing that both methyl groups of trans-2,6-dimethyloxane cause equal decreases in  $IP_1$ . Considering the unique effect of an axial methyl group on  $IP_2$ , it may have been expected that the axial methyl group would also exert a unique influence on  $IP_1$ . The equal magnitude of the  $IP_1$  decreases for both axial and equatorial methyl groups suggests that the mechanism for stabilizing the radical cations might also be the same. (This is particularly relevant to the discussions concerning the effect of substituents on the IPs of the 1,3-dioxanes.) Referring back to the HOMO, or equatorial lone-pair in the orbital contour diagrams (Figure 3), it is evident that the lone-pair is admixed with the vicinal CC bonds. This is the primary interaction in this orbital. The influence of a

substituent on this orbital will be a secondary interaction, since another substituent cannot be attached to the oxygen, but is bonded to carbon. This secondary interaction involves a  $\pi$ -CH<sub>3</sub> orbital of the methyl group, not the CC bond. Since an equivalent  $\pi$ -CH<sub>3</sub> orbital can be drawn for both an axial and an equatorial substituent, it is reasonable that they should have an equal influence on the HOMO of oxane.

The CC bond orbitals of the ring can destabilize the HOMO and stabilize the radical cation resulting from ionization from this orbital of oxane by a hyperconjugative mechanism. These effects are not dependent on the presence of substituents and also occur in the parent molecule. The "equatorial" lone-pair is nearly parallel to the vicinal CC bond orbitals, Figure 5. Therefore, it is not surprising that we have not observed a dramatic decrease in the IP of the HOMO with any substitution pattern. The SHOMO is nearly perpendicular to the vicinal CC bonds of the ring and is destabilized by axial 2-methyl substituents. The radical cation arising from ionization from this orbital can be stabilized by hyperconjugation. Thus, a significantly larger decrease in the SHOMO IP is expected when an axial 2-methyl group is present, compared to the decrease expected for an equatorial methyl substituent. The decrease observed due to the 2-axial methyl group (at least 0.3 eV) is comparable in magnitude to the decrease observed for an axial methyl substituent in the piperidines (vide supra).

The results for the 1,3-dioxanes are less obvious, due to a lack of sufficient numbers of definitive samples and, more importantly, the inability to assign and verify, with certainty, all the lone pair combinations in the spectra as the methyl groups are added. The spectra show the first four ionizations to be reasonably separated, but the remainder are poorly resolved. The possibility that the ionization order may change is an added uncertainty.

The addition of two equatorial methyl groups to 1,3-dioxane to form cis-4,6-dimethyl-1,3-dioxane causes a 0.29 eV decrease in  $IP_1$  (the  $n_{eq}^-$  combination), relative to 1,3-dioxane, or 0.15 eV per methyl group since both should be equivalent.  $IP_2$  (the  $n_{ax}^+$  combination) decreases 0.23 eV, or 0.12 eV per methyl group. 0.31 and 0.32 eV decreases are observed for  $IP_3$  ( $\sigma$ ) and  $IP_4$  ( $n_{ax}^-$ ), respectively, or 0.16 eV per methyl group in each case.

Altering the position of one of the methyl groups to form cis-2,4-dimethyl-1,3-dioxane, causes essentially no changes in the first two IPs, or the per methyl equivalents (cf. Table 6). The decreases in  $IP_3$  and  $IP_4$  are 0.37 and 0.46 eV, respectively. Since we have already determined the per methyl equivalent for the 4-methyl group to be 0.16 eV for these two IPs, the remainder represents the contribution from the 2-methyl group; the increments are 0.21 and 0.30 eV, respectively, for  $IP_3$  and  $IP_4$ .

Assuming that substituent effects are additive and temporarily disregarding the possibility of a hyperconjugative

influence, the IPs of 2,2,4,6-tetramethyl-1,3-dioxane may be predicted from the previous results.  $IP_1$  is expected to decrease by 0.60 eV ( $4 \times 0.15$  eV),  $IP_2$  should decrease by 0.48 eV ( $4 \times 0.12$  eV),  $IP_3$  should decrease 0.74 eV ( $2 \times 0.16$  eV +  $2 \times 0.21$  eV), and  $IP_4$  should decrease by 0.92 eV ( $2 \times 0.16$  eV +  $2 \times 0.30$  eV). The observed decreases are 0.63 eV, 0.63 eV, 0.74 eV, and 0.76 eV, respectively.  $IP_1$  and  $IP_3$  are in excellent agreement with those predicted, while  $IP_2$  is lower than predicted and  $IP_4$  is higher. If the additive effects above remain valid, the axial-2-methyl group causes a 0.27 eV decrease in  $IP_2$ , the  $n_{ax}^+$  combination. This decrease is more than double that expected, similar in magnitude to that observed in the oxanes and piperidines. This stereochemical dependence is not as well-substantiated due to the small number of samples.

The smaller decrease than expected in  $IP_4$  is not understood. The ionization is assigned to the  $n_{ax}^-$  orbital in the parent, but the possibility exists that a change in the ionization order has occurred. The nature of the  $\sigma$  orbital and the effect of substituents on it are uncertain.

STO-3G calculations on oxane which has a slightly puckered conformation according to microwave spectroscopy,<sup>54-55</sup> and the replacement of various  $\alpha$ -hydrogens by a standard methyl group reproduce the experimentally observed stereochemical dependence.

Table 7. STO-3G Orbital Energies for Oxanes (Tetrahydropyrans)

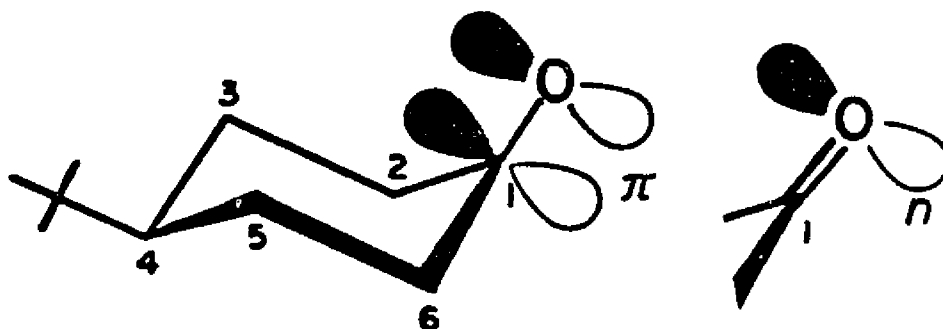
Oxane Substituent	$-\epsilon_1$ (eV)	$\Delta\epsilon_1^a$	$-\epsilon_2$ (eV)	$\Delta\epsilon_2^a$
---	8.50	---	9.75	---
eq-2-Me	8.25	-0.25	9.63	-0.12
ax-2-Me	8.32	-0.18	9.47	-0.28

=====

(a) Relative to oxane.

The calculated IPs (Table 7) indicate that an equatorial-2-methyl group exerts a slightly greater influence on the HOMO than does an axial-2-methyl group. Conversely, the axial-2-methyl group influences the SHOMO much more than the equatorial-2-methyl group. While the absolute magnitudes of the effects indicated by the calculations may be incorrect, the trends are in reasonable agreement with the experimental results. The stereochemical dependence of an axial-2-methyl group, the substance of the hyperconjugative mechanism, is reproduced.

METHYL SUBSTITUTED 4-*tert*-BUTYLCYCLOHEXANONES



The HOMO of cyclohexanone, 4-*tert*-butylcyclohexanone, and numerous other ketones<sup>56-59</sup> is an oxygen lone-pair orbital which may be admixed with other orbitals of appropriate symmetry. The SHOMO of most ketones is the  $\pi_{C=O}$  orbital which may also be admixed with others, as in the case of cyclohexanone (vide infra).

The pes spectrum of cyclohexanone shows the first ionization



band (lone-pair, IP = 9.18 eV) to be well-separated from the remainder, but the second band has merged into the  $\sigma$  framework. The spectrum of 4-tert-butylcyclohexanone shows a well separated first band and two additional, but poorly resolved, bands below 11 eV. In addition, the region between 12 and 14 eV is intensified, and rather featureless, as seems typical of compounds with a tert-butyl substituent. The first of the poorly resolved bands below 11 eV has been attributed to the  $\pi_{C=O}$  by one author from a study of 2-chlorocyclohexanone.<sup>56</sup> The second of these two poorly resolved bands was assigned to a  $\sigma$  ionization.

We have examined a small number of methyl-substituted 4-tert-butylcyclohexanones to determine whether the conformational dependence shown in the previous studies might also exist between the carbonyl group and an axial methyl group. The spectra (Figure 6) are very similar in appearance. Only minimal changes are observed in the first three IPs as single methyl groups are added (Table 8). Relative to 4-tert-butylcyclohexanone, the lone-pair IP (IP<sub>1</sub>) is changed less than experimental error ( $\pm 0.05$  eV) when a 2-methyl group is added, regardless of the axial or equatorial position. Two methyl groups cause a 0.1 eV decrease, again with essentially no differentiation between the cis and trans-2,6-dimethyl-4-tert-butylcyclohexanone conformers. These results are not too surprising, as the lone pair is mixed primarily with the vicinal CC bonds to the carbonyl carbon atom. A through-space interaction<sup>60</sup> could be envisioned, or electron-

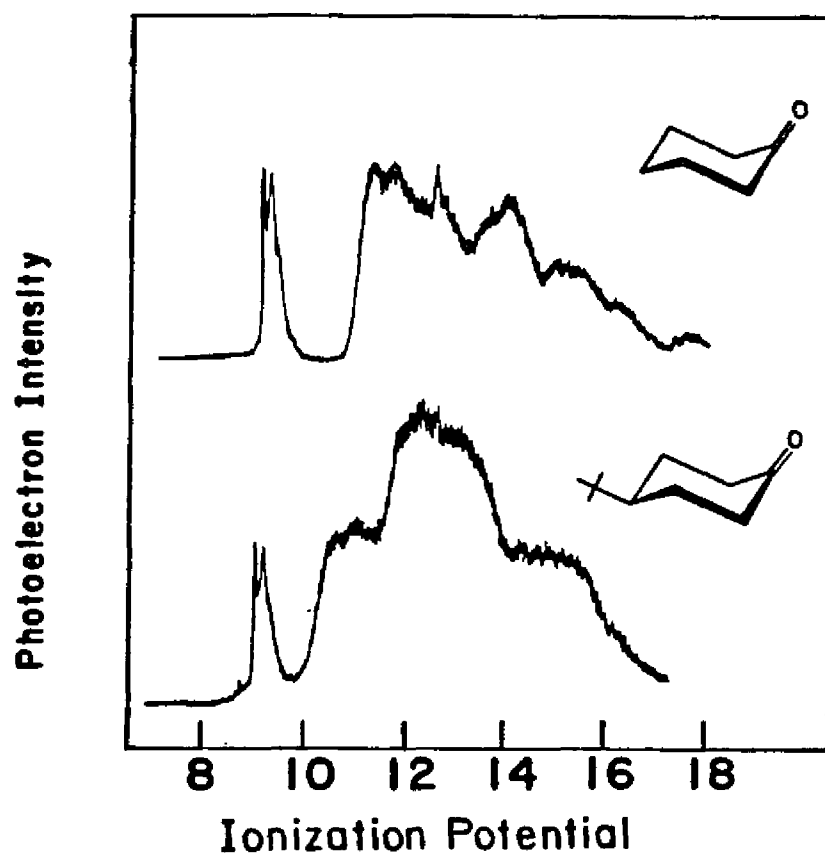


Figure 6. Photoelectron Spectra of Cyclohexanone and 4-tert-Butylcyclohexanone.

Table 8. Ionization Potentials of 4-tert-Butylcyclohexanones

4- <u>tert</u> -Butylcyclohexanone Substituent(s)	IP <sub>1</sub> , eV <sup>a</sup>	IP <sub>2</sub> , eV <sup>a</sup>	ΔIP <sub>1</sub>	ΔIP <sub>2</sub>
---	9.06 (9.04 <sup>c</sup> )	10.62 (10.54 <sup>c</sup> )	---	---
eq-2-Me	9.08	10.50	+0.02	-0.12
ax-2-Me	9.06	10.55	---	-0.07
<u>cis</u> -2,6-di-Me (eq, eq)	8.96	10.42	-0.12	-0.20
<u>trans</u> -2,6-di-Me (eq, ax)	8.97	10.39	-0.11	-0.23

=====

(a)  $\pm$  0.05 eV; previously reported values are enclosed in parentheses.

(b) Changes in IPs, relative to the parent species.

(c) Reference 56.

donation to the  $\pi$  orbital, which could increase the electron density on oxygen, and consequently decrease the lone-pair IP. However, the flattening of the ring suggests that there should be little if any differentiation between the axial and equatorial positions for interaction with either the lone-pair or  $\pi$  orbital (vide infra).

The trends for the second IPs are also quite similar. The second IP decreases 0.12 eV due to an equatorial-2-methyl group, but only by 0.07 eV for an axial-2-methyl group. The equatorial (second) methyl group of the cis-2,6-dimethyl derivative causes an additional 0.10 eV decrease, while the axial methyl group of the trans-2,6-dimethyl isomer causes a decrease of 0.11 eV, compared to 2-methyl-4-tert-butylcyclohexanone. The IP decreases, when compared to the IPs of 4-tert-butylcyclohexanone, are quite small, with little distinction between axial and equatorial substituents. The third IP decreases 0.08 eV for the first methyl substituent and 0.05 eV for the second methyl substituent, in both isomers.

The poor resolution of the second and third ionizations, and the subsequent uncertainty in the assignment of these bands, coupled with the significant flattening of the carbonyl end of the ring, all tend to make the above results inconclusive. The stereochemical dependence found earlier does not seem to be present in these cyclohexanones.

The crystal structure of 4-tert-butylcyclohexanone<sup>61</sup> indicates that the carbonyl end of the ring is flattened by 17°

from the ideal chair conformation. (The opposite end is also slightly flattened.) Using this geometry, but without the tert-butyl group, STO-3G calculations have been performed on 2-methylcyclohexanone, with the methyl group in both the axial and equatorial positions. The HOMO is the oxygen lone pair while the SHOMO is the  $\pi_{C=O}$ , as shown in the contour diagrams of Figure 7. The addition of the standard methyl group showed the equatorial-2-methyl conformer to be favored by 1.93 kcal/mole. The calculated IPs (Table 9) of the equatorial conformer (8.46 eV and 10.29 eV) are slightly higher than those of the axial-2-methyl conformer (8.42 eV and 10.20 eV). The calculations indicate a slight stereochemical dependence, but apparently this dependence is too small to be observed experimentally.

#### SUMMARY

In these three studies of piperidines, oxanes, and 1,3-dioxanes, hyperconjugation, polarizability, and inductive effects have been considered and evaluated as possible mechanisms to stabilize radical cations. An inductive mechanism should be dependent only on the number of bonds separating the substituent from the lone-pair or carbonyl group. This mechanism clearly does not allow for the stereochemical dependence found experimentally. The only series in which inductive effects may be of consequence, based on the experimental IPs is the cyclohexanones; here, the

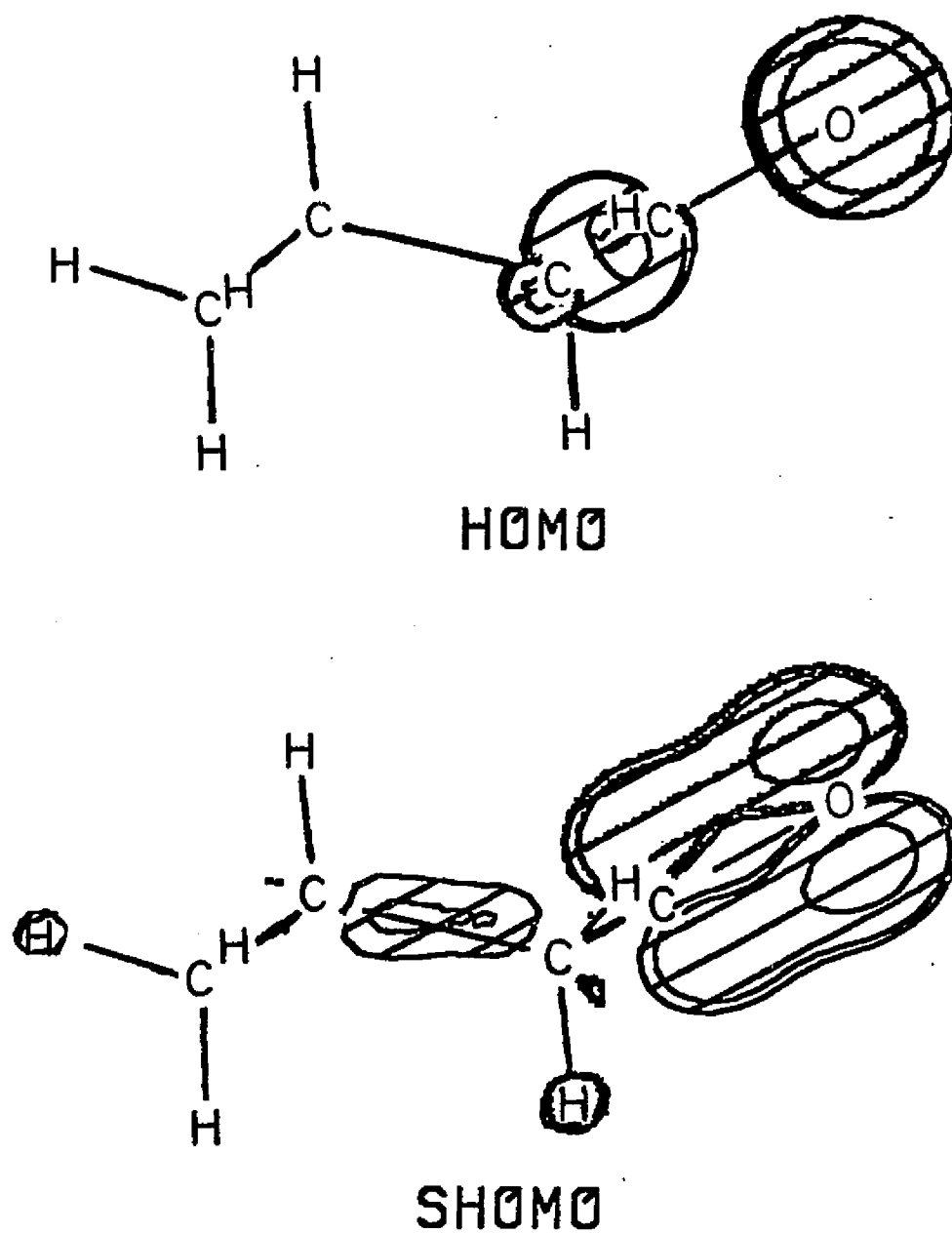


Figure 7. Orbital Contour Plots of the HOMO and SHOMO of Cyclohexanone.

Table 9. ST0-3G Orbital Energies for Cyclohexanones

Cyclohexanone Substituent	$-\epsilon_1$ (eV)	$\Delta\epsilon_1^a$	$-\epsilon_2$ (eV)	$\Delta\epsilon_2^a$
---	8.51	---	10.33	---
eq-2-Me	8.46	-0.05	10.29	-0.04
ax-2-Me	8.42	-0.09	10.20	-0.13

=====

(a) Relative to cyclohexanone.

changes are quite small and essentially equal for both equatorial and axial methyl substituents.

The polarizability mechanism (the charge inducing a dipole in the substituent) has been both experimentally and computationally ruled out as the predominant mechanism of IP change by methyl substituents in piperidines. The polarizability mechanism should have shown a greater influence on the IP from the 3-axial position, as well as from the 2-equatorial position, which are both closer to the lone pair than an axial-2-methyl group. In view of the similarities between piperidines, oxanes, and 1,3-dioxanes, it is suggested that polarizability is not the predominant mechanism in the oxanes and 1,3-dioxanes, even though it is not ruled out as effectively as in the piperidine case.

The hyperconjugation mechanism in which a stereochemical dependence exists between the lone-pair and the substituent for the delocalization of a bonding pair of electrons is consistent with the experimentally determined IPs and the calculated IPs. This has been effectively demonstrated for the piperidines, oxanes, and 1,3-dioxanes in this study.



# REFERENCES

1. Aue, D. H.; Webb, H. M.; Bowers, M. T. J. Am. Chem. Soc. 1976, 98, 311, 318.
2. Brauman, J. I.; Blair, L. K. J. Am. Chem. Soc. 1969, 92, 2126.
3. Brauman, J. I.; Riveros, J. M.; Blair, L. K. J. Am. Chem. Soc. 1971, 93, 3911, 3914.
4. Henderson, W. G.; Taagepera, M.; Holtz, D.; McIver, Jr., R. T.; Beauchamp, J. L.; Taft, R. W. J. Am. Chem. Soc. 1972, 94, 4728.
5. Taft, R. W.; Taagepera, M.; Abboud, J. L. M.; Wolf, J. F.; DeFrees, D. J.; Hehre, W. J.; Bartmess, J. E.; McIver, Jr., R. J. J. Am. Chem. Soc. 1978, 100, 7765.
6. Yoder, C. S.; Yoder, C. H. J. Am. Chem. Soc. 1980, 102, 1245.
7. Marchington, A. F.; Moore, S. C. R.; Richards, W. G. J. Am. Chem. Soc. 1979, 101, 5529.
8. Ingold, C. K. Structure and Mechanism in Organic Chemistry 2nd ed., Cornell University Press, Ithaca, N. Y., 1969.
9. Levitt, L. S.; Widing, G. F. Progress in Physical Organic Chemistry 1976, 12, 119.
10. Previous indirect evidence has been provided for the hyperconjugative mechanism of ionization potential lowering by methyl groups: Houk, K. N.; McAlduff, E. J.; Mollere, P. D.; Strozler, R. W.; Chang, Y.-M. J. Chem. Soc., Chem. Comm. 1977, 141.
11. Taft, R. W.; Taagepera, M.; Abboud, J. L. M.; Wolf, J. F.; Defrees, D. J.; Hehre, W. J.; Bartmess, J. E.; McIver, Jr., R. T. J. Am. Chem. Soc. 1978, 100, 7765.
12. Dewar, M. J. S. Hyperconjugation Ronald Press Company, New York, 1962.
13. Baker, J. W. Hyperconjugation Oxford University Press, Fair Lawn, N. J., 1952.

14. Parker, W.; Tranter, R. L.; Watt, C. I. F.; Chang, L. W. K.; Schleyer, P. V. R. J. Am. Chem. Soc. 1974, 96, 7121.
15. Bingham, R. C.; Schleyer, P. V. R. J. Am. Chem. Soc. 1971, 93, 3189.
16. Shiner, Jr., V. J.; Murr, B. L.; Heinemann, G. J. Am. Chem. Soc. 1963, 85, 2413.
17. Shiner, Jr., V. J.; Jewett, J. G. J. Am. Chem. Soc. 1964, 86, 945.
18. Shiner, Jr., V. J.; Humphrey, Jr., J. S. J. Am. Chem. Soc. 1963, 85, 2416.
19. Karabatsos, G. J.; Sonnichsen, G. C.; Papaioannou, C. G.; Scheppele, S. E.; Shone, R. L. J. Am. Chem. Soc. 1967, 89, 463.
20. Kresge, A. J.; Preto, R. J. J. Am. Chem. Soc. 1967, 89, 5510.
21. Jewett, J. G.; Dunlap, R. P. J. Am. Chem. Soc. 1968, 90, 409.
22. DeFrees, D. J.; Hehre, W. J.; Sunko, D. E. J. Am. Chem. Soc. 1979, 101, 2323.
23. DeFrees, D. J.; Taagepera, M.; Levi, B. A.; Pollack, S. K.; Summerhays, K. D.; Taft, R. W.; Wolfsberg, M.; Hehre, W. J. J. Am. Chem. Soc. 1979, 101, 5532.
24. Schmidt, H.; Schweig, A. Angew. Chem. Int. Ed. Engl. 1973, 12, 307.
25. Turner, D. W.; Baker, C.; Baker, A. D.; Brundle, C. R. Molecular Photoelectron Spectroscopy Wiley-Interscience, New York, 1970.
26. Rabalais, J. W. Principles Of Ultraviolet Photoelectron Spectroscopy Wiley, New York, 1975.
27. Eland, J. H. D. Photoelectron Spectroscopy Butterworths, London, 1974.
28. Calson, T. A. Photoelectron And Auger Spectroscopy Plenum, New York, 1975.

29. Katrib, A. Libyan J. Sci. 1975, 4B, 35.
30. Aue, D. H.; Bowers, M. T. in Gas Phase Ion Chemistry Vol. II, Academic Press, New York, 1979, Ch. 9 and references therein.
31. Eliel, E. L.; Kandasamy, D.; Yen, C.-Y.; Hargrave, K. J. Am. Chem. Soc. 1980, 102, 3698.
32. Blackburne, I. D.; Katritzky, A. R.; Takeuchi, Y. Accts. Chem. Res. 1975, 8, 300.
33. Lambert, J. B.; Featherman, S. I, Chem. Rev. 1975, 75, 611.
34. Blackburn, I. D.; Duke, R. P.; Jones, R. A. Y.; Katritzky, A. R.; Record, K. A. F. J. C. S. Perkin Trans. II 1973, 332.
35. Eliel, E. L.; Vierhapper, F. W. J. Am. Chem. Soc. 1975, 97, 2424.
36. Crowley, P. J.; Robinson, M. J. T.; Ward, M. G. J. C. S. Chem. Comm. 1974, 825.
37. The Program GAUSSIAN 70, by Hahre, W. J.; Lathan, W. A.; Ditchfield, R.; Newton, M. D.; Pople, J. A., QCPE 236 (1973) was used for these calculations.
38. Smail, E. J.; Sheldrick, G. M. Acta Cryst. 1973, B29, 2027.
39. Allinger, N. L. J. Am. Chem. Soc. 1977, 99, 8127.
40. Profeta, Jr., S., Ph. D. Dissertation, University of Georgia, Athens, Georgia, 1978, and references therein.
41. We thank Professor William L. Jorgensen for the program used to generate these plots (QCPE 340).
42. Epiotis, N. D. Theory of Organic Reactions Springer-Verlag, New York, 1978.
43. Krueger, P. J.; Jan, J. Can. J. Chem. 1970, 48, 3229, 3236.
44. Profeta, Jr., S; Kollman, R. A.; Allinger, N. A. manuscript in preparation.

45. Bachler, V.; Olbrich, G. Theoret. Chim. Acta. (Berl.) 1980, 57, 329.
46. Potts, A. W.; Streets, D. G. J. C. S. Faraday Trans. II 1974, 875.
47. Murrell, J. N.; Schmidt, W. J. C. S. Faraday, Trans. II 1972, 1709.
48. Jorgensen, W. L.; Salem, L. The Organic Chemist's Book of Orbitals Academic Press, New York, 1973, and references therein.
49. Fleming, I. Frontier Orbitals and Organic Chemical Reactions Wiley, Chichester, 1976.
50. Sweigart, D. A.; Turner, D. W. J. Am. Chem. Soc. 1972, 94, 5599.
51. Kobayashi, T.; Nagakura, S. Bull. Chem. Soc. Japan 1973, 46, 1558.
52. Planckaert, A. A.; Doucet, J.; Sandorfy, C. J. Chem. Phys. 1974, 60, 4846.
53. Eliel, E. L.; Allinger, N. L.; Angyal, S. J.; Morrison, G. A. Conformational Analysis Wiley-Interscience, New York, 1965.
54. Rao, V. M.; Kewley, P. Can. J. Chem. 1969, 47, 1289.
55. Breed, H. E.; Gundersen, G.; Seip, R. Acta. Chem. Scand. 1979, 33A, 225.
56. Loudet, M.; Grimaud, M.; Metras, F.; Pfister-Guillouzo, G. J. Mol. Struct. 1976, 35, 213.
57. Cocksey, B. J.; Eland, J. H. D.; Danby, C. J. J. Chem. Soc. (B) 1971, 790.
58. Chadwick, D.; Frost, D. C.; Weiler, L. Tetrahedron Lett. 1971, 4543.
59. Rao, C. N. R.; Basu, P. K.; Hegde, M. S. Applied Spectroscopy Reviews 1979, 15, 1.

60. Hoffmann, R. Accts. Chem. Res. 1971, 4, 1.
61. Lectard, A.; Lichanot, A.; Metras, F.; Gaultier, J.; Hauw, C. Cryst. Struct. Comm. 1975, 4, 527.
62. Aue, D. H.; Webb, H. M.; Bowers, M. T. J. Am. Chem. Soc. 1975, 97, 4137.
63. Bodor, N.; Dewar, M. J. S.; Jennings, W. B.; Worley, S. D. Tetrahedron 1970, 36, 4109.

CHAPTER III. N-ARYLAZACYCLOALKANES

## INTRODUCTION

The influence of N-aryl substitution upon the solution basicities of azacycloalkanes (cyclic imines) has been studied by Searles and Seyedrezaei.<sup>1</sup> The basicities of aziridine and N-methylaziridine are ~3 pKa units lower than those of the azetidine, pyrrolidine, and piperidine analogs. This has been attributed to the high s character and low basicity of the aziridine nitrogen lone pair.<sup>1-3</sup> However, the N-phenyl derivatives show a curious anomaly. N-phenylpiperidine is ~2 pKa units less basic than the corresponding azetidine and pyrrolidine. Non-regular behavior is also observed for 2-tolyl-, 2,4-xylyl-, and 2,6-xylyl- derivatives. This unusual behavior may result from a complex interplay of hybridization, conformational effects, aryl  $\pi$ - $n_N$  lone-pair conjugation, and solvation differences for the different ring sizes and substitution patterns.

As the ring size is changed, the hybridization about the nitrogen can also change, and this can change the basicity in different ways.<sup>2-3</sup> On the one hand, maximum overlap can occur between a pure p-lone-pair orbital on nitrogen and the  $\pi$  orbitals of the aromatic ring; the resultant resonance delocalization will decrease the basicity of the amine. In opposition to this effect, as the amount of s character increases, the basicity is expected to decrease. The amount of overlap (conjugation) between the aromatic- $\pi$  orbitals and the amine lone-pair is depends on the conformation.

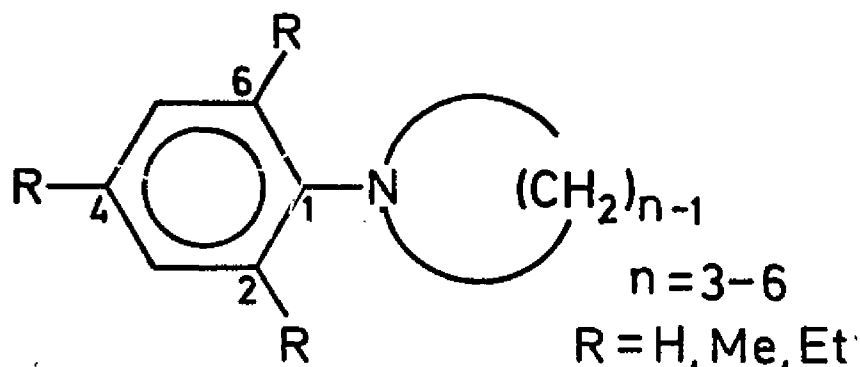
Rotation from a coplanar arrangement decreases the overlap. The hybridization about the nitrogen affects the amount of conjugation. As the amount of s character in the lone-pair orbital increases, the ability to conjugate with the aromatic  $\pi$  orbitals decreases. A pure p orbital would be parallel to the  $\pi$  orbitals, tilting toward a perpendicular orientation for sp hybridization. An s orbital would not overlap to any appreciable extent with the p orbitals of the aromatic ring.

Differences exist between observed solution and gas-phase basicities of amines. Solvation effects are assumed to be responsible for these differences, but are vague and hard to define, much less quantitate.

Photoelectron spectroscopy has been shown to be a sensitive probe for conjugation between two  $\pi$  systems, between a lone-pair and a  $\pi$  system, and thus of conformation.<sup>4</sup> Lone-pair ionization potentials are known to correlate with gas phase proton affinities.<sup>5</sup> Furthermore, Aue has reported a determination of the lone-pair hybridization from a determination of the photoelectron spectral line shape.<sup>6</sup> Thus, in principle, pes can isolate the important inherent conformational and electronic factors related to gas phase basicities, and by comparison to solution data, it is possible to determine the role of solvation on pKa's, as well. In order to identify some of these conformational and electronic factors present in aryl-substituted azacycloalkanes, we have examined the photoelectron spectra of the extensive series of arylazacyclo-



alkanes indicated below.



Particularly relevant to this study, the photoelectron spectra of a number of alkyl-substituted anilines have been studied previously. Cowling and Johnstone<sup>7</sup> assigned the first two ionizations in a series of anilines to the  $b_1$  and  $a_2$ -like orbitals of benzene, while the third band was presumed to arise from an ionization of the nitrogen lone-pair. Maier and Turner<sup>8</sup> reversed the assignments of the lone-pair and  $b_1$  orbitals. Our analysis,<sup>9</sup> which follows, is in agreement with the latter of these assignments.<sup>8,10</sup> For most anilines, three ionization potentials are observed below 11 eV. All three arise from  $\pi$ -like orbitals which may be formally derived from the nitrogen lone-pair and the degenerate HOMO's of benzene,<sup>11-12</sup> as shown in Figure 8.

The mixing, which occurs in the planar molecule, precludes the designation of any orbital of aniline as a pure "nitrogen lone-pair" orbital. For simplicity, however, we will refer to the HOMO based on its appearance in the spectra, as the "nitrogen lone-pair" ( $n_N$ ) orbital. It is typically a broad band. The other two

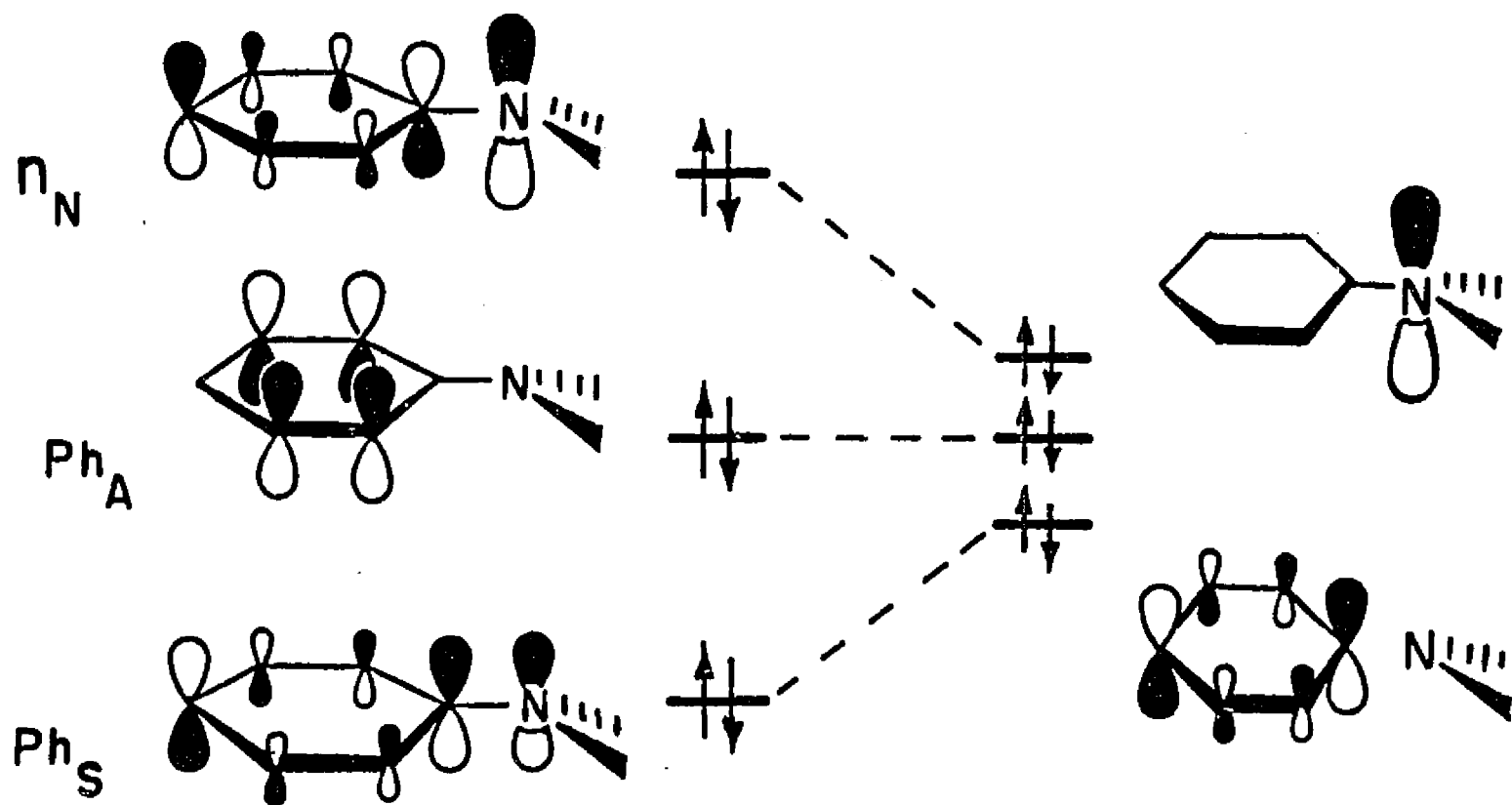


Figure 8. The Three Highest Occupied Molecular Orbitals of N-Arylazacycloalkanes.

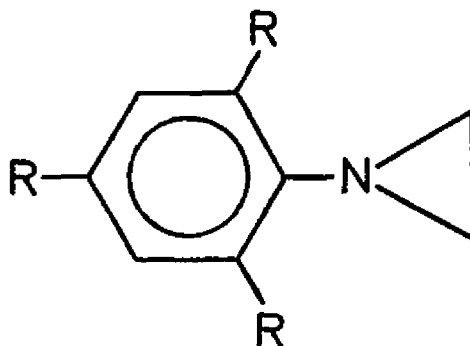
orbitals will be referred to as  $\text{Ph}_A$  ( $a_2$ ) and  $\text{Ph}_S$  ( $b_1$ ). These are the  $\pi$  orbitals primarily localized on benzene. They are antisymmetric (A) and symmetric (S) with respect to the symmetry plane perpendicular to the benzene ring. Methyl substituent(s) on the phenyl ring or rotation about the phenyl-N bond destroy the planar symmetry and allow additional orbitals to mix with each other, making these descriptions more qualitative, but still useful. As the nitrogen lone-pair is rotated toward a conformation in which the lone-pair is perpendicular to the plane of the benzene fragment, the contribution of  $\text{Ph}_S$  to  $n_N$ , and vice versa, will be less than when the two orbitals are coplanar.

Whereas the spectrum of N,N-dimethylaniline gives three bands at 7.45, 9.60, and 9.85 eV, indicative of planarity and similar to other anilines, the spectrum of N,N,2-trimethylaniline revealed some deviation from a planar conformation.<sup>8</sup> Although three low-energy IP's are observed, the first band was noticeably broadened, the second band had a slight increase in relative intensity, and the resolution between the second and third bands was noticeably decreased. The spectrum of N,N,2,6-tetramethylaniline revealed only two low-energy bands with a further intensity increase in the second band.

Maier and Turner<sup>8</sup> attempted to quantitate the degree of rotation present for these three N,N-dimethylanilines, based on the splitting between the first and third IPs. Planarity was assumed for N,N-dimethylaniline; the difference in IPs for the

$n_N$  orbital and the  $Ph_S$  orbital (2.40 eV) defined the maximum splitting possible for a planar, fully-conjugated species. The difference between the IP of trimethylamine (8.54 eV) and the second IP of toluene (9.25 eV) was used to define the minimum splittings expected for non-conjugated amine and aromatic orbitals. These parameters lead to the estimation of a 50-55° dihedral angle between the lone pair and the phenyl orbital for N,N,2-trimethylaniline and a 68-69° dihedral angle for N,N,2,6-tetramethylaniline, in reasonable agreement with other estimates.<sup>13-14</sup>

#### N-ARYLAZIRIDINES



The spectra of N-phenylaziridine and N-(2,6-xylyl)aziridine are shown in Figure 9 and the IPs are tabulated in Table 10, along with those of the other compounds studied here and appropriate models. The spectrum of N-(2,4-xylyl)aziridine is not shown, but is very similar in appearance to those in Figure 9. Three well-resolved bands are observed in the 7-11 eV region and are assigned to the  $n_N$ ,  $Ph_A$ , and  $Ph_S$  orbitals, respectively.

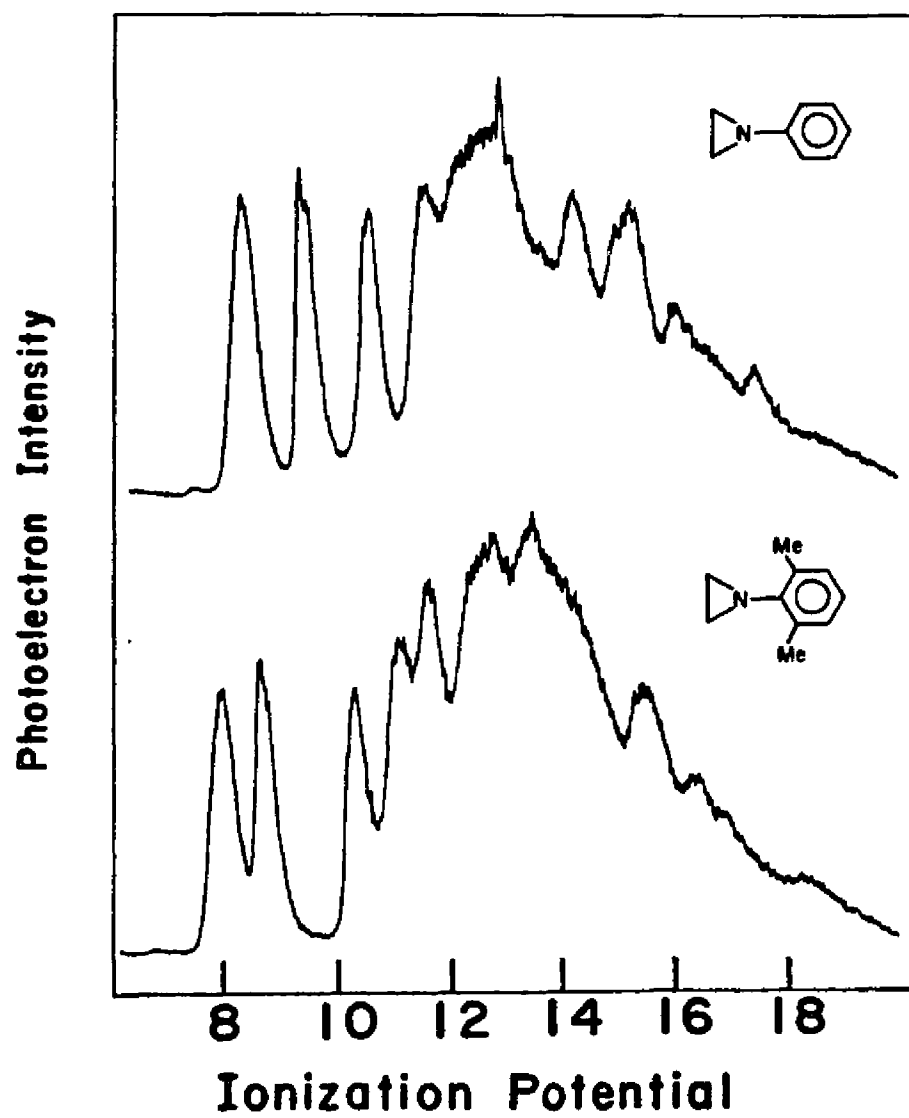
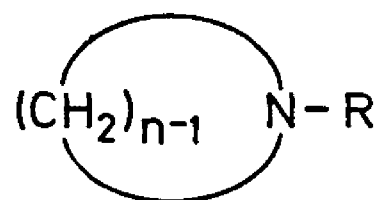


Figure 9. Photoelectron Spectra of *N*-phenylaziridine and *N*-(2,6-Xylyl)aziridine.

Table 10. Ionization Potentials<sup>a</sup> (eV) of Azacycloalkanes

<u>n</u>	<u>R</u>	<u>IP<sub>1</sub></u>	<u>IP<sub>2</sub></u>	<u>IP<sub>3</sub></u>
3	H	(9.80 <sup>b</sup> , 9.85 <sup>c</sup> )		
4	H	(9.04 <sup>b</sup> )		
5	H	(8.77 <sup>c</sup> )		
6	H	(8.66 <sup>b</sup> , 8.64 <sup>c</sup> )		
3	Me	(9.26 <sup>b</sup> )		
4	Me	---		
5	Me	(8.41 <sup>b,c</sup> )		
6	Me	(8.29 <sup>b,c</sup> )		
3	Phenyl	8.19	9.16	10.37
4	Phenyl	7.61	9.08	9.95
5	Phenyl	7.23	8.89	9.76
6	Phenyl	7.72	9.09	9.72
4	2-tolyl	7.67	8.78	9.80
5	2-tolyl	7.73	8.80	9.52
6	2-tolyl	7.84	8.81	9.28

Table 10. (continued)

<u>n</u>	<u>R</u>	<u>IP<sub>1</sub></u>	<u>IP<sub>2</sub></u>	<u>IP<sub>3</sub></u>
3	2,4-xylyl	7.80	8.70	9.93
4	2,4-xylyl	7.48	8.66	9.56
5	2,4-xylyl	7.60	8.66	9.21
6	2,4-xylyl	7.70	8.72	9.02
3	2,6-xylyl	7.88	8.57	10.17
4	2,6-xylyl	7.76	8.56	9.75
5	2,6-xylyl	7.67	8.51 <sup>d</sup>	8.51
6	2,6-xylyl	7.78	8.64 <sup>d</sup>	8.52
<u>N,N</u> -dimethylaniline		(7.37 <sup>e</sup> (7.48 <sup>f</sup> (7.45 <sup>g</sup>	8.96 9.06 9.06	9.80) 9.80) 9.85)
<u>N,N</u> ,2,4-tetramethyl- aniline		7.79	8.74	9.10
<u>N,N</u> ,2,6-tetramethyl- aniline		7.83 (7.85 <sup>g</sup>	8.61 8.60	8.93 8.85)
<u>N</u> -ethylaniline		7.67	9.10	10.20
2,6-diethylaniline		7.77	8.58	10.56
<u>N,N</u> ,2,6-tetraethyl- aniline		7.77	8.51 <sup>d</sup>	8.51

Table 10. (continued)

- a)  $\pm 0.06$  eV.
- b) References 5 and 6.
- c) Reference 15.
- d) Only one band is observed, resulting from both  $\text{Ph}_A$  and  $\text{Ph}_S$ .
- e) Reference 16.
- f) Reference 17.
- g) Reference 8.



The  $n_N$  band shape is narrower in the aziridines than in the larger ring size amines, as described later, and is indicative of minor geometry changes upon ionization. However, the first band is the broadest, and similar in appearance to those of the other amine lone-pair IPs.

The IP changes observed in these aziridines for all the low-energy orbitals as the methyl groups are added in differing locations to the phenyl ring are readily explained based on the coefficient sizes in the benzene orbitals. The para coefficients are largest in the  $n_N$  and  $Ph_S$  orbitals, while the ortho coefficients are largest in the  $Ph_A$  orbital for the planar species (cf. Figure 8). For the perpendicular species, the aromatic coefficients are zero in the  $n_N$  orbital.

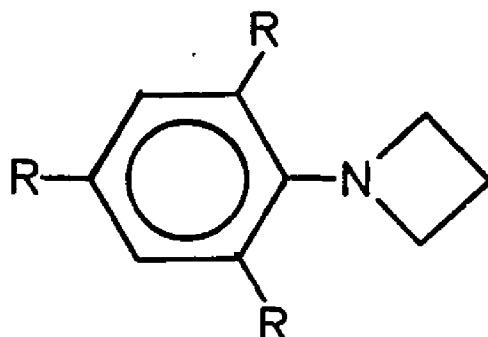
The  $n_N$  IP decreases from 8.19 eV in N-phenylaziridine to 7.80 eV for N-(2,4-xylyl)aziridine. The ortho-methyl group is at a site with a small coefficient, while the para-methyl group is at a large coefficient site. The  $n_N$  IP of N-(2,6-xylyl)aziridine at 7.88 eV is actually 0.08 eV higher than that of N-(2,4-xylyl)-aziridine (7.88 eV). Both methyl groups are now at small coefficient sites.

The  $Ph_A$  orbital experiences a 0.46 eV decrease in IP upon conversion of N-phenylaziridine (IP = 9.16 eV) to N-(2,4-xylyl)-aziridine (IP = 8.70 eV), and an additional 0.13 eV decrease in N-(2,6-xylyl)aziridine (IP = 8.57 eV). In the 2,6-xylyl derivative, both methyl groups are at large coefficient sites,

whereas the para-methyl group of the 2,4-xylyl derivative is located at a node.

The shifts in the  $\text{Ph}_S$  orbital IPs are in the same direction and slightly magnified compared to the shifts in the  $n_N$  IPs, providing support to the assignment of the HOMO as  $n_N$  and the THOMO as  $\text{Ph}_S$ . A 0.44 eV decrease in the  $\text{Ph}_S$  IP is observed upon conversion of N-phenylaziridine (10.37 eV) to N-(2,4-xylyl)aziridine (9.93 eV). The IP of N-(2,6-xylyl)-aziridine is actually raised 0.24 eV, relative to the 2,4-xylyl derivative (10.17 eV), since both methyls are now at small coefficient sites.

The trends in these aziridine  $n_N$  and  $\text{Ph}_S$  orbital IPs do not follow thoses observed for the substituted N,N-dimethyl-anilines, acyclic analogs of the aziridines, also listed in Table 10. The ortho-methyl group(s) cause a rotation about the phenyl-nitrogen bond in the anilines. The smaller aziridine C-N-C bond angle, and/or a different hybridization about the nitrogen decreases the steric requirement between the ortho substituents on the phenyl ring and the hydrogens attached to the carbons  $\alpha$  to the nitrogen, making rotation unnecessary. The band shapes remain sharp and well-resolved, in marked contrast to the ortho-methyl-anilines previously reported.

N-ARYLAZETIDINES

The spectra of N-phenylazetidine, N-(2-tolyl)azetidine, and N-(2,6-xylyl)azetidine are shown in Figure 10, and the IPs are tabulated in Table 10, along with those of N-(2,4-xylyl)azetidine and N-(2,6-diethylphenyl)azetidine. The spectrum of the 2,4-xylyl derivative is very similar to that of the tolyl derivative and the spectrum of the diethylphenyl compound is very similar to that of the 2,6-xylyl compound.

Three bands are still observed in all cases, and the assignments are the same as in the aziridines:  $\nu_N$ ,  $\text{Ph}_A$ , and  $\text{Ph}_S$ . The relative intensities and band widths are noticeably altered in two cases, N-(2,6-xylyl)azetidine and the 2,6-diethylphenyl analog. The increased intensity and band width of the middle band, the increased width of the first band, and the reduced intensity of the third band, all indicate the presence of multiple conformations in these species. A coplanar conformation gives rise to three well-resolved bands of nearly equal intensity, as in the N-phenylazetidine and the aziridines. Rotated, non-planar conformations give rise to unequal band intensities and over-

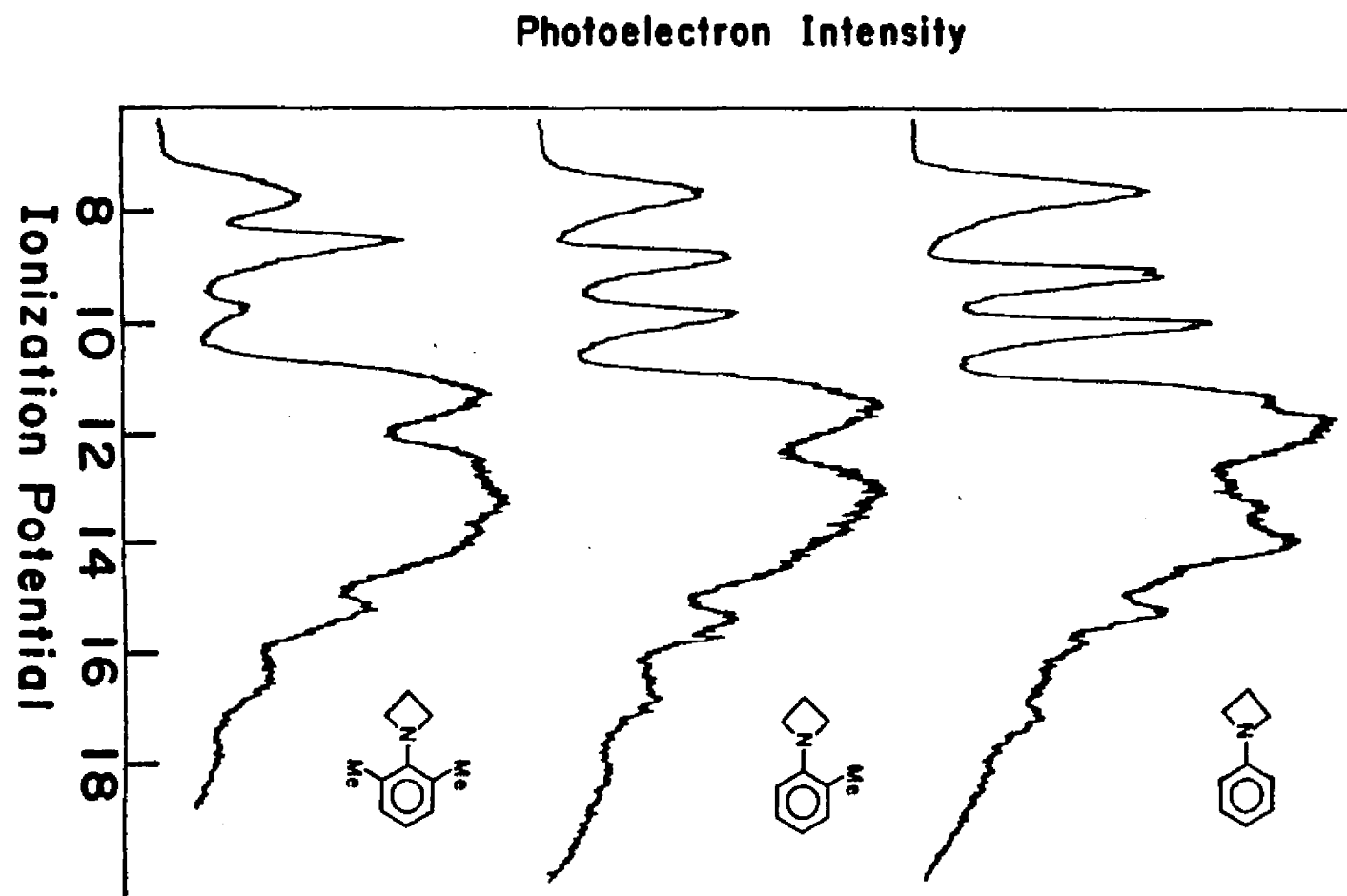


Figure 10. Photoelectron Spectra of N-Phenylazetidine, N-(2-Tolyl)azetidine, and N-(2,6-Xylyl)azetidine.

lapping  $\text{Ph}_A$  and  $\text{P}_S$  bands in the 2,6-substituted-phenyl derivatives.

The  $n_N$  IPs of conformations with differing rotational angles have different values due to differing contributions from the  $\text{Ph}_S$  orbital. Slight changes in the nitrogen lone pair hybridization are also possible, especially upon rotation, which would cause the ground state molecule to be bent further. Reorganization upon ionization would contribute toward a broader  $n_N$  band.

Introduction of an ortho-methyl group to N-phenylazetidine to form N-(2-tolyl)azetidine raises the  $n_N$  IP by 0.06 eV, an effect opposite to that anticipated based on the aziridine results. This apparent anomaly is the result of a small hyperconjugative lowering of the IP by the methyl group attached to the phenyl ring, counteracted by rotation to minimize the steric interaction between the azetidine ring and the hydrogens of the methyl group. Addition of the second methyl group to give N-(2,4-xylyl)azetidine does not affect the rotation, but does lower the  $n_N$  IP, since the para position is a large coefficient site.

When two ortho methyl groups are introduced to form N-(2,6-xylyl)azetidine, the  $n_N$  orbital has a higher IP than the N-phenyl-, N-(2-tolyl)-, or N-(2,4-xylyl)azetidine derivatives. This must result from an even greater degree of rotation about the phenyl-nitrogen bond, since ortho-methyls would otherwise decrease

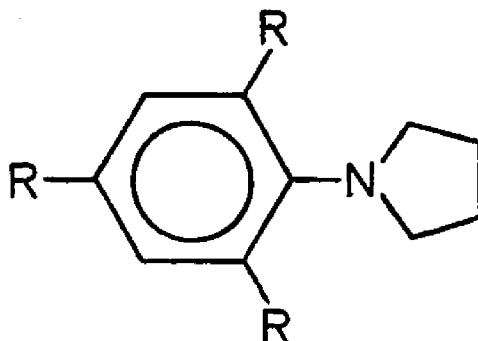
the  $n_N$  IP, relative to N-phenylazetidine. The  $n_N$  IP of N-(2,6-diethylphenyl)azetidine was determined to be only 0.06 eV lower than the corresponding methyl derivative. Within experimental error, these values can be considered equal. The tendency toward a lower IP in the 2,6-diethylphenyl derivative is due to the slightly greater electron donation by ethyl than by methyl groups. Both of these compounds are significantly non-planar.

The magnitudes of the  $Ph_A$  IP decreases are very nearly the same as those observed for the corresponding aziridines. Upon conversion of N-phenylazetidine (IP = 9.08 eV) to N-(2,4-xylyl)-azetidine (IP = 8.66 eV), a decrease of 0.42 eV is observed. Conversion to N-(2,6-xylyl)azetidine (IP = 8.56 eV) results in an additional 0.10 eV decrease.

The trends in the  $Ph_S$  IPs are also the same as those of the corresponding aziridines, and the magnitudes of the substituent effects are very similar. An ortho methyl group causes a 0.15 eV decrease; addition of a para methyl group to form the 2,4-xylyl derivative decreases the IP an additional 0.24 eV; moving the para methyl group to the ortho' position to give the 2,6-xylyl derivative raises the IP by 0.19 eV. Rotation of the aryl group is expected to decrease the IP of the  $Ph_S$  orbital, but no large effect is seen. The loss of conjugation is somewhat counteracted by the change in the size of the orbital coefficient. That is, rotation causes the THOMO ( $Ph_S$ ) to become more

heavily localized on the phenyl ring, and thus to be influenced more by methyl substitution than the HOMO (lone-pair).

#### N-ARYLPYRROLIDINES



The spectra of N-phenylpyrrolidine, N-(2-tolyl)pyrrolidine, and N-(2,6-xylyl)pyrrolidine are shown in Figure 11, and the IPs are tabulated in Table 10. The spectrum of N-(2,4-xylyl)-pyrrolidine is similar to that of the 2-tolyl derivative; the spectrum of N-(2,6-diethylphenyl)pyrrolidine is similar to that of the 2,6-xylyl derivative. The spectrum of N-phenylpyrrolidine is very similar to that of the aziridines and N-phenylazetidine, as described earlier, and the three low-energy IPs are assigned as before to the  $n_N$ ,  $Ph_A$ , and  $Ph_S$  orbitals. The spectra of N-(2-tolyl)pyrrolidine and N-(2,4-xylyl)pyrrolidine are similar to that of N-(2,6-xylyl)azetidine, indicating non-planarity and multiple conformations of similar energy. The  $n_N$  band is noticeably broadened, and the intensity of the center band is increased due to rotation about the phenyl-nitrogen bond.

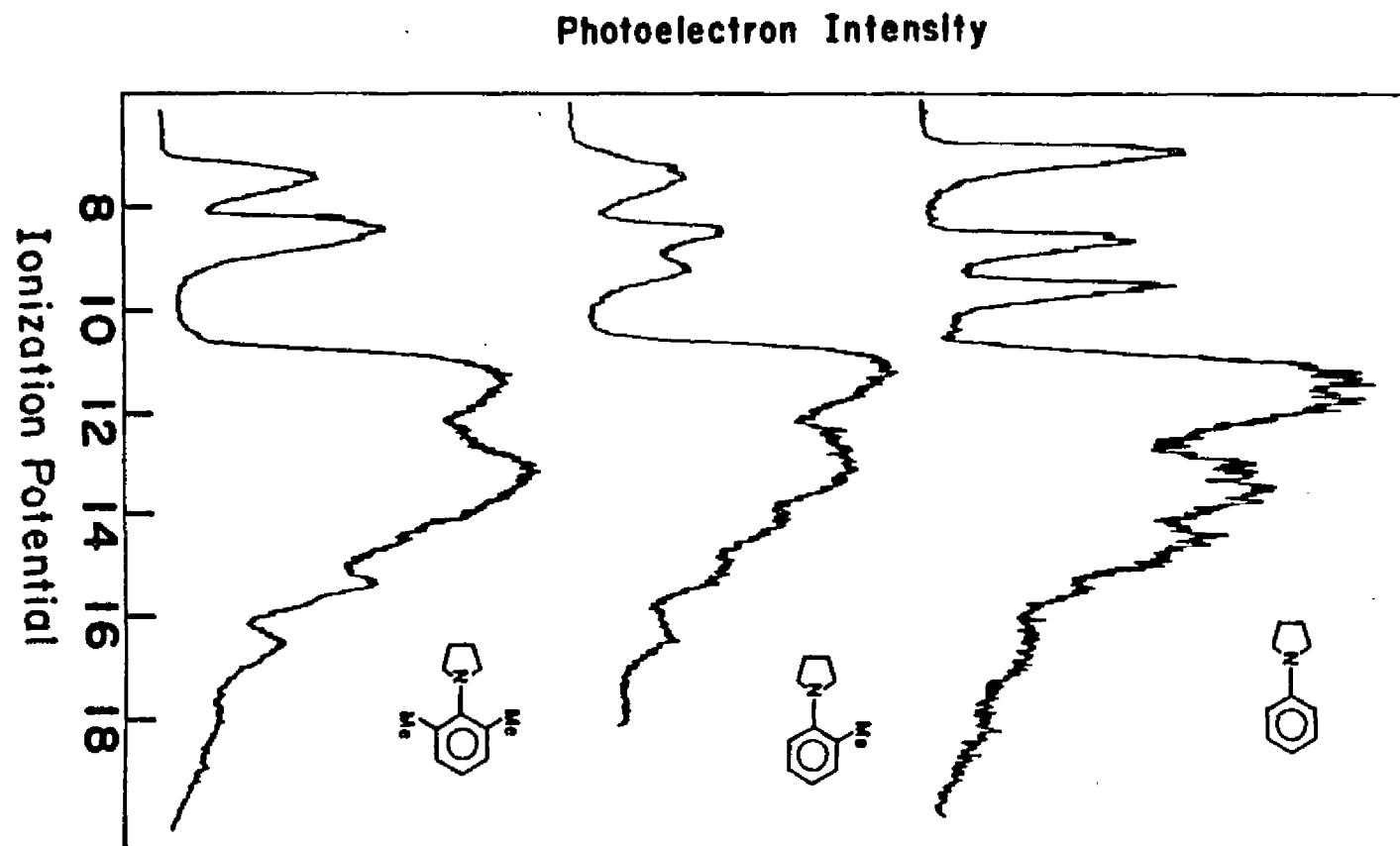


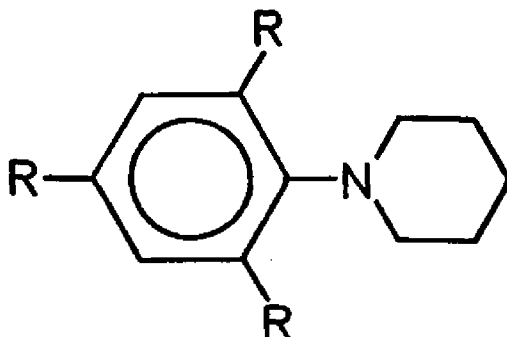
Figure 11. Photoelectron Spectra of N-Phenylpyrrolidine, N-(2-Tolyl)pyrrolidine, and N-(2,6-Xylyl)pyrrolidine.



A 0.50 eV decrease in the  $n_N$  IP is observed upon conversion of N-phenylpyrrolidine (IP = 7.23 eV) to N-(2-tolyl)-pyrrolidine (IP = 7.73 eV), followed by an additional 0.13 eV decrease when a second, para methyl group is added, slightly less than that observed in the corresponding azetidine.

Relative to N-phenylpyrrolidine, the  $Ph_A$  IP decreases 0.09 eV for the 2-tolyl derivative and an additional 0.14 eV for the 2,4-xylyl derivative. The  $Ph_S$  decreases are 0.16 eV and 0.31 eV respectively for these two derivatives.

In N-(2,6-xylyl)- and N-(2,6-diethylphenyl)pyrrolidine, only two bands are resolved, indicative of a greater degree of rotation about the phenyl-nitrogen bond. The  $n_N$  IP increases 0.07 eV, compared to the 2,4-xylyl compound, and decreases 0.07 eV due to the enhanced effect of ethyl compared to methyl.  $Ph_A$  and  $Ph_S$  have merged in both compounds. The expected increase in the  $Ph_S$  IP as the methyl group is moved to the ortho' position is strongly counteracted by the loss of conjugation between the lone pair and the aromatic orbitals. The degree of rotation is considerably greater than that observed for N-(2,6-xylyl)azetidine.

N-ARYLPYPERIDINES

The spectra of N-phenylpyperidine, N-(2-tolyl)pyperidine, and N-(2,6-xylyl)pyperidine are shown in Figure 12. The IPs are tabulated in Table 10, along with those of N-(2,4-xylyl)pyperidine whose spectrum is similar to that of the 2-tolyl derivative. The spectrum of N-phenylpyperidine has three low-energy IPs assigned with the same order as before. The  $n_N$  band is broadened relative to those of the planar N-phenyl amines described previously. The second and third bands overlap slightly and are decidedly less sharp than those previous. Thus, even N-phenylpyperidine appears to be non-planar.

A comparison of the  $n_N$  IPs of all these pyperidines shows that the lone pair IP is relatively insensitive to the presence of methyl substituents on the phenyl ring. Using the data and trends previously presented, this behavior appears consistent only if a rotation from planarity is postulated in all cases, including N-phenylpyperidine. An ortho-methyl substituent causes further phenyl-nitrogen bond rotation, reducing the interaction between

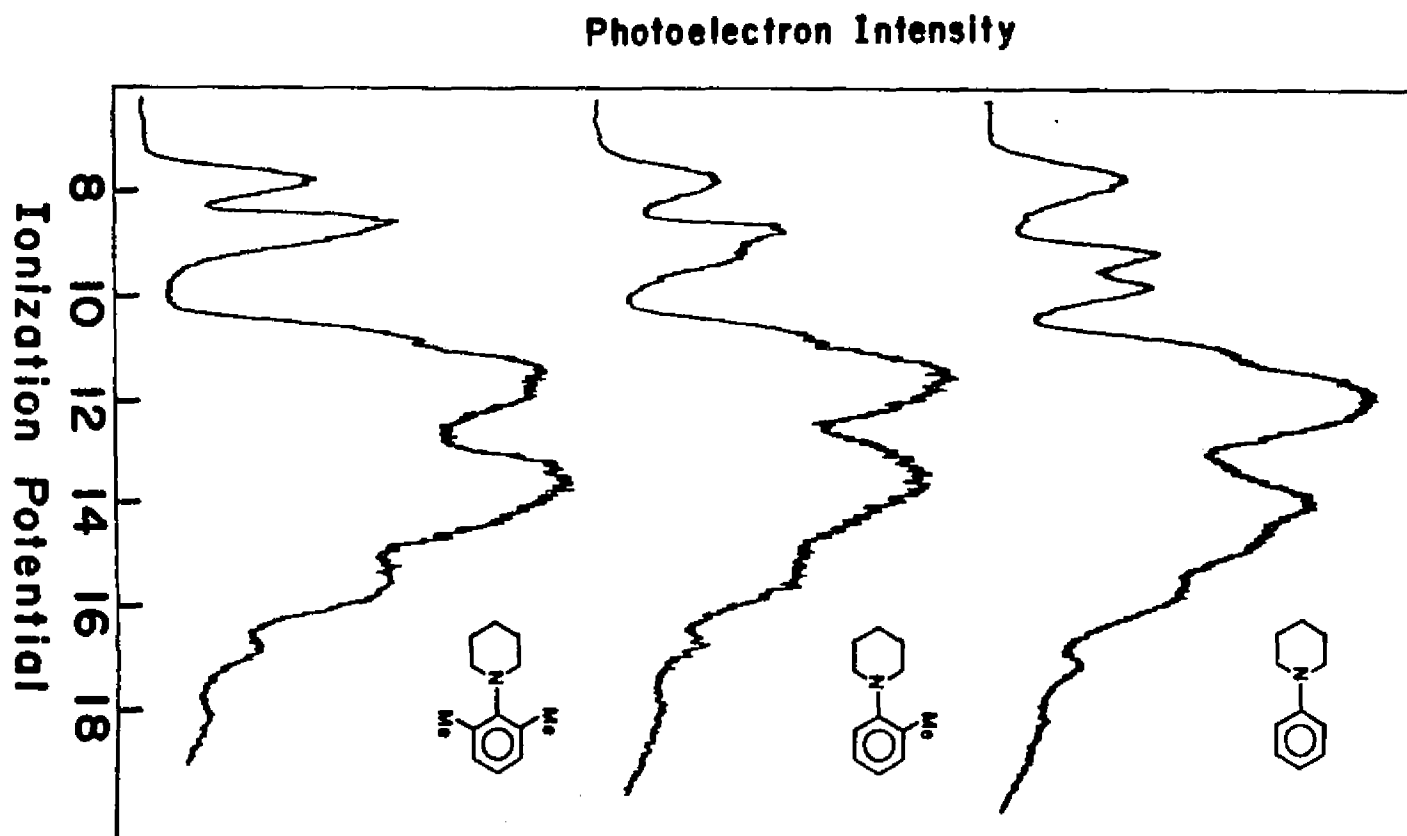


Figure 12. Photoelectron Spectra of N-Phenylpiperidine, N-(2-Tolyl)piperidine, and N-(2,6-Xylyl)piperidine.

$n_N$  and  $Ph_S$ , and the IP increases by 0.12 eV. A para-methyl lowers the IP 0.14 eV through hyperconjugation without causing further rotation. Moving the second methyl substituent to the ortho' position forces the amine ring to rotate further, and the IP again increases as a result of the diminished interaction. The continual decrease and merging of the  $Ph_A$  and  $Ph_S$  orbitals upon methylation also indicate a decreasing interaction between  $Ph_S$  and the nitrogen lone-pair.

As an aid to these interpretations of conformation, ab initio STO-3G calculations were carried out on N,N-dimethylaniline using standard bond lengths and bond angles. The dihedral angle between the nitrogen lone-pair and the phenyl  $\pi$  orbitals was varied from  $0^\circ$  (coplanar) to  $90^\circ$  (perpendicular) in  $10^\circ$  increments. The orbital order, according to calculations, is  $Ph_S$ ,  $Ph_A$ , and  $n_N$ , and the effects of rotation on the various orbitals are shown in Figure 13. The ordering of the  $Ph_S$  and  $n_N$  orbitals is believed to be reversed from the order observed in the spectra, based on the IPs of trimethylamine (8.54 eV) and benzene (9.25 eV), which indicate that the nitrogen lone-pair of a tertiary amine should be lower than the phenyl  $\pi$  orbitals. The trends observed for the orbital energies as the dimethylamino group is rotated remain relevant. The HOMO energy is highest for the planar conformation and decreases in energy as rotation occurs, with a minimum at the perpendicular conformation (Figure 13). The

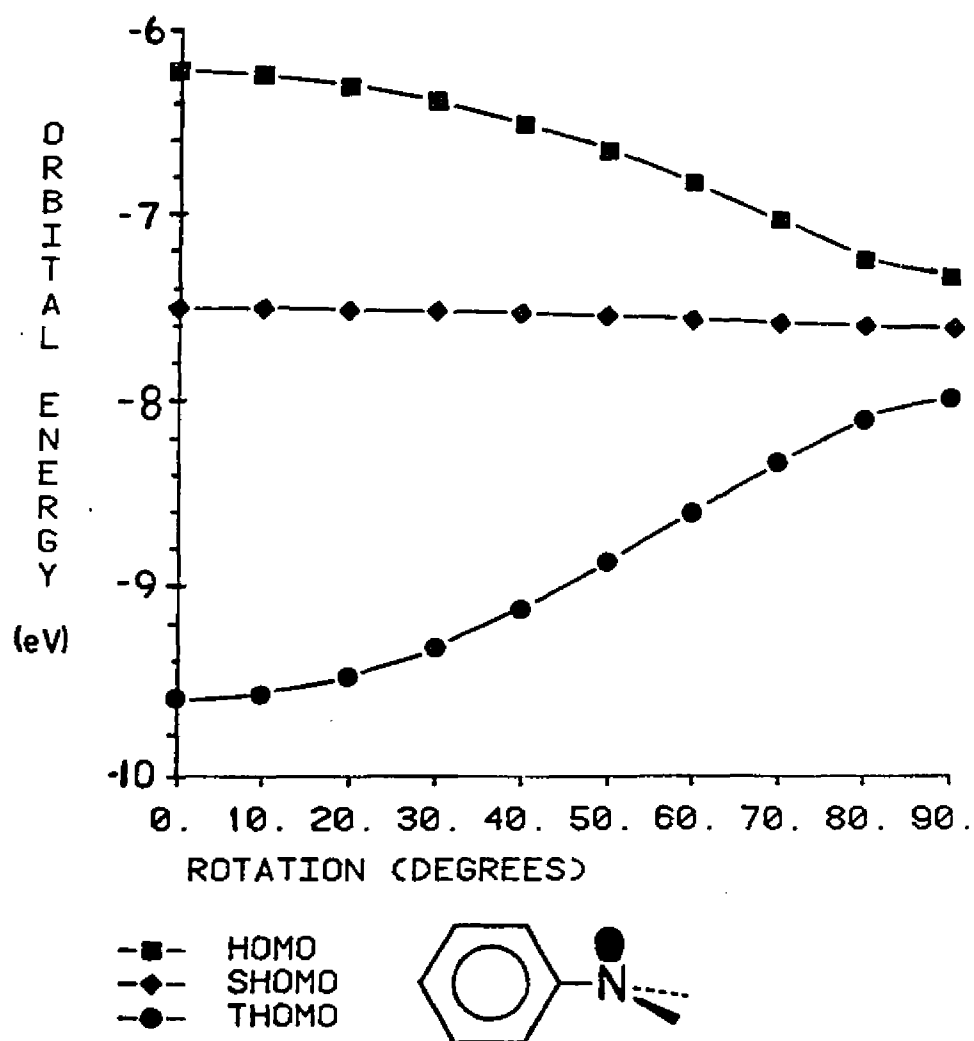


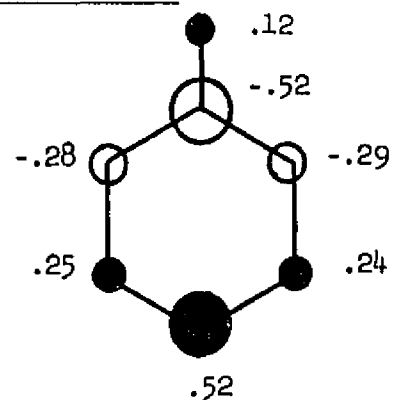
Figure 13. STO-3G Orbital Energies as a Function of Rotational Angle.

SHOMO energy changes only slightly as the dihedral angle changes, since the nitrogen is attached to a nodal site in  $\text{Ph}_A$ . The third highest occupied molecular orbital (THOMO) energy is at a maximum for the planar conformation and decreases upon rotation. Even though the calculated order is incorrect, the same trends in the IPs should result.  $\text{Ph}_S$  and  $n_N$  mixing and separation is maximized in the planar conformation and minimal in the perpendicular conformation. This is readily apparent in the calculated molecular orbital coefficients shown in Figure 14 for coplanar (conjugating) and perpendicular (nonconjugating) N,N-dimethylaniline.

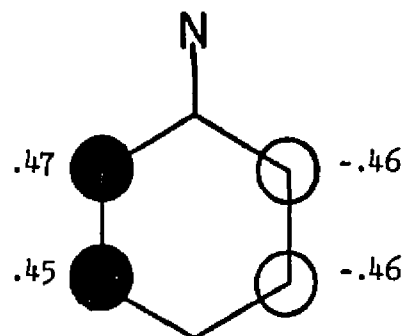
#### DETERMINATION OF CONFORMATIONS

The band shapes and ionization potentials observed in the photoelectron spectra lead to the qualitative conclusions summarized in Table 11 by the indications "coplanar" or "non-coplanar". The dashed line separates the coplanar and non-coplanar species. In order to provide a more quantitative estimate of the degree of non-planarity in these compounds, we have used a technique similar to that of Maier and Turner.<sup>8</sup> The maximum splits between  $n_N$  and  $\text{Ph}_S$  were taken from the spectra of N-phenylazetidine and N-phenylpyrrolidine, and including an extrapolation for N-phenylpiperidine, to be 2.34, 2.53, and 2.64 eV, respectively. The minimum splits, expected for the perpendicular

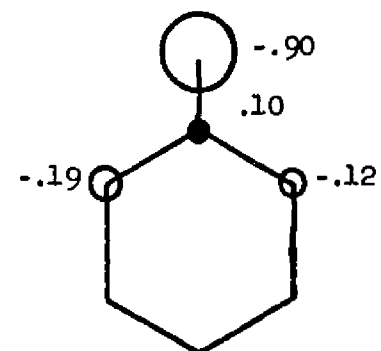
PERPENDICULAR



HOMO



SHOMO



THOMO

COPLANAR

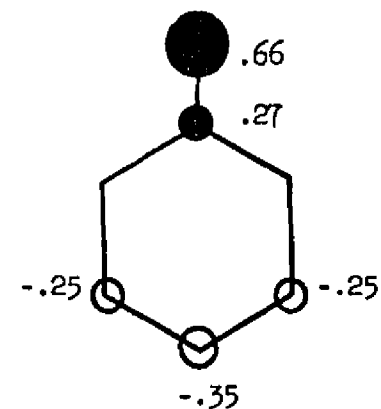
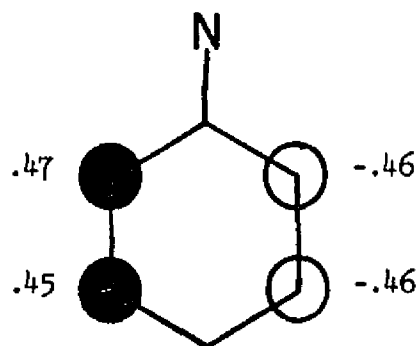
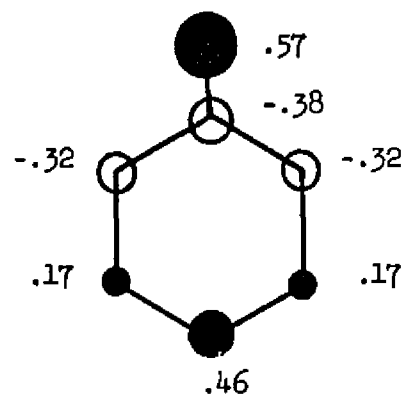
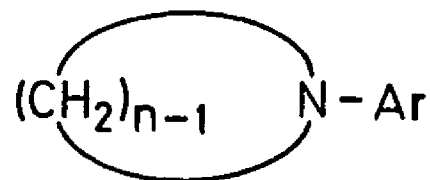


Figure 14. STO-3G Orbital Coefficients of N,N-Dimethylaniline in Perpendicular and Coplanar Conformations.

Table 11. Conformations of N-Arylazacycloalkanes.



Substituent	Ring Size			
	3	4	5	6
Phenyl	coplanar (0°)	coplanar (0°)	coplanar (0°)	non-coplanar (48°)
2-tolyl	b	coplanar (23°)	non-coplanar (52°)	non-coplanar (68°)
2,4-xylyl	coplanar (0°)	coplanar (28°)	non-coplanar (58°)	non-coplanar (72°)
2,6-xylyl	coplanar (0°)	non-coplanar (33°)	non-coplanar (81°)	non-coplanar (85°)

a) "Coplanar" or "non-coplanar" were determined from band shapes and substituent effects. Degrees given in parentheses were determined, based on the difference in IP between IP( $n_N$ ) and IP(Ph<sub>5</sub>), as discussed in the text. See also reference 8.

b) This compound was not available, but it is presumed to be coplanar.



conformations, were taken as the difference between the lone-pair IP of N-methylazetidine, N-methylpyrrolidine, and N-methylpiperidine, and the second IP of toluene (9.25 eV). This resulted in points parallel to those observed by Maier and Turner for the N,N-dimethylanilines. Assuming a  $\cos\theta$  relationship between the change in IP and the angle,  $\theta$ , between the lone-pair and the aromatic  $\pi$  orbitals, the numerical values given in Table 11 were found. Although they are only approximate, these angles do give a quantitative idea of the preferred angle of rotation for the non-planar species. N-(2-Tolyl)- and N-(2,4-xylyl)azetidine are the only two compounds for which the conformation, as deduced from the spectral line shape, differs from the conformation determined by the difference between the  $n_N$  and  $Ph_g$  IPs. With reference to Figure 13, the minimum degree of rotation from planarity required to cause significant changes in the IPs appears to be ca. 30°; thus, the angle predicted from the line shapes of N-(2-tolyl)- and N-(2,4-xylyl)azetidine (23° and 28°) is in a region where minor angle changes may have a major impact on the spectral line shape.

#### PROTON AFFINITIES

Finally, we can use the  $n_N$  IPs determined here to estimate the gas-phase proton affinities of these compounds. For the parent azacycloalkanes and N-methyl derivatives included in Table 10, there is a reasonable ( $r=0.996$ ) linear correlation between proton

affinity and IP:  $PA(\text{kcal/mole}) = 296.1 - 8.13IP(\text{eV})$ . However, the predicted PA for N,N-dimethylaniline (255.5 kcal/mole) is 11.7 kcal/mole too high. In classical terms, this must be due to the resonance stabilization of aniline which is interrupted upon protonation. In molecular orbital terms, the HOMO is no longer a localized orbital in aniline as it is in alkylamines; thus, the PA is not as high for aniline as it is for a saturated amine with an identical IP. There is also some indication that anilines are protonated on the aromatic ring, not on the nitrogen.<sup>8</sup>

For perpendicular N-arylazacycloalkanes, we can use the correlation given above to estimate the proton affinities, while the planar species are expected to have PAs 11.7 kcal/mole lower. In order to provide a single estimate of PA as a function of both IP and rotational angle, we have defined the following equation:

$$PA(\text{est.}) = 296.1 - 8.13 IP_1 - 11.7\cos\theta$$

where  $IP_1$  is the first IP of the N-arylazacycloalkane, and  $\theta$  is the angle of rotation ( $\theta = 0^\circ$  for a planar species). Using the values of  $\theta$  listed in Table 11, the PAs listed in Table 12 are obtained.

These predicted PAs qualitatively follow the order of measured  $pK_a$ s ( $\pm 1 pK_a$  unit) with three notable exceptions, N-phenylpyrrolidine, N-(2,4-xylyl)azetidine, and N-(2,6-xylyl)-

Table 12. Experimental and Calculated Proton Accepting Properties of Azacycloalkanes.<sup>a</sup>



<u>n</u>	<u>R</u>	<u>pK<sub>a</sub></u>	<u>Δv<sup>b</sup></u>	<u>PA (exp)<sup>c</sup></u>	<u>PA (calc)<sup>d</sup></u>
3	H	8.04	221	215.7	
4	H	11.29	259	222.7	
5	H	11.27	262	224.3	
6	H	11.22	259	225.4	
3	Me	7.86	269	221.5	
4	Me	10.40	293		
5	Me	10.46	292	227.8	
6	Me	10.08	287	228.8	
3	Phenyl	1-2	198		218
4	Phenyl	3.62	174		222
5	Phenyl	3.57	172		226
6	Phenyl	5.22	180		226
4	2-tolyl	3.97	181		223
5	2-tolyl	5.01	187		226
6	2-tolyl	4.68	184		228

Table 12. (continued)

<u>n</u>	<u>R</u>	<u>pK<sub>a</sub></u>	<u>Δv<sup>b</sup></u>	<u>PA (exp)<sup>c</sup></u>	<u>PA (calc)<sup>d</sup></u>
3	2,4-xylyl	2.	205		221
4	2,4-xylyl	4.31	188		225
5	2,4-xylyl	5.28	196		228
6	2,4-xylyl	5.02	186		230
3	2,6-xylyl	3.48	208		220
4	2,6-xylyl	4.64	196		223
5	2,6-xylyl	4.81	188		232
6	2,6-xylyl	3.44	187		232
Ammonia		9.21 <sup>e</sup>		205.0	
Methylamine		10.62 <sup>e</sup>		214.1	
Aniline		4.6 <sup>e</sup>		211.5	
Dimethylamine		10.64 <sup>e</sup>		220.5	
Trimethylamine		9.76 <sup>e</sup>		224.3	
N,N-dimethyl- aniline		4.26	165	223.8	

=====

a) Reference 1, unless otherwise noted.

b)  $\text{cm}^{-1} \pm 2 \text{ cm}^{-1}$ .

c) Reference 18, kcal/mole.

d) estimated from the equation  $\text{PA} = 296.1 - 8.13(\text{IP}) - 11.7\cos\theta$ .

e) Reference 19.

piperidine, all of which have  $pK_a$ s  $\sim 2$   $pK_a$  units too low. The remaining compounds seem to have maximum  $pK_a$ s of about 5.5, even when the estimated PAs are quite high, which can be attributed to steric hindrance to solvation of the ammonium cations. Of the three compounds noted above with especially low  $pK_a$ s, only the last would seem to provide especially high steric hindrance to solvation.

#### CONCLUSION

The pes studies have shown that the conformations of the N-arylazacycloalkanes may be quite different for different amine ring sizes. Furthermore, the conformations of the aryl group with respect to the amine lone-pair influence not only the IP, but also gas phase proton affinities, and solution  $pK_a$ s because of steric hindrance to solvation of ammonium cations.

REFERENCES

1. Seyedrezai, S. E., Ph.D. Dissertation, University of Missouri-Columbia, Missouri, 1980, and references therein.
2. Bottini, A. T.; Nash, C. P. J. Am. Chem. Soc. 1962, 84, 734.
3. Wepster, B. M. in Progress in Stereochemistry Vol. II, ed. by Klyne and de la Mare, Academic Press, New York, 1958, Chapter 4.
4. Klessinger, M.; Raademacher, P. Angew. Chem. Int. Ed. Engl. 1979, 18, 826, and references therein.
5. Aue, D. H.; Webb, H. M.; Bowers, M. T. J. Am. Chem. Soc. 1976, 98, 311, 318.
6. Aue, D. H.; Webb, H. M.; Bowers, M. T. J. Am. Chem. Soc. 1975, 97, 4136, 4137.
7. Cowling, S. A.; Johnstone, R. A. W. J. Electron Spectrosc. Relat. Phenom. 1973, 2, 161.
8. Maier, J. P.; Turner, D. W. J. C. S. Faraday Trans. II 1973, 69, 521.
9. Rozeboom, M. D.; Houk, K. N.; Searles, Jr., S.; Seyedrezai, S. E. J. Org. Chem. submitted for publication.
10. Schafer, W.; Schweig, A. Angew. Chem. Int. Ed. Engl. 1972, 11, 836.
11. Rabalais, J. W. Principles of Ultraviolet Photoelectron Spectroscopy Wiley-Interscience, New York, 1977.
12. Turner, D. W.; Baker, C.; Baker, A. D.; Brundle, C. R. Molecular Photoelectron Spectroscopy Wiley, London, 1970.
13. Kleven, H. B.; Platt, J. R. J. Am. Chem. Soc. 1948, 71, 1714.
14. Katritzky, A. R.; Topsom, R. D. Angew. Chem. Int. Ed. Engl. 1970, 9, 87.
15. Yoshikawa, K.; Hashimoto, M.; Morishima, I. J. Am. Chem. Soc. 1974, 96, 228.

16. Kobayashi, T.; Nagakura, S. Bull. Chem. Soc., Japan 1974, 47, 2563.
17. Egdell, R.; Green, J. C.; Rao, C. N. R. Chem. Phys. Lett. 1975, 33, 600.
18. Aue, D. A.; Bowers, M. T. in Gas Phase Ion Chemistry Vol. II, Academic Press, New York, 1979, Ch. 9.
19. Arnett, E. M. Prog. Phys. Org. Chem. 1963, 1, 223 (319 for numbers).

## CHAPTER IV. PHENCYCLIDINES



## INTRODUCTION

Phencyclidine [N-(1-phenylcyclohexyl)piperidine, PCP, or angel dust] and close analogs have become major drugs of abuse. Originally introduced as a general anesthetic, phencyclidine has been found to be a potent psychotomimetic, which exacerbates psychopathologies.<sup>1</sup> Phencyclidine and its analogs are weakly bound by rat brain muscarinic and opiate receptors.<sup>2</sup> There have also been reports of the existence of a rat brain membrane receptor which is specific for phencyclidine and its analogs, but does not show significant binding to other common biogenic amines, such as neurotransmitters, neurotransmitter agonists and antagonists, amino acids, peptides, or benzodiazepines.<sup>3</sup> However, Maayani and Weinstein have shown that the rapid filtration technique used to substantiate the specific receptor hypothesis produces artifacts;<sup>4</sup> there is no remaining experimental evidence to prove that a specific receptor exists for phencyclidine.

Through quantum mechanical studies, Weinstein et al. have shown electronic similarities between phencyclidine and acetylcholine which are suggested to lead to anticholinergic properties of the phencyclidines (Figure 15).<sup>5</sup> In particular, the trimethylammonio group of acetylcholine and the protonated nitrogen of phencyclidine provide similar regions of positive charge which can coordinate with a negatively charged, or electron rich, site of the muscarinic receptor; the ester oxygen of the

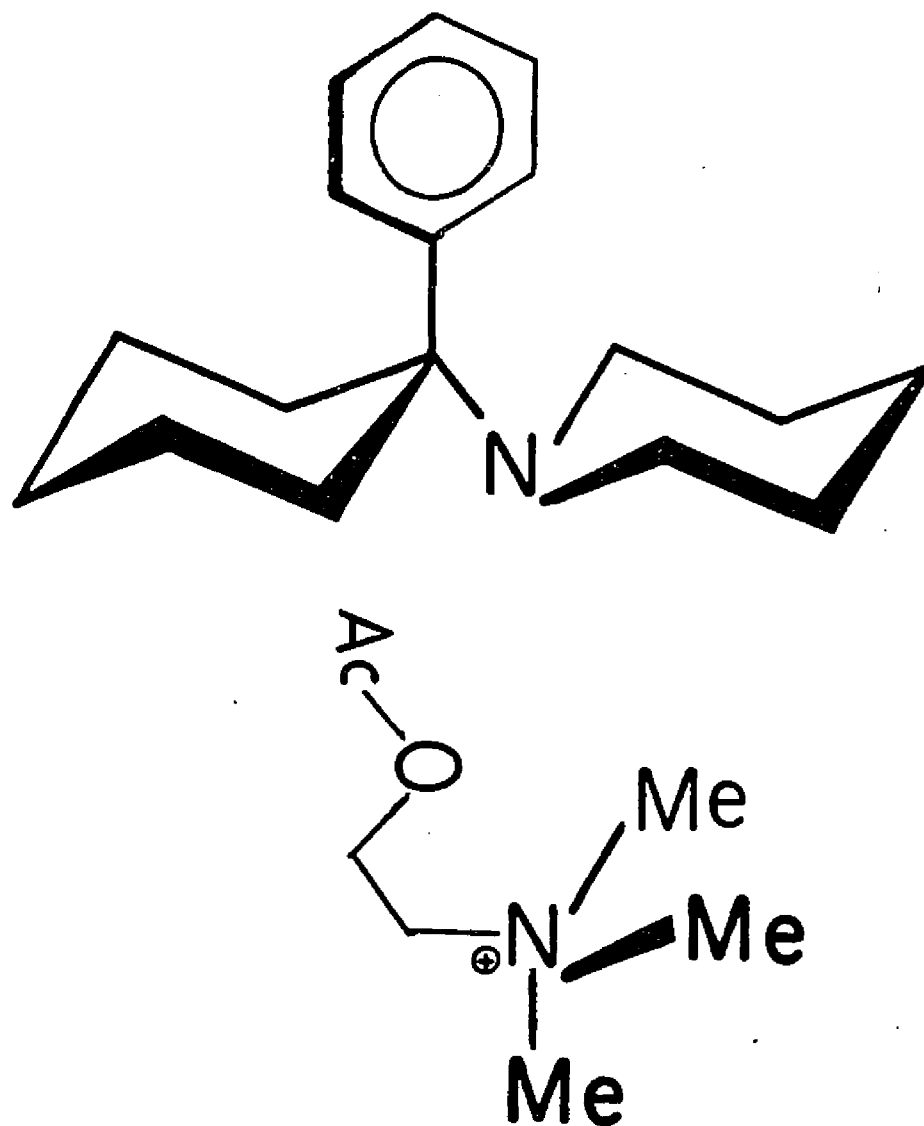


Figure 15. The Similarities Between Acetylcholine and PCP. The Protonated Nitrogen of the Piperidinium Moiety Mimics the Trimethyl-ammonium Moiety of Acetylcholine, while the Phenyl  $\pi$ -Cloud Resembles the Electron-rich Region About the Acetoxy Oxygen.

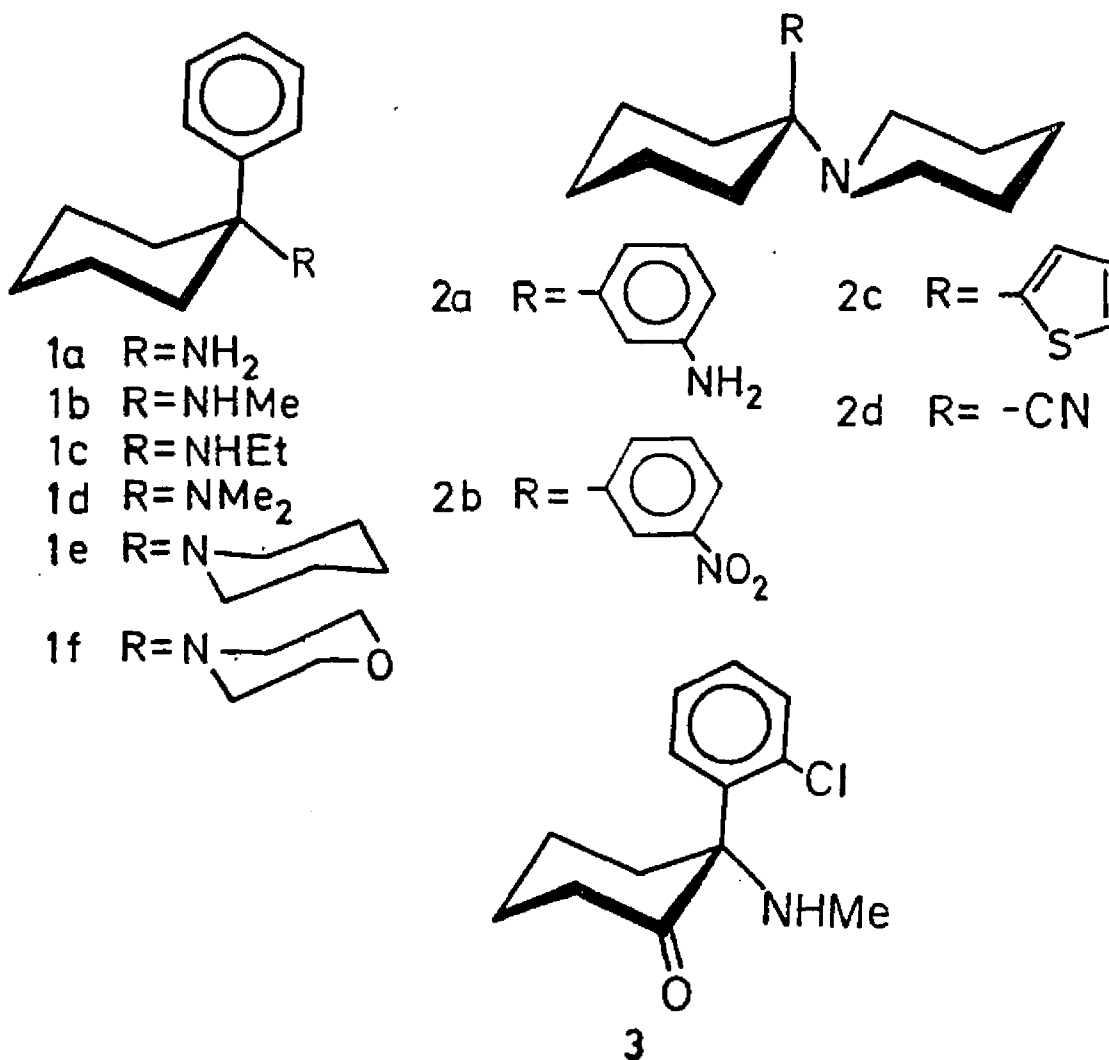
acetoxy group in acetylcholine, and the aromatic ring of phencyclidine and its derivatives provide similar regions of attraction for electron deficient sites in the receptor. Because of the similar dispositions of the positive and negative regions in space for both acetylcholine and phencyclidine, these molecules have a common muscarinic receptor interaction pharmacophore, and both types of molecules may bind to the muscarinic receptor.<sup>5</sup>

Analogues of phencyclidine with electron rich moieties, such as the thienyl or ethynyl groups, exhibit interaction pharmacophores, determined by quantum mechanical calculations, and pharmacological properties similar to those of the parent phencyclidine. If a sterically similar, but electron deficient group, such as a nitrile, is substituted for the phenyl moiety, activity decreases, which is attributed to the grossly altered regions of attraction for electrophilic moieties by the nitrile. Addition of an electron donating amino group to the phenyl ring of phencyclidine enhances binding and behavioral potency (in rats), while the addition of an electron withdrawing nitro group diminishes in vitro and in vivo activities.<sup>6</sup>

To acquire experimental information about the electronic structures of phencyclidines, we have studied the photoelectron spectra of phencyclidine and several analogs. As described in detail elsewhere,<sup>7</sup> this technique affords quantitative information on the electron donor properties of various parts of a molecule, and can also provide conformational information in some cases.

PHOTOELECTRON SPECTRA

The photoelectron spectra of PCP and a number of its analogs as shown below have been examined and are displayed in Figures 16, 17, and 18. The low-energy IPs are assembled in Table 13.



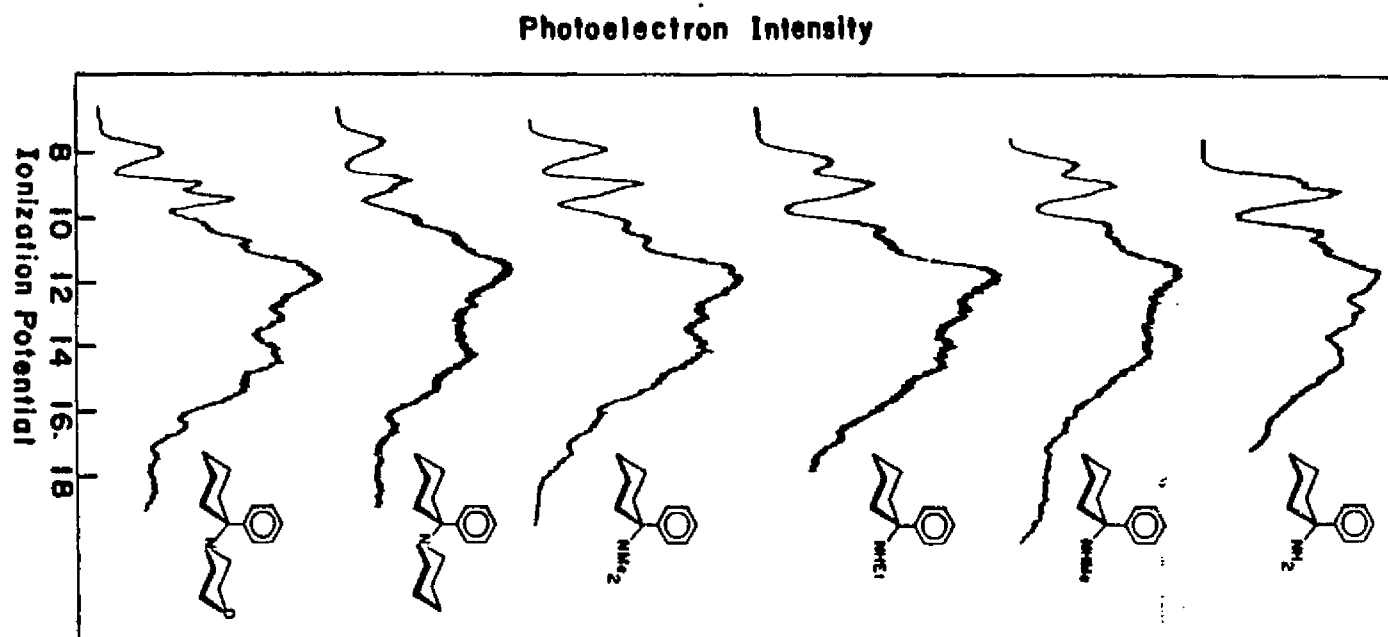


Figure 16. Photoelectron Spectra of 1-Phenylcyclohexylamine, N-(1-Phenylcyclohexyl)-methylamine, N-(1-Phenylcyclohexyl)ethylamine, N,N-(1-Phenylcyclohexyl)-dimethylamine, N-(1-Phenylcyclohexyl)piperidine, and N-(1-Phenylcyclohexyl)-morpholine.

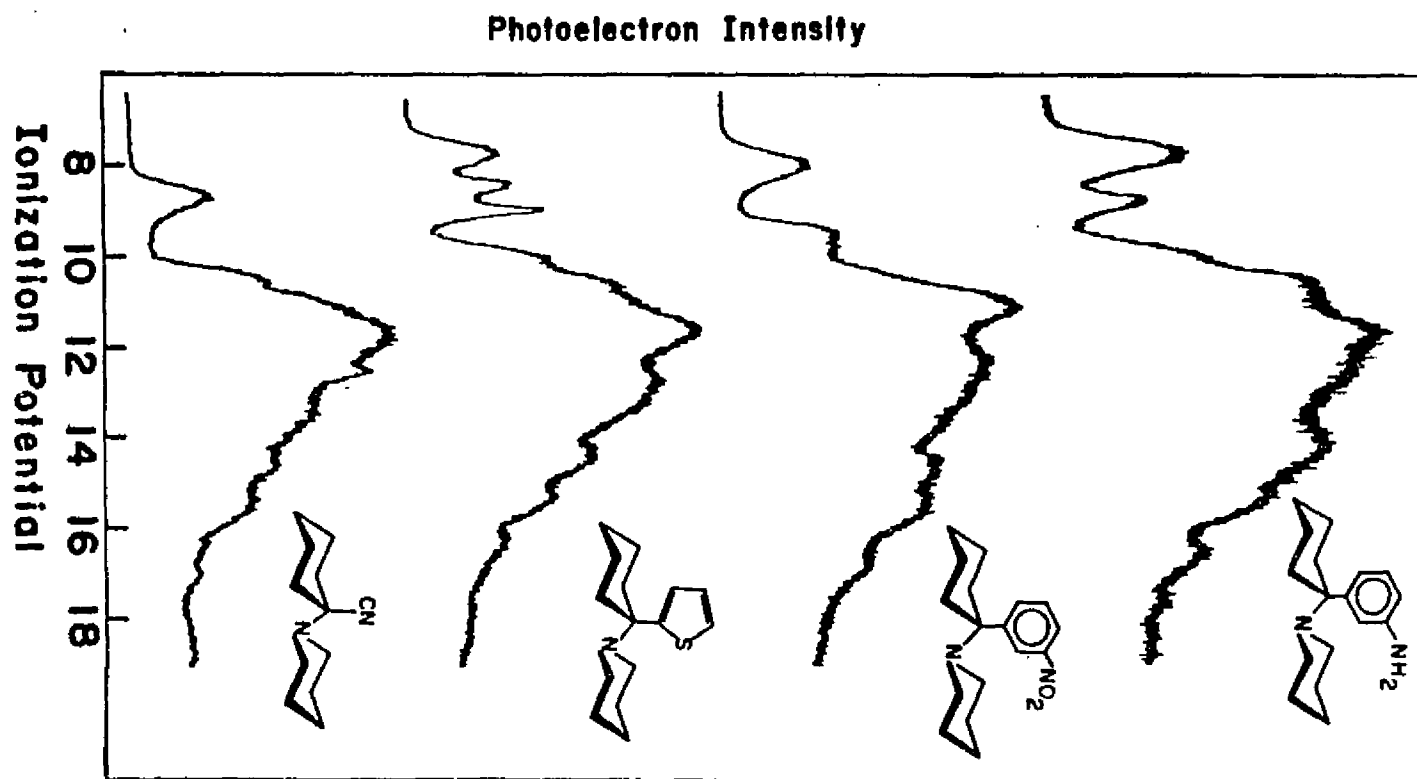


Figure 17. Photoelectron Spectra of *N*-[1-(3-Aminophenyl)cyclohexyl]piperidine, *N*-[1-(3-Nitrophenyl)cyclohexyl]piperidine, *N*-[1-(2-Thienyl)cyclohexyl]piperidine, and *N*-(1-Cyanocyclohexyl)piperidine.

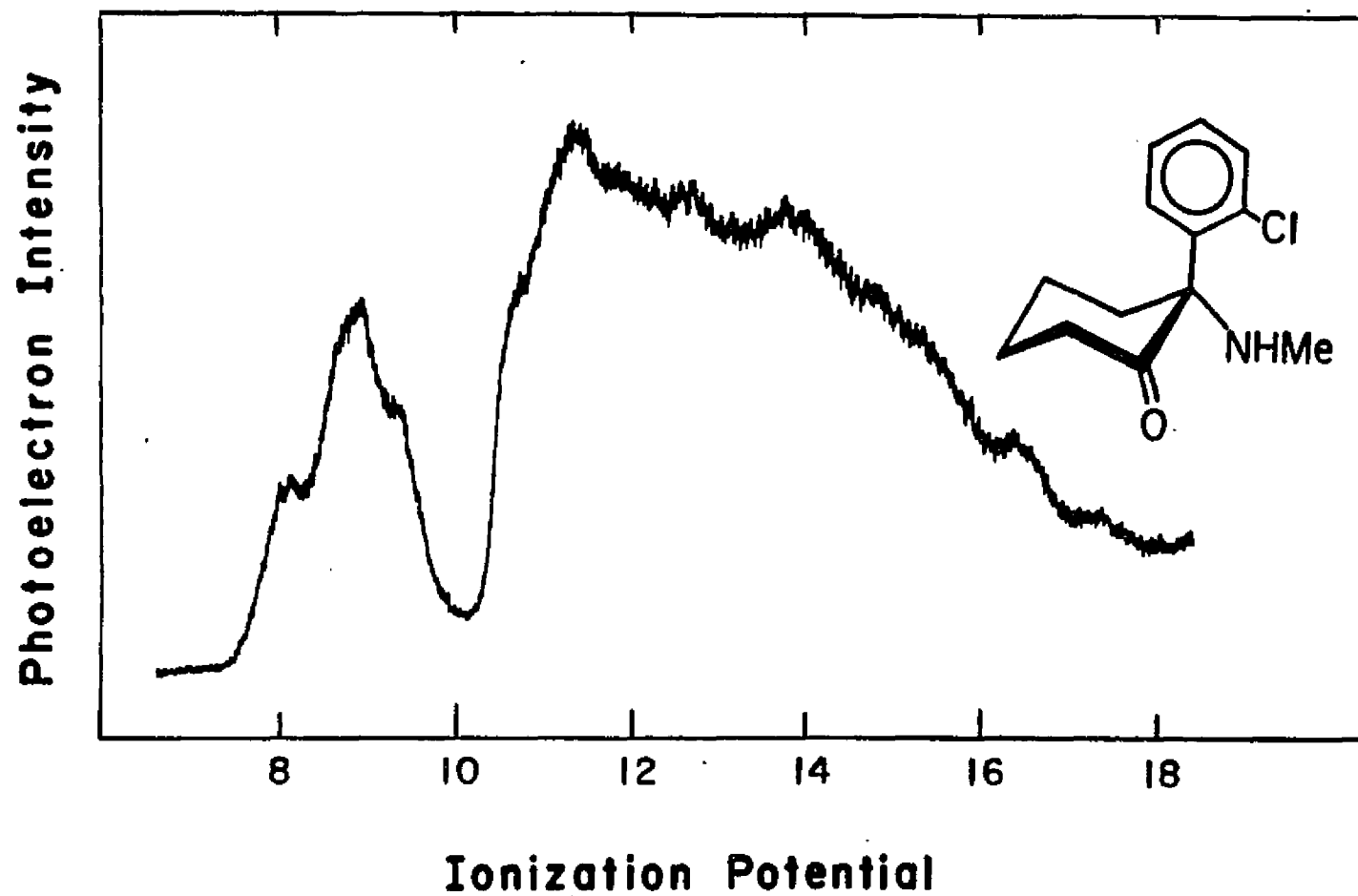
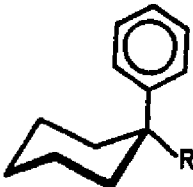
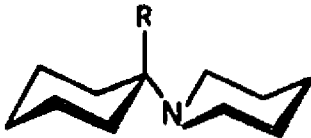


Figure 18. Photoelectron Spectrum of Ketamine.

Table 13. Ionization Potentials of Phencyclidine (PCP) and Analogs

	R	IPs (eV)	
		n	Aromatic IPs
	<u>1a</u> NH <sub>2</sub>	8.81	9.12, 9.3
	<u>1b</u> NHMe	8.35	8.99, 9.1
	<u>1c</u> NEt	8.24	8.93, 9.1
	<u>1d</u> NMe <sub>2</sub>	7.91	8.94, 9.1
	<u>1e</u> piperidino	7.70	8.85, 9.1
	<u>1f</u> morpholino	8.00 (n = 9.46)	8.97, 9.1?
	<u>2a</u> <u>meta</u> -aminophenyl	7.72	7.9, 8.75
	<u>2b</u> <u>meta</u> -nitrophenyl	8.05	9.51, 9.8
	<u>2c</u> 2-thienyl	7.79	8.45, 9.00
	<u>2d</u> cyano	8.68	10.52
Ketamine	<u>3</u>	8.41 (n <sub>CO</sub> = 9.54)	9.04, 9.18

a)  $\pm 0.06$  eV.

b) A second aromatic IP has been estimated from shoulders which are poorly resolved.



With the exception of the cyano analog, 2d, all the compounds are expected to have at least three low-energy ionizations. In most cases, the first ionization is a very broad band due to the nitrogen lone-pair, with three potential exceptions: 1a ( $R = NH_2$ ), 2a ( $X = \text{meta-aminophenyl}$ ) and 3 (ketamine). This broad band is similar in shape to the lone pair ionizations of other alkylamines<sup>8</sup> and the piperidines<sup>9</sup> (Chapter II) and is indicative of both the pyramidal geometry at nitrogen in the ground state and the planar geometry of the radical cation state formed upon ionization. Two other low-energy ionizations are expected to arise from the orbitals of the aromatic moieties.

Three poorly resolved ionizations are observed in the low-energy region of the spectrum of 1-phenylcyclohexylamine, 1a. The first ionization at 8.81 eV is broader and less intense than the second ionization band and it may be tentatively assigned to the nitrogen lone pair. This band is the only one which is appreciably affected by the nitrogen substituents of 1b, 1c, and 1d. For comparison, the lone pair IP of isopropylamine occurs at 9.32 eV and the lone pair IP of tert-butylamine occurs at 9.25 eV.<sup>10</sup> The additional carbons which constitute the cyclohexyl ring have lowered the IP by 0.16 eV in cyclohexylamine (IP = 9.16 eV) relative to isopropylamine. The 1-phenylcyclohexyl moiety resembles the tert-butyl group, but should be a better electron donor because of the additional carbons of the cyclohexyl ring and the phenyl group which replaces one of the methyls. The phenyl ring influences the

IP only by induction since the nitrogen is removed from conjugation and the  $\pi$  orbitals are orthogonal to the nitrogen lone-pair, based upon the crystal structure of phencyclidine hydrochloride.<sup>11</sup>

The second band in the spectrum of 1a at 9.12 eV is sharper and more intense than the first band and arises from the two aromatic  $\pi$  orbitals. Inductive electron-withdrawal by the nitrogen diminishes the electron donation of the cyclohexyl group to the phenyl ring, making the 1-aminocyclohexyl group approximately as good an electron donor as the methyl group. (cf. The first IP of tert-butyl benzene is at 8.68 eV, by photoionization spectroscopy.<sup>12</sup>) Toluene and other monoalkylbenzenes<sup>12-14</sup> have two ionizations appearing as a broad band between 8.85-9.34 eV, which nicely bracket this band of 1a. Finally, around 10 eV, the sigma ionizations and higher energy aromatic  $\pi$  orbital ionization give rise to a near continuum of ionization bands.

The spectra of N-(1-phenylcyclohexyl)methylamine, 1b, (lone-pair IP = 8.35 eV), and N-(1-phenylcyclohexyl)ethylamine, 1c, (lone-pair IP = 8.24 eV), are quite similar in appearance. The first band is somewhat better resolved in each case than in 1a, and is again assigned as the lone-pair. The decreases observed, relative to the first IP of 1a are 0.46 and 0.57 eV, respectively. These are in the range expected for the conversion of a primary amine to a secondary amine. (The IP of methylamine decreases 0.73 eV when a second methyl is added; the IP of ethylamine decreases 0.63 eV when a methyl group is added.<sup>10</sup>) A slightly larger

decrease is expected with the ethyl analog, compared to the methyl analog, due to the greater electron donating ability of the ethyl group. The second band is assigned as before to two ionizations from the  $\pi$  orbitals. They are not resolved, although the band is slightly wider than in la. The added methyl and ethyl group cause the  $\pi$  IPs to be lowered by 0.13 and 0.19 eV, respectively. The intensity ratio in these two compounds between the first and second bands is not appreciably different than that observed for la, lending credence to the tentative assignments made above.

The spectrum of N-(1-phenylcyclohexyl)dimethylamine, ld, has a lone-pair IP of 7.91 eV, which is well resolved, and the IP decreases by 0.46 eV, relative to lb above. This decrease is a result of the conversion of a secondary amine to a tertiary amine, and the magnitude of the decrease is comparable to that observed for the conversion of dimethylamine (IP= 8.93 eV) to trimethylamine (IP = 8.54), a decrease of 0.39 eV. The two  $\pi$  ionizations are not resolved, as before, and the IP decrease is only 0.05 eV, relative to lb, a further indication that the lone pair influences the  $\pi$  orbitals only by induction. The intensity ratio between the lone-pair and  $\pi$  ionization bands is essentially unchanged.

The spectrum of PCP, le, is again very similar to those discussed previously. Both bands are slightly broader, but the assignments are the same. The first IP at 7.70 eV is the lone-pair and is decreased by 0.21 eV, relative to ld, by the additional electron donating ability of the extra carbons which comprise the

piperidine ring. This decrease due to the extra carbons is only slightly greater than observed for the extra carbons in the conversion of isopropyl amine to cyclohexylamine (*vide supra*). The  $\pi$  orbitals are very poorly resolved and their appearance and IPs are essentially the same as those of toluene. Again, the intensity ratio is the same.

The spectrum of N-(1-phenylcyclohexyl)morpholine, 1f, shows the nitrogen lone-pair IP at 8.00 eV, an increase relative to piperidine due to electron withdrawal by the oxygen. The oxygen lone-pair ionization overlaps with the  $\pi$  ionization(s), making the exact positions uncertain. In any case, the second band at 8.97 eV is assigned to the  $\pi$  orbital(s) by comparison to the other spectra in Figure 16. The third band at 9.46 eV is assigned to the oxygen lone-pair, which is essentially the same as in oxane.<sup>16</sup> The 1-phenylcyclohexyl moiety has inductively lowered the nitrogen lone-pair IP considerably, compared to morpholine (nitrogen lone-pair IP = 8.88 eV; oxygen lone-pair IP = 9.77 eV<sup>17-18</sup>) which also lowers the oxygen lone-pair IP by 0.31 eV in 1f.

The spectrum of N-[1-(3-amino)phenylcyclohexyl]piperidine, 2a, shows some similarities to the previous spectra which aid in the assignments. Based on the intensity ratio, the first band at 7.72 eV arises from two overlapping ionizations: the piperidine nitrogen lone-pair, and a  $\pi$  orbital. The piperidine lone-pair ionization in 2a should not be altered very much from that in PCP, 1e, since the lone-pair is not conjugated with the phenyl ring

and is influenced only by induction. Meta-aminotoluene has two low-energy  $\pi$  ionizations at 7.66 and 8.71 eV,<sup>19</sup> suggesting the presence of a  $\pi$  ionization in this band. Meta substituents interact most strongly with the  $\text{Ph}_A$  orbital, which has large coefficients at both meta carbons. Therefore, this lowest  $\pi$  ionization should arise from the  $\text{Ph}_A$  orbital. The second resolved band at 8.75 eV corresponds closely to the second IP of meta-aminotoluene, and is due to the  $\text{Ph}_S$  orbital. The "lone-pair like" orbital of meta-aminotoluene has an IP of 10.45 eV, and the corresponding orbital of 2a is not readily identifiable in this spectrum, although the shoulder at 9.88 eV may arise from this orbital.

The meta-nitro analog, 2b, has an amine lone-pair IP of 8.05 eV, approximately 0.3 eV higher than that of 1e and 2a. Thus, the nitro group has a large effect on the piperidine lone-pair IP, even though these groups are separated by five bonds. The aromatic IPs appear at 9.5-10 eV, approximately in the same region as the IPs of meta-nitrotoluene which occur at 9.48 and 10.03 eV. Since the aromatic IPs are in their normal positions, the large increase in the piperidine lone-pair IP is again attributed to an inductive effect.

The spectrum of N-[1-(2-thienyl)cyclohexyl]piperidine, 2c, has three low-energy ionization bands. The first band at 7.79 eV is assigned to the nitrogen lone-pair, due to its position and shape. The amine lone-pair IP of 2c is slightly higher than that of 1e, indicative of less electron donation by the thiophene ring

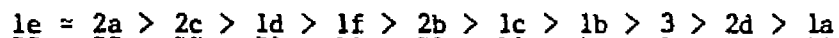
than the benzene ring. The second and third bands at 8.45 and 9.00 eV correspond to ionizations from the highest two  $\pi$  orbitals of the thiophene ring. The corresponding IPs of thiophene are 8.80 and 9.44 eV, while these are 8.32 and 8.96 eV in 2-methylthiophene.<sup>20</sup> As before, the 1-piperidinocyclohexyl group is nearly as efficient an electron donor as the methyl group.

The spectrum of N-(1-cyanocyclohexyl)piperidine, 2d, shows only one low-energy ionization at 8.68 eV which is assigned to the piperidine lone-pair. The cyano group exerts a strong electron withdrawing effect on the lone-pair IP. The ionizations from the cyano group are typically at much higher energy and are not identifiable. We have previously observed this "long range" inductive effect by the cyano group in other examples.<sup>21-22</sup>

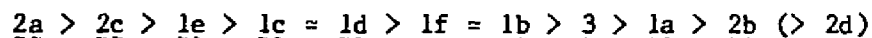
Finally, ketamine, 3, a compound pharmacologically similar to PCP, has rather broad, poorly resolved, bands. The analysis is based on the previous analogs of PCP and on a few model compounds. The first broad band centered at 8.41 eV arises from the secondary amine lone-pair ionization. This is somewhat higher than the corresponding IP of 1b and 1c. The carbonyl and chlorine are both electron-withdrawing and should further increase the lone-pair IP. The second broad band centered at 9.18 eV should arise from two ionizations: the carbonyl lone-pair, (cf. cyclohexanone IP = 9.14 eV<sup>23</sup>) and the first aromatic IP, which appears at 8.82 eV in ortho-chlorotoluene.<sup>24</sup> The third band is a shoulder whose IP corresponds roughly to the second IP of chlorobenzene.

### DISCUSSION

The lone-pair ionization potentials of amines are known to correlate with gas phase basicities and solution basicities in limited series.<sup>8</sup> Thus, the predicted basicities of the compounds studied here are:



The IP of the aromatic moiety is related to the degree of electron donation possible by the aromatic ring. On this basis, the order of electron donation is:



For PCP (1e) and its phenyl-substituted derivatives, 2b and 2c, the order of activity in rat behavioral studies and binding assays follows the order of IPs: the most electron-rich species have the greatest activity. For the remaining compounds, no direct activity comparisons are available. Our studies provide experimental support for the Weinstein et al. hypothesis,<sup>5</sup> that the electron-richness of the aromatic portion of PCP, and the ability of this portion to interact attractively with a neighboring

positive center, influences the binding ability and pharmacological action of PCP and its analogs.



## REFERENCES

1. (a) "PCP", NIDA Research Monograph #21, 1978; (b) Shulgin, A. T.; MacLean, D. E. Clinical Toxicology 1976, 9, 553.
2. Vincent, J. P.; Cavey, D.; Kamenka, J. M.; Geneste, P.; Lazdunski, M. Brain Res. 1978, 152, 176.
3. Vincent, J. P.; Kartalovski, B.; Geneste, P.; Komenka, J. M.; Lazdunski, M. Proc. Nat. Acad. Sci., U.S.A. 1979, 76, 4678; Zukin, S. R.; Zukin, R. S. Proc. Nat. Acad. Sci., U.S.A. 1979, 76, 5372.
4. Maayani, S.; Weinstein, H. Life Sciences 1980, 26, 2011.
5. Wienstein, H.; Maayani, S.; Srebrenik, S.; Cohen, S.; Sokolovsky, M. Molecular Pharm. 1973, 9, 820.
6. Weinstein, H.; Maayani, S.; Glick, S. D.; Meibach, R. C., in Domanio, E. F., Ed., PCP (Phencyclidine): Historical and Current Perspectives NPP Books, Ann Arbor, Michigan, in press.
7. Domelsmith, L. N.; Houk, K. N. in "Photoelectron Spectroscopic Studies of Hallucinogens: The Use of Ionization Potentials in QSAR", in QuaSAR Research Monograph 22, Barnett, G.; Trsic, M.; Willette, R.; Eds., NIDA, 1978.
8. Aue, D. H.; Webb, H. M.; Bowers, M. T. J. Am. Chem. Soc. 1976, 98, 311.
9. Rozeboom, M. D.; Houk, K. N. submitted for publication.
10. Aue, D. H.; Bowers, M. T. in Gas Phase Ion Chemistry Vol. II, Academic Press, New York, 1979, Ch. 9 and references therein.
11. Argos, P.; Barr, R. E.; Weber, A. H. Acta Cryst. 1970, 2, 369.
12. Watanabe, K.; Nakayama, T.; Mottl, J. R. J. Quant. Spectroscopy. Rad. Transfer 1977, 2, 369.
13. Turner, D. W.; Baker, C.; Baker, A. D.; Brundle, C. R. Molecular Photoelectron Spectroscopy Wiley-Interscience, New York, 1970.

14. Rabalais, J. W. Principles of Ultraviolet Photoelectron Spectroscopy Wiley, New York, 1975.
15. Sweigart, D. A.; Turner, D. W. J. Am. Chem. Soc. 1972, 94, 5599.
16. Kobayashi, T.; Nagakura, S. Bull. Chem. Soc. Japan 1973, 46, 1558.
17. Colonna, F. P.; Distefano, G.; Pignataro, S.; Pitacco, G.; Valentin, E. J. C. S. Faraday Trans. II 1975, 71, 1572.
18. Domelsmith, L. N.; Houk, K. N. Tetrahedron Lett. 1977, 1981.
19. Kobayashi, T.; Nagakura, S. Bull. Chem. Soc. Japan 1974, 47, 2563.
20. Baker, A. D.; Betteridge, D.; Kemp, N. R.; Kirby, R. E. Anal. Chem. 1970, 42, 1064.
21. Paquette, L. A.; Ku, A. Y.; Santiago, C.; Rozeboom, M. D.; Houk, K. N. J. Am. Chem. Soc. 1979, 101, 5972.
22. Paquette, L. A.; Rozeboom, M. D.; Houk, K. N. J. Am. Chem. Soc. 1979, 101, 5981.
23. Chadwick, D.; Frost, D. C.; Weiler, L. Tetrahedron Lett. 1971, 4543.
24. Baker, A. D., Mayo, D. P.; Turner, D. W. J. Chem. Soc. (B) 1968, 22.

## CHAPTER V. EXOCYCLIC ALKENES

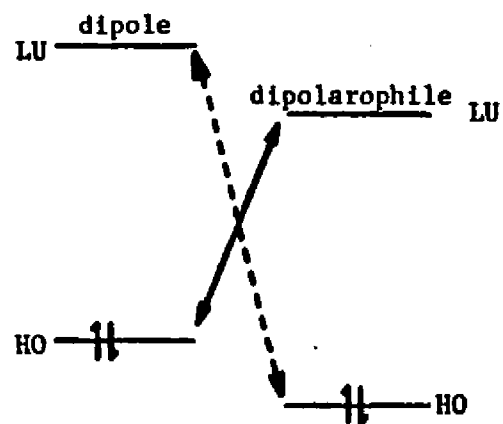
## INTRODUCTION

The Diels-Alder reaction<sup>1-2</sup> is the cycloaddition of alkenes to dienes. It constitutes a very useful method for the formation of six-membered carbocyclic rings. Analogous to these reactions are cycloadditions in which an alkene, or dipolarophile, adds to a three atom moiety, or dipole, bearing four electrons in a  $\pi$  system. This reaction gives rise to five-membered rings, generally containing at least one heteroatom and is known as a 1,3-dipolar cycloaddition. This type of reaction has been extensively studied by Huisgen,<sup>3</sup> Sustmann,<sup>4</sup> and Firestone,<sup>5</sup> and their respective coworkers.

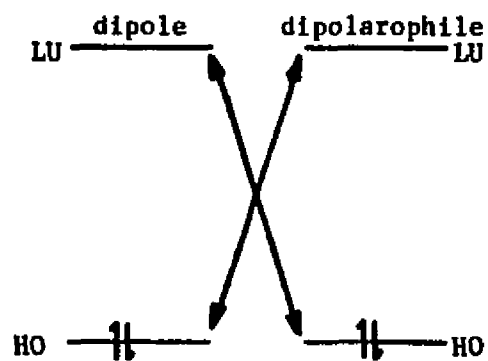
For cycloaddition reactions, the observed regioselectivities have been explained in various ways, among them the frontier molecular orbital approach.<sup>6</sup> For the 1,3-dipolar cycloaddition, regioselectivity refers to the relative orientation of the dipole and the dipolarophile in the cycloaddition process. Two major tenets<sup>6-9</sup> which will not be derived here, but are implicit in this explanation are: 1) the important interaction(s) which have the greatest energy-lowering effect on the transition state are the mixing of filled orbitals of one reactant with unfilled orbitals on the other, particularly the interaction between the highest occupied molecular orbital (HOMO) of one of the species and the lowest unoccupied molecular orbital (LUMO) of the other; these two orbitals are the "frontier molecular orbitals". The largest

amount of transition state stabilization is expected when the energy difference between the HOMO and LUMO is smallest, and the reaction rate should be fastest. The products are expected to show the greatest regioselectivity when the energy difference between the regioisomeric transition states caused by frontier orbital interactions is greatest (vide infra). 2) The joining of the termini with larger frontier molecular orbital (fmo) coefficients to form one bond, coupled with the union of the termini with smaller fmo coefficients to form the second bond in the cycloaddition results in a greater stabilization than the interaction of a large coefficient terminus with a small coefficient terminus to form the bond. (There would be two such large/small interactions in the cycloaddition.)

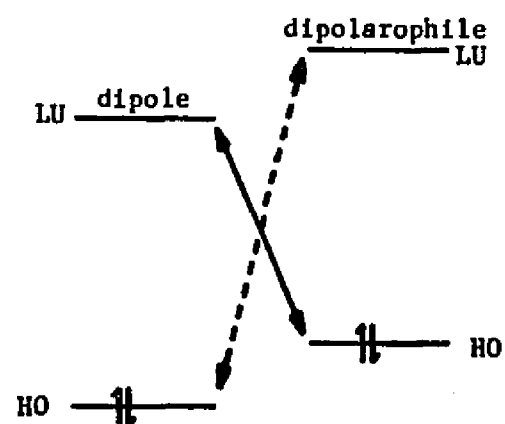
Given these two principles and excluding such things as steric effects, the regioselectivity observed is a consequence of the three different types of possible HOMO/LUMO interactions shown in Figure 19. Using the classification of Sustmann,<sup>5</sup> the Type I interaction is controlled by the smaller energy gap between the HOMO of the dipole and the LUMO of the dipolarophile compared to the gap between the dipolarophile HOMO and dipole LUMO. The rate of reaction should be fastest when the energy gap between these two orbitals is smallest. The regioselectivity is determined by the extent of polarization found in the interacting HOMO and LUMO. A strongly polarized HOMO and LUMO should give a single product. In the Type II interaction, the two possible



Type I  
(HO controlled)



Type II  
(HO, LU controlled)



Type III  
(LU controlled)

Figure 19. Sustmann's Classification Scheme for 1,3-Dipolar Cycloadditions.

HOMO/LUMO gaps are essentially equal. A mixture of regioisomers may result from the reaction if the HOMO(a)/LUMO(b) interaction leads to a different product than the HOMO(b)/LUMO(a) interaction, or if no orbitals are appreciably polarized. In Type III interactions, the smaller gap is between the LUMO of the dipole and the HOMO of the dipolarophile, i.e. the opposite interaction being important compared to Type I control of the reaction. Again, the fastest reaction rate is expected when the energy gap is smallest. For a strongly polarized HOMO and LUMO, only one product should be observed. Both Type I and Type III reactions lead to the same regioisomers when the HOMO and LUMO of each of the reactants are polarized in opposite directions. When the HOMO and LUMO of one of the reactants are polarized in the same direction while the HOMO and LUMO of the other reactant are polarized in opposite directions, then a more accurate assessment of the orbital energies is necessary to correctly classify the reaction, using Sustmann's scheme.

Azides add to alkenes to give two possible regioisomers, the preference for formation of one of these depending on the nature of the substituents attached, particularly on the dipolarophile.<sup>5,8-11</sup> Reactions with electron-rich dipolarophiles are usually Type III controlled (HOMO of dipolarophile, LUMO of dipole). Since the larger terminal coefficients are on the unsubstituted nitrogen of the azide in the LUMO and on the unsubstituted terminus of the dipolarophile in the HOMO, the

5-substituted  $\Delta^2$ -triazolines are favored.<sup>8</sup> Reactions of azides with electron-deficient dipolarophiles are often Type I controlled, and lead to the 4-substituted  $\Delta^2$ -triazolines, as rationalized by terminal coefficients.<sup>8</sup>

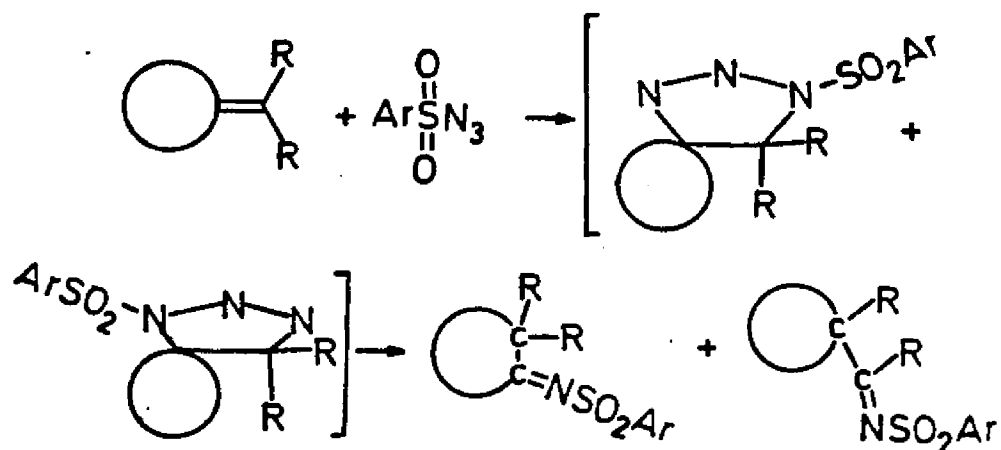
Cycloadditions of azides with alkenes are examples where the classification of the reaction type is delicately controlled. The dipole HOMO controls the cycloaddition with simple and electron-deficient alkenes while the dipole LUMO controls the cycloaddition with electron-rich alkenes, i.e. a Type II interaction.<sup>11</sup> The orbital coefficients of the HOMO and LUMO of azides are polarized in opposite directions. The HOMO and LUMO of electron-rich alkenes are also oppositely polarized; thus both sets of frontier orbital interactions lead to the same regioisomer in these cases.<sup>9</sup> For conjugated and electron-deficient alkenes, polarization of the HOMO and LUMO are not opposite, thus leading to product mixtures.<sup>6</sup> The crucial test of frontier orbital approach involves the cases where only low regioselectivity is observed. Such cases have traditionally been considered to involve a delicate balance between electronic and steric effects.<sup>8</sup>

Product mixtures may also be obtained from cycloadditions in which the polarization present in the alkene moiety are very small or non-existent. The ideal example of a non-polarized frontier orbital is a symmetrically substituted alkene. Other alkenes which are unsymmetrically substituted by very similar substituents will have very small polarizations.

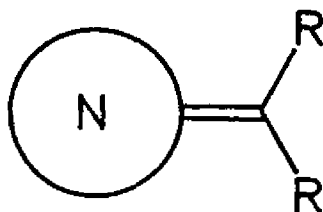


In 1,3-dipolar cycloadditions of phenyl azide, the reactivity is found to be increased both by electron donating and withdrawing substituents on the alkene.<sup>11</sup> Since phenyl azide is a reactant throughout, its HOMO and LUMO energies give rise to a constant term in the calculation of energy differences. Therefore, only the HOMO and LUMO energies of the olefins (dipolarophiles) are necessary to classify the reaction according to Sustmann's scheme. Photoelectron spectroscopy provides a measure of HOMO energies of reagents. The LUMO energies are not known, but trends observed for different types of substituents enable one to estimate trends in LUMO energies. Predictions are then possible concerning the reaction of other dipolarophiles with the same dipole. The occurrence of "wrong" regiochemical results will then indicate when other factors, such as secondary orbital interactions, are important in the transition state.

The 1,3-dipolar cycloadditions of a more electron-deficient 1,3-dipole, such as para-nitrobenzenesulfonyl azide,<sup>12-13</sup> involve a shift toward more electrophilic behavior. The HOMO and LUMO would both be lower in energy than those of phenyl azide. The HOMO and LUMO will both be polarized in the same direction by the electron withdrawing substituent, with the larger coefficient on the opposite end. The decrease in LUMO energy will favor Type III reactions in which the energies of the alkene HOMO and the dipole LUMO govern the rate and regioselectivity of the reaction.



#### PHOTOELECTRON SPECTRA



In collaboration with Professor McManus of the University of Alabama-Huntsville, who has studied the 1,3-dipolar cycloaddition of para-nitrobenzenesulfonyl azide with various exocyclic alkenes,<sup>12-13</sup> we have examined the photoelectron spectra of some exocyclic alkenes, two of which are shown in Figure 20. The IPs of the alkenes studied are assembled in Table 14 along with those of some related compounds. The spectra are all remarkably similar in appearance, especially the first ionization band which arises from the  $\pi$  orbital. Vibrational fine structure is clearly evident in

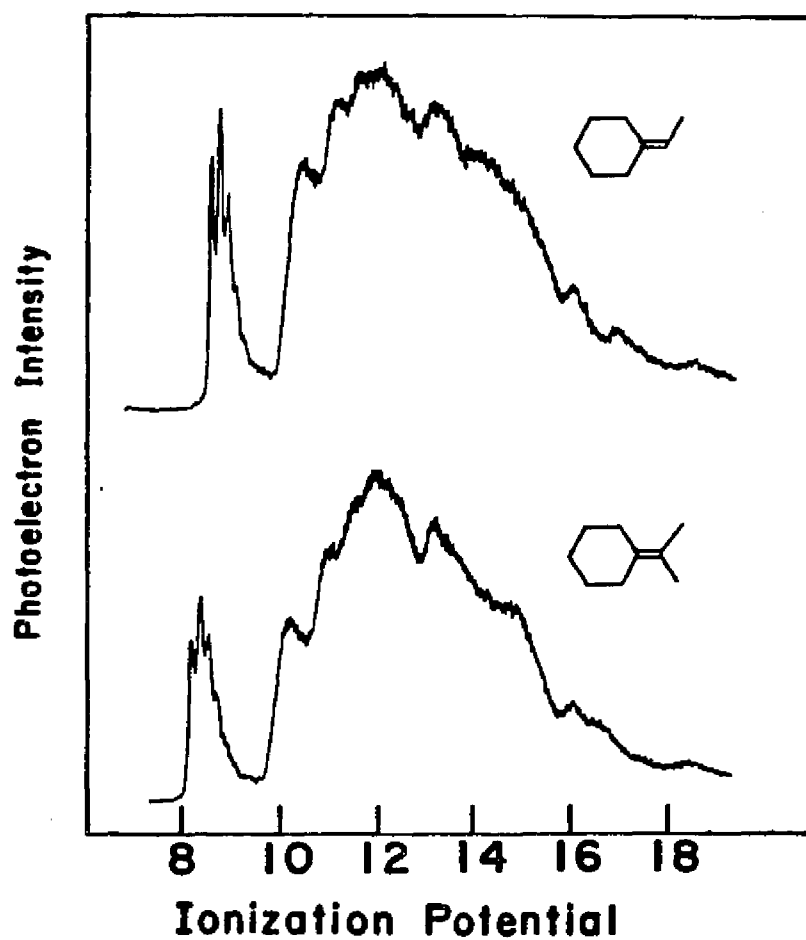


Figure 20. Photoelectron Spectra of Ethylidenecyclohexane and Isopropylidenecyclohexane.

Table 14. Ionization Potentials of Endocyclic Alkenes and Exocyclic Alkenes<sup>a</sup>



N	IP (eV)			
5	(9.01) 9.18 <sup>b</sup>	9.15 <sup>b</sup>	(8.56) 8.72	(8.19) 8.37
6	(8.94) 9.12 <sup>b</sup>	9.13 <sup>b</sup>	(8.56) 8.84	(8.18) 8.36
7	(8.87) 9.04 <sup>b</sup>	9.0 <sup>c</sup>	(8.45) 8.60	(8.12) 8.29
8	(8.82) 8.98 <sup>b</sup>	8.9 <sup>c</sup>	(8.36) 8.48	(8.05) 8.17

=====

a) All IPs are accurate to  $\pm 0.05$  eV. The  $0 \leftarrow 0$  band is the adiabatic IP which is given in parentheses. The  $1 \leftarrow 0$  band is the vertical band listed in the table.

b) Reference 15.

c) Estimated IPs, from data on the smaller ring-sized alkenes.

all the spectra, including those of the endocyclic alkenes. In each case, the  $1 \leftarrow 0$  transition shows the greatest intensity. This is the transition with the largest Franck-Condon factor, or greatest vibrational overlap of the initial and final states. Roughly speaking, this indicates that the radical cation geometry is slightly different from the ground state geometry, the former having a slightly longer C=C bond length. With the exception of the spectrum of cyclopentene, where both the  $0 \leftarrow 0$  and  $1 \leftarrow 0$  transitions have equal intensities, this tendency is also evident in the endocyclic alkenes. The  $\pi$  ionization leads to a radical cation in which the CC stretching frequency is decreased to  $1200\text{--}1450\text{ cm}^{-1}$ , compared to a radical cation vibrational frequency of  $1230 \pm 50\text{ cm}^{-1}$  in ethylene.<sup>14</sup>

### Cyclopentanes

The  $\pi$  ionization of methylenecyclopentane occurs at 9.14 eV,<sup>15</sup> only slightly lower than that of cyclopentene (IP = 9.20 eV).<sup>16-17</sup> This represents a decrease of 0.10 eV, relative to isobutene (IP = 9.24 eV<sup>18</sup>), due to the additional carbons which make up the ring (cf. 2-ethyl-1-butene, IP = 9.06 eV;<sup>18</sup> the two extra carbons lower the IP by 0.18 eV). Substitution of a methyl group for one of the vinyl hydrogens of methylenecyclopentane to give ethylenecyclopentane lowers the IP to 8.72 eV, a 0.42 eV decrease. The second methyl substituent in isopropylidene-

cyclopentane lowers the IP to 8.37 eV, an additional decrease of 0.35 eV. The corresponding decreases in the conversion of isobutene to 2-methyl-2-butene to 2,3-dimethyl-2-butene are 0.56 and 0.41 eV, respectively.<sup>18</sup> The extra ring carbons have slightly diminished the effects of the methyl substituents on the IPs of these acyclic alkenes.

#### Cyclohexanes

The IP of cyclohexene (9.12 eV)<sup>15</sup> is the same as that of methylenecyclohexane.<sup>17</sup> Substitution of a methyl substituent to form ethylidenecyclohexane lowers the IP by 0.38 eV to 8.74 eV. The second methyl substituent lowers the IP by an equal amount, 0.38 eV, to 8.36 eV. The decreases observed are in good agreement with those observed in the cyclopentane series and with the expected decreases as a result of addition of a third and fourth substituent to the ethylene unit.

#### Cycloheptanes

The IP of cycloheptene occurs at 9.04 eV.<sup>15</sup> A comparison of the IPs of the endocyclic alkenes of smaller ring size (three, four, five, and six-membered rings) with the methylenecycloalkanes indicates that the IPs of the endocyclic alkenes are slightly more sensitive to ring size than the exocyclic alkenes. From the data

given above for the cyclopentanes and cyclohexanes, the IP of methylenecycloheptane would be predicted to be slightly lower than that of cycloheptene, i.e. approximately 9.0 eV. Using this value, the addition of a methyl substituent lowers the IP to 8.60 eV for ethylenecycloheptane, a decrease of 0.40 eV, in good agreement with the previously reported decreases. The second methyl group (isopropylidenecycloheptane) lowers the IP by an additional 0.31 eV, only slightly smaller than the previous results.

#### Cyclooctanes

The IP of cis-cyclooctene occurs at 8.98 eV.<sup>15</sup> From this and the previous discussion, the IP of methylenecyclooctane is estimated to be approximately 8.9 eV. The first methyl substituent lowers the IP to 8.48 eV, a decrease of 0.42 eV, reaffirming the previous decrease due to the methyl group, and solidifying the assumed IP. The second methyl group lowers the IP by an additional 0.31 eV, the same amount as in the cycloheptanes.

#### DISCUSSION

The  $\pi$  ionization potentials of methylene-, ethylidene-, and isopropylidene-cyclopentanes and cyclohexanes are essentially identical. This is contrary to the endocyclic alkene IPs which show

a difference of 0.06 eV between the IPs of cyclopentene and cyclohexene (see Table 14). The constancy of the alkylidene IPs is also unusual and different from observations on acyclic alkenes, whose IPs are determined primarily by the number of carbon atoms in the substituents attached to the alkene.<sup>18</sup> Approximately 0.1 eV decreases in the  $\pi$  IPs are observed as the alkylidene cyclohexane ring size is increased by a methylene unit to form the alkylidene cycloheptanes. A similar decrease is observed as another methylene is inserted into the ring to form the alkylidene cyclooctanes. The  $\pi$  IP decreases observed when a methylene unit is inserted into a cyclopropene or cyclobutene ring are larger than 0.1 eV per methylene unit.

This lack of change with a ring-size increase for these two sets of compounds is even more unusual when compared to the decreases caused by the methyl groups which are sequentially added to the double bond. Each methyl group causes a 0.3-0.4 eV decrease in alkene IP. It may be argued that substituting directly on the double bond should have a greater effect than an increase in ring size. An increase in ring size would still be expected to have an observable effect on the IP for five- and six-membered rings.

The  $\pi$  ionization potential of a number of alkenes was shown to correlate with the rate of cycloaddition for phenyl azide.<sup>11</sup> The reactivities of the alkenes studied here are predicted to be:



isopropylidenes > ethylidenes > methylenecycloalkanes

that is, the same as the order of increasing ionization potential. Within each group, the reactivities of the various sized rings should be

$$5 \approx 6 < 7 < 8$$

The reactivities found by McManus were determined from the approximate time required for the disappearance of the azide.<sup>13</sup> The less substituted methylenecycloalkanes are more reactive than the ethylenecycloalkanes and isopropylidenecycloalkanes. The alkylidenecyclopentanes and alkylidenecycloheptanes react at comparable rates, followed by the alkylidenecyclooctanes, which are slightly faster than the alkylidenecyclohexanes.

While frontier orbital interactions do not fare well in the prediction of relative reactivities for this study, it must be pointed out that the reactivities of cyclopentene and cyclohexene with phenyl azide are also noticeably different.<sup>11</sup> Frontier molecular orbital theory does predict the observed regioisomers in the majority of examples. The HOMO of methylenecycloalkanes and ethylenecycloalkanes should be polarized such that the larger coefficient is found on the less-substituted terminus of the alkene. For these cases, the observed product results from addition of the unsubstituted (electrophilic terminus with larger

coefficient) terminus of the azide to the less-substituted terminus of the alkene, which also has the larger coefficient, i.e. the "correct" product, as predicted from frontier molecular theory. The "wrong" product results from addition of the substituted azide terminus to the less-substituted alkene terminus.

Only the correct product is observed in cycloadditions of the methylenecycloalkanes and ethylidenecycloalkanes to para-nitrobenzenesulfonyl azide. A mixture of products results from cycloaddition of the azide to isopropylidenecycloalkanes. The frontier molecular orbitals of isopropylidenes should be only slightly polarized (in the same direction as before) since the double bond has four alkyl substituents. The observed ratios of "correct": "wrong" regioisomers for the isopropylidenecycloalkanes for the various ring size cycloalkanes are:<sup>13</sup>

5 (1.7:1) ; 6 (1.5:1) ; 7 (1.1:1) ; 8 (1:1.7).

The trend toward an increase in the amount of "wrong" regioisomer (substituted terminus of the azide adding to the methyl-substituted end of the alkene) is directly opposite to what is predicted from frontier molecular orbital theory, based on IPs. As ring size increases, the ionization potential decreases, which means that the cyclooctane ring is a better donor than the cycloheptane ring which is better than the cyclohexane and cyclopentane rings. The opposite trends of IPs and product ratios

indicate that other factors, such as steric effects and/or conformational effects of the methyl substituents and the hydrogens of the cycloclakane are overriding the frontier molecular orbital preference. Additional study, either computationally or experimentally, is required for a better understanding. The curious identity of IPs for alkylidene-cyclopentanes and alkylidenecyclohexanes also merits additional study.

REFERENCES

1. Wassermann, A. Diels-Alder Reactions Elsevier, London, 1965.
2. Hamer, J. 1,4-Cycloaddition Reactions - The Diels-Alder Reaction in Heterocyclic Syntheses Academic Press, New York, 1967.
3. See for example: Huisgen, R. Angew. Chem. Int. Ed. Engl. 1963, 2, 633; J. Org. Chem. 1968, 33, 2291, and references therein.
4. See for example: Firestone, R. A. J. Org. Chem. 1968, 33, 2285; 1972, 37, 2181, and references therein.
5. See for example: Sustmann, R. Tetrahedron Lett. 1971, 2717, 2721, and references therein.
6. Fleming, I. Frontier Orbitals and Organic Chemical Reactions Wiley, Chichester, 1976, and references therein.
7. Houk, K. N. Acc. Chem. Res. 1975, 8, 361.
8. Houk, K. N.; Sims, J.; Watts, C. R.; Luskus, L. J. J. Am. Chem. Soc. 1973, 95, 7301, and references therein.
9. Houk, K. N.; Sims, J.; Duke, Jr., R. E.; Strozler, R. W.; George, J. K. J. Am. Chem. Soc. 1973, 95, 7287, and references therein.
10. Herndon, W. C. Chem. Rev. 1972, 72, 157, and references therein.
11. Sustmann, R.; Trill, H. Angew. Chem. Int. Ed. Engl. 1972, 11, 838, and references therein.
12. Abramovitch, R. A.; Ortiz, M.; McManus, S. P. J. Org. Chem. 1981, 46, 330.
13. McManus, S. P.; Ortiz, M.; Abramovitch, R. A. J. Org. Chem. 1981, 46, 336.
14. Turner, D. W.; Baker, C.; Baker, A. D.; Brundle, C. R. Molecular Photoelectron Spectroscopy Wiley-Interscience, New York, 1970.
15. Bischof, P.; Heilbronner, E. Helv. Chim. Acta 1970, 53, 1677.

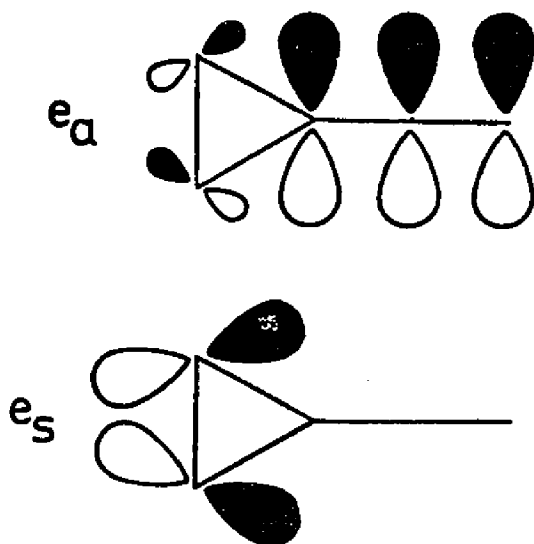
16. Wiberg, K. B.; Ellison, G. B.; Wendoloski, J. J.; Brundle, C. R.; Kuebler, N. A. J. Am. Chem. Soc. 1976, 98, 7179.
17. Asmus, P.; Klessinger, M. Tetrahedron 1974, 30, 2477.
18. Masclet, P.; Grosjean, D.; Mouvier, G.; Dubois, J. J. Electron Spectroscopy. Relat. Phenom. 1973, 2, 225.
19. Houk, K. N.; Williams, Jr., J. C.; Mitchell, P. A.; Yamaguchi, Y. J. Am. Chem. Soc. 1981, 103, 949.

## CHAPTER VI. CUMENES AND CYCLOPROPYLBENZENES

## INTRODUCTION

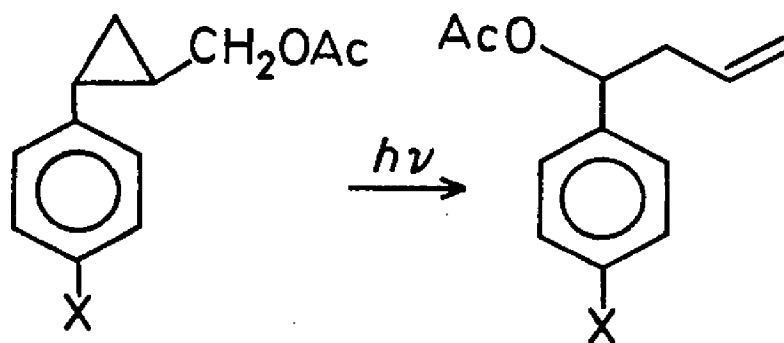
A number of comparisons have been made between a  $\pi$  bond and a cyclopropane ring.<sup>1</sup> The possibility of conjugation between the ring and an adjacent  $\pi$  system has led to a variety of experimental probes to evaluate the amount of conjugation.

Walsh predicted that the plane of the cyclopropane ring should be perpendicular to the plane of the unsaturated side chain,<sup>2</sup> i.e. a "bisected" conformation. In molecular orbital terms, the bisected conformation would provide for maximum overlap of one of the degenerate HOMOs of the cyclopropane ring and a  $\pi$  system, as shown:



The ultraviolet absorption spectrum of cyclopropylbenzene was successfully predicted from molecular orbital calculations on the molecule in the bisected conformation.<sup>3</sup> It was noted by Strait *et al.*<sup>4</sup> that the conjugation between the cyclopropane Walsh orbitals and the para-substituted benzene ring was strong only for electron-withdrawing substituents. Goodman and Eastman<sup>5</sup> failed to observe any significant difference between the ultraviolet spectra of spiro[cyclopropane-1,1'-indan] and benzobicyclo[3.1.0]hexane, i.e. a bisected and non-bisected "cyclopropylbenzene".

Hixson and co-workers<sup>6-8</sup> have been studying the photochemistry of para-substituted cyclopropylbenzenes.



They have determined that electron-donating substituents decrease the reactivity while electron-withdrawing substituents increase the reactivity. Electron-withdrawing substituents greatly decrease the lifetime of the singlet state while electron-donating groups increase the lifetime only slightly. These photochemical results suggest that there is an increased interaction between the



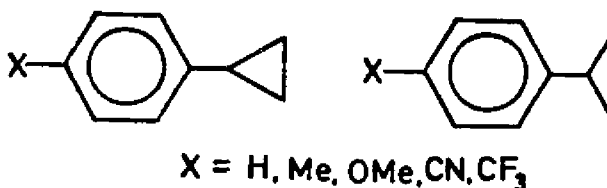
cyclopropane and benzene rings which contain electron-withdrawing substituents.

Pes has been used in conjunction with some photochemical reactivity studies. The facile photochemical ring closure of norbornadienes to quadricyclanes is a widespread occurrence<sup>9-10</sup> as a consequence of the orbital sequence which places the  $\pi_-$  combination over the  $\pi_+$  level. Electronic excitation promotes an electron from an orbital which is antibonding, with respect to the individual ethylene fragments, to a bonding orbital. Studies of some other non-conjugated dienes, such as cyclohexadienes, in which the ethylene fragments bear a spatial resemblance to norbornadiene,<sup>11-12</sup> but also containing high-lying  $\sigma$  orbitals have separated through-bond and through-space effects.<sup>13</sup> In these cases, the  $\pi$  levels are reversed and the photochemical cyclization products were not observed.

Photoelectron spectroscopy has been successful in studying conjugative interactions in spiro[cyclopropylalkenes]<sup>14-15</sup> with a bisected conformation. These studies reveal an interaction between the Walsh orbitals and the  $\pi$  orbital. Pes studies on alkenylidenecyclopropanes<sup>16</sup> have determined that an interaction can occur between a  $\pi$  orbital and the cyclopropane ring, even in the non-bisected conformation. An evaluation of the splittings observed in the spectra of 1-alkyl-1-phenylcyclopropanes<sup>17</sup> have suggested that the non-bisected conformation is preferred in

cyclopropylbenzene and para-methoxycyclopropylbenzene. Supportive MIEHM (Modified Iterative Extended Hückel Method) calculations<sup>17</sup> predicted a large splitting in the  $\pi$  levels, even in the non-bisected conformation. For all angles of rotation about the connecting bond, the Walsh  $e_g$  orbital contained a substantial carbon-2p contribution in the cyclopropane ring plane.

#### PHOTOELECTRON SPECTRA



In collaboration with Professor Hixson of the University of Massachusetts, we have recorded and analyzed the photoelectron spectra of several para-substituted cyclopropylbenzenes. Three benzobicyclo[3.1.0]hexanes were also analyzed as rigid models of non-bisected cyclopropylbenzenes. Several cumenes were also examined as acyclic models of a non-conjugating cyclopropyl substituent. Some representative spectra are shown in Figure 21, and the IPs are assembled in Table 15, along with those of some model compounds.

The spectra of cumene and cyclopropylbenzene have been contrasted previously.<sup>18</sup> The first band of cumene is vertical

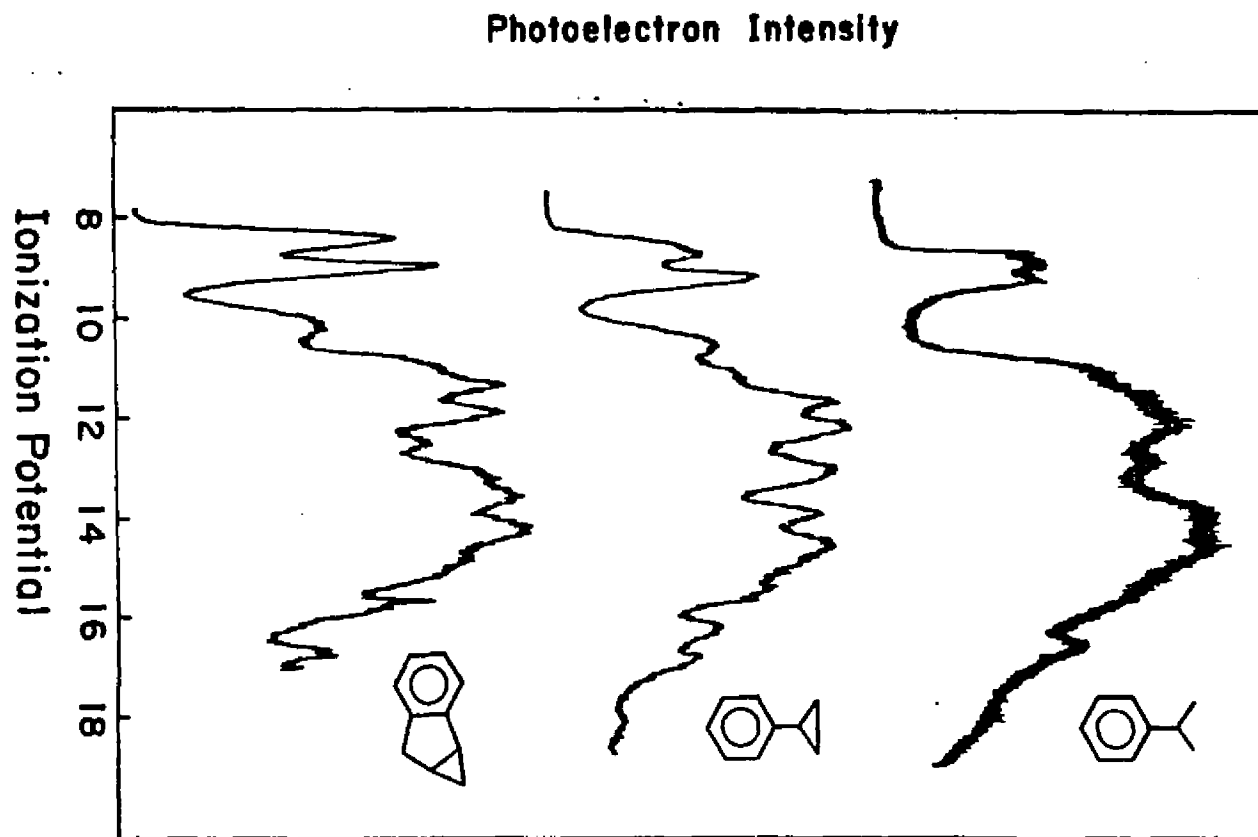
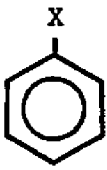


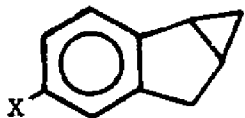


Figure 21. Photoelectron Spectra of Cumene, Cyclopropylbenzene, and Benzobicyclo[3.1.0]hexane.

Table 15. Ionization Potentials of Substituted Benzenes.

		IPs (vert., eV)			
		IP	IP	HIGHER IPs	
	H <sup>c</sup>	9.25	9.25		
	Me <sup>c</sup>	8.72	9.24		
	OMe <sup>c</sup>	8.42	9.21	11.02 <sup>e</sup>	
	CN <sup>c</sup>	9.70	10.13		
	CF <sub>3</sub> <sup>d</sup>	9.90	11.9		
	H	8.97	9.29		
	Me	8.55	9.10		
	OMe	8.10	9.04	10.78 <sup>e</sup>	
	CN	9.37	9.86		
	CF <sub>3</sub>	9.36	9.70		
	H	8.72	9.19	10.54	11.13
	Me	8.41	9.04	10.34	10.99
	OMe	8.10	9.00	10.18 <sup>f</sup>	10.64 <sup>f</sup>
	CN	9.08	9.84	10.97	11.39
	CF <sub>3</sub>	9.15	9.69	10.94	11.49
	H	8.43	8.92	10.23	
	OMe	7.80	8.89	9.99 <sup>f</sup>	10.28 <sup>f</sup>
	CN	8.87	9.53	10.02	11.10

=====

Table 15. (continued)

- a)  $\pm 0.05$  eV.
- b) These are the cyclopropane Walsh orbitals, unless otherwise noted.
- c) Reference 19.
- d) Reference 20.
- e) Oxygen lone pair IP.
- f) One of these two bands also contains an oxygen lone pair IP.

according to one author,<sup>19</sup> but non-vertical by another group.<sup>20</sup> Our examination of the spectrum shows a well-defined adiabatic IP which is only slightly less-intense than the vertical IP. This means the ground state of the neutral molecule ionizes with equal probabilities to the first and second vibrational levels of the cation. All the cumenes except the para-methoxy derivative show a well-defined adiabatic ionization potential which is also the vertical IP in two instances. The first band of cyclopropylbenzene is definitely non-vertical which means there is a significant difference between the shapes of the potential curves for the neutral and cationic ground states of cyclopropylbenzene. The difference arises from an interaction of the highest-occupied  $b_1$ -like benzene orbital<sup>21</sup> and an alkyl  $\sigma$  bonding orbital, i.e. a Walsh orbital. The band arising from the  $a_2$ -like orbital is poorly resolved in both cases. The cyclopropylbenzenes have two additional bands which are separated from the  $\pi$  ionizations and arise from the Walsh orbitals.

The vertical IPs of cumene are found at 8.97 eV and 9.29 eV and are assigned to the  $b_1$ -like ( $Ph_S$ ) and the  $a_2$ -like ( $Ph_A$ ) orbitals, respectively. The IPs of cyclopropylbenzene are found at 8.72 eV, 9.19 eV, 10.54 eV, and 11.13 eV. The first two ionizations are assigned to the  $Ph_S$  and  $Ph_A$  orbitals, similar to the cumenes. The last two ionizations arise from the originally degenerate Walsh HOMOs of cyclopropane.

Donors at the para position of cyclopropylbenzene or cumene

are expected to cause the largest decrease to be observed in the  $\text{Ph}_S$  IP since the two groups are attached to "large" coefficient sites, with little or no effect on the  $\text{Ph}_A$  IP, since  $\text{Ph}_A$  has a nodal plane through these sites. The Walsh  $e_a$  orbital of the cyclopropane ring should preferentially interact with the phenyl ring ( $\text{Ph}_S$  orbital) and be raised in energy, relative to the Walsh  $e_s$  orbital which has a node at the site of attachment to the phenyl ring. The substituent may influence the electron density in the cyclopropane ring through the  $e_a$  orbital which can then cause changes in the IP of the  $e_s$  orbital.

The adiabatic ionization potential of para-cymene (para-methylcumene) at 8.43 eV is also the vertical ionization potential. For an accurate comparison of the various cumene derivatives and their cyclopropylbenzene counterparts, it is preferable to compare the same process, i.e. we must compare the ionization which involves the same state of the radical cation in as many examples as possible, which may mean comparing one of the vibrational bands in the pes, not just the vertical IPs. Based on the nonadiabatic ionization at 8.55 eV, a para-methyl substituent causes a 0.42 eV decrease in the first IP of cumene. The second IP is lowered by 0.19 eV in accord with expectations.

The spectra of all the cyclopropylbenzenes are similar, with clear indications that the shapes of the potential curves for the neutral and cation ground states are different. The first two ionizations of para-methylcyclopropylbenzene occur at 8.41 eV and

9.04 eV, which correspond to decreases of 0.31 eV and 0.15 eV, respectively, slightly smaller in magnitude but in the same direction as the cumenes. The cyclopropyl Walsh orbital IPs at 10.34 eV and 10.99 eV are lowered by 0.20 eV and 0.14 eV, respectively, relative to cyclopropylbenzene.

As stated previously, an adiabatic ionization process is not readily identifiable for para-methoxycumene. The para-methoxy substituent lowers the first IP of cumene by 0.87 eV to 8.10 eV. The second IP is lowered by 0.25 eV to 9.04 eV. The  $\pi$  IPs of the cyclopropylbenzene analog are lowered by 0.72 eV and 0.19 eV, respectively, to 8.00 eV and 9.00 eV. The Walsh orbital IPs are decreased by 0.36 eV and 0.49 eV to 10.18 eV and 10.64 eV, respectively. All the decreases caused by the methoxy group are larger than those caused by the methyl group, consistent with the larger electron donating ability of the methoxy group. The oxygen lone pair ionization in para-methoxycumene is tentatively assigned to the well-defined shoulder at 10.78 eV in the spectrum. The location of this ionization in the cyclopropylbenzene analog is uncertain.

For electron-donating groups, we have compared the IPs of the cumenes and cyclopropylbenzenes. The  $\text{Ph}_A$  orbital has a node at the site of attachment and does not conjugate with the substituent, resulting in minimal changes in the IP. Electron-withdrawing substituents decrease the charge density in the



aromatic ring and cause both  $\pi$  ionizations to occur at lower energy. This necessitates the inclusion of an additional consideration in the assignments and the evaluation of trends in the IPs. With these electron-withdrawing groups, a noticeable change is observed in the  $\text{Ph}_A$  IP. We can no longer compare the substituted derivative directly to the parent hydrocarbon without comparing the effect that electron-withdrawing groups have on the IPs of benzene. Kobayashi<sup>19</sup> has indicated that the ionization order remains unchanged, with the  $\text{Ph}_S$  orbital below  $\text{Ph}_A$ . As will be seen, our results are consistent with this order.

The adiabatic IP of para-cyanocumene at 9.25 eV is also the vertical IP. As referred to earlier, to be consistent in our comparison, the IP of the first vibrational band at 9.37 is used. The cyano group raises the first IP of cumene by 0.28 eV, while the second IP is raised by 0.57 eV. This result may seem anomalous until one examines the influence the cyano group has on the IPs of benzene. One of the  $\pi$  orbitals is raised by 0.46 eV and the second is raised by 0.89 eV by the cyano group in benzonitrile.<sup>20</sup>

Similar comparisons are made for para-cyanocyclopropylbenzene (IPs = 9.08 eV and 9.84 eV). The increases in the IPs (0.36 eV and 0.65 eV), relative to cyclopropylbenzene are larger than for the cumenes, but smaller than for benzene. More correctly, the decreases in the IPs (0.62 eV and 0.29 eV), when compared to benzonitrile, are larger for the cyclopropylbenzenes, indicating that the cyclopropyl group interacts more strongly with the

aromatic ring than with the isopropyl group, in keeping with the results observed earlier for the electron-donating substituents. The Walsh orbital ionizations occur at 10.97 eV and 11.39 eV.

The adiabatic IP of the  $\text{Ph}_S$  orbital in para-trifluoromethylcumene has noticeably decreased in intensity compared to the vertical IP at 9.36 eV. This represents a 0.39 eV increase in the first IP, as compared to cumene. The  $\text{Ph}_A$  IP increases to 9.70 eV, a 0.41 eV increase. As with the cyano derivatives, it is preferable to compare the IPs with those of trifluoromethylbenzene,<sup>20</sup> in which the  $\pi$  ionizations are not separated, at 9.90 eV. Compared in this manner, the isopropyl group causes a 0.54 eV decrease in  $\text{Ph}_S$  and a 0.20 eV decrease in  $\text{Ph}_A$ .

The  $\pi$  IPs in para-trifluoromethylcyclopropylbenzene occur at 9.15 eV and 9.69 eV, and are assigned as before to ionizations from the  $\text{Ph}_S$  and  $\text{Ph}_A$  orbitals. The IPs at 10.94 eV and 11.49 eV are assigned to the Walsh orbitals. Relative to cyclopropylbenzene, increases of 0.43 eV and 0.50 eV are observed. Relative to the IP of trifluoromethylbenzene, the IPs decrease by 0.75 eV and 0.21 eV, respectively. As before, the cyclopropyl group interacts more strongly with the phenyl ring than the isopropyl group does.

As referred to earlier, three benzobicyclo[3.1.0]hexanes have also been analyzed as model compounds. While the cyclopropane ring may not be rotated exactly 90° from the bisected conformation in these models, the conjugation should be effectively interrupted to

allow a determination as to whether the bisected conformation is necessary for an effective interaction between the two rings.

The IPs of the parent benzobicyclo[3.1.0]hexane are at 8.43 eV and 8.92 eV. Compared to cyclopropylbenzene, both IPs have been lowered by an average of 0.28 eV due to the extra methylene of the ring. A methoxy substituent para to the cyclopropyl group (IP = 7.80 eV and 8.89 eV) causes a 0.20 eV decrease in the first IP and a 0.11 eV decrease in the second IP, relative to para-methoxycyclopropylbenzene. The extra methylene unit does not cause as great a decrease as in the parent. The extra methylene unit in the para-cyano analog (IPs = 8.87 eV and 9.53 eV) causes a 0.21 eV decrease in the first IP and a 0.31 eV decrease in the second IP, relative to para-cyanocyclopropylbenzene.

#### DISCUSSION

Electron-donating groups in mono-substituted benzenes generally affect only the  $\text{Ph}_\text{S}$  orbital energy, lifting the degeneracy found in benzene. The energy of the  $\text{Ph}_\text{A}$  orbital is lowered very slightly, but shows very minor changes with the substituents. Electron-withdrawing groups, meanwhile, decrease the electron density in the phenyl ring by both conjugative and inductive electron-withdrawal and lower the energy of both orbitals. The degeneracy may or may not be lifted by the substituent. One can determine which interaction is stronger with the  $\text{Ph}_\text{S}$  orbital,

either the low-lying vacant orbital or a high-lying filled orbital, based on the relative ordering of the  $\text{Ph}_S$  and  $\text{Ph}_A$  orbitals.

In benzonitrile, the  $\text{Ph}_S$  orbital is said to be destabilized due to interaction with the high-lying filled orbitals of the cyano group.

The conformation of the cyclopropane ring, relative to the phenyl ring, should have a direct influence on the phenyl IPs and vice-versa. In the bisected conformation, the  $e_a$  orbital can conjugate with the  $\text{Ph}_S$  orbital, which should lower the IP. In the non-bisected conformation, the cyclopropyl ring should inductively lower the IP.

A comparison of the relative strengths of the isopropyl and cyclopropyl groups and the conformation of the cyclopropylbenzenes can be made by comparing the changes observed when substituents are present. When the  $\text{Ph}_S$  IP for each of these two series is plotted against the  $\text{Ph}_S$  orbital of the monosubstituted benzene derivatives, the slope of the line for the cyclopropylbenzenes (1.298) is larger than the slope for the cumenes (1.131), Figure 22. This indicates that the cyclopropylbenzenes are more sensitive to the nature of the substituent, compared to the cumenes.

There are no obvious indications of a change in slope for the cyclopropylbenzenes. A change in slope is expected if the conformation changes, due to the loss of conjugation upon rotation. Since no change in slope appears, it is to be concluded that the conformation does not change in this series of compounds. Either the bisected conformation is preferred for all members, or

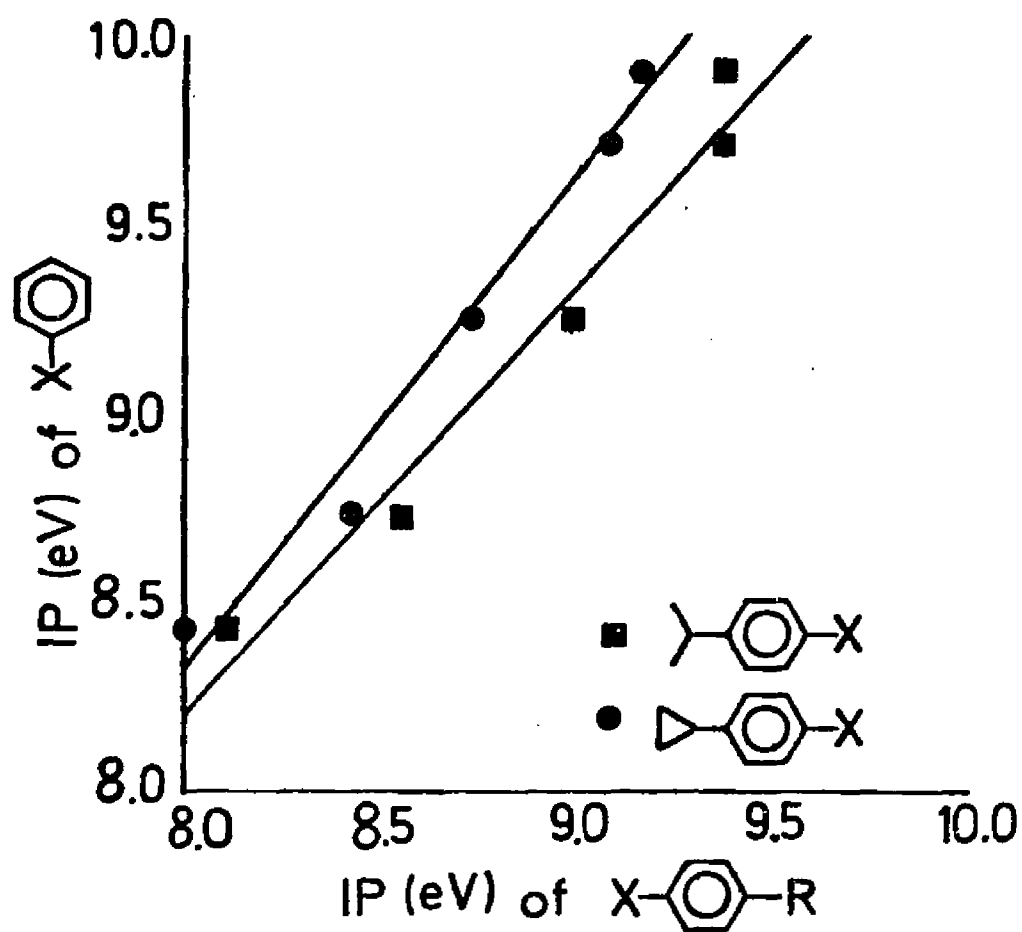


Figure 22. Plot of  $\text{Ph}_S$  IP of Substituted Benzenes vs  $\text{Ph}_S$  IP of Substituted Cumenes and Cyclopropylbenzenes.

none of them exist in the bisected conformation.

Cyclopropylbenzene and the para-methoxy derivative were both indicated to favor the non-bisected conformation.<sup>17</sup> One of the supporting indications was that the difference in energy between the two ionizations assigned to the Walsh orbitals remained nearly constant, regardless of the alkyl substituent also attached to the cyclopropane ring.

An alternative explanation is that both Walsh-type orbitals of the cyclopropane ring are equally effective in lowering the  $\text{Ph}_g$  IP, completely obscuring a change in conformation. The conformation may be dependent on the nature of the substituent. However, if the  $e_g$  orbital is equally efficient in destabilizing the  $\text{Ph}_g$  orbital in the non-bisected conformation, compared to the destabilization of the  $\pi$  orbital by the  $e_a$  orbital in the bisected conformation, then a change in the slope would not be observed. The ultraviolet studies with spiro[cyclopropane-1,1'-indan] and benzobicyclo[3.1.0]hexane, the IPs of the bicyclic compounds studied here, and the alkenylidenecyclopropane pes results are consistent with this alternative.

Our results for the substituted cyclopropylbenzenes do not enable us to solve this conformational problem. Our results for the electron-donating substituents are consistent with the earlier pes study. The  $\pi$  IPs follow the expected trends and the difference in the Walsh orbital IPs remains nearly constant. However, the ultraviolet studies and our own pes data on the bicyclic compounds are

consistent with the fact that the the  $e_g$  orbital can lower the phenyl IPs.

Molecular orbital theory has been used to make logical extensions to the excited state with varying degrees of success.<sup>22</sup> Acceptors should favor the bisected conformation which provides for better overlap between the  $Ph_g$  and the  $e_a$  orbitals, while donors may favor the non-bisected conformation. The photochemical reactivity differences for donor and acceptor substituted cyclopropylbenzenes may be related to the different effects of the donor and the acceptor. The key may lie in the Walsh orbital IPs which are not as well-defined in the spectra, nor is their assignment obvious, since they lie very close to, and overlap with the  $\sigma$  framework in many examples.

REFERENCES

1. Charton, M. "Olefinic Properties of Cyclopropanes" in The Chemistry of Alkenes Vol 2, Zabicky, J., Ed., Interscience, New York, 1970, ch. 10.
2. Walsh, A. D. Trans. Faraday Soc. 1949, 45, 179.
3. Music, J. F.; Matsen, F. A. J. Am. Chem. Soc. 1950, 72, 5256.
4. Strait, L. A.; Ketcham, R.; Janbotkar, D.; Shah, V. P. J. Am. Chem. Soc. 1964, 86, 4628.
5. Goodman, A. L.; Eastman, R. H. J. Am. Chem. Soc. 1964, 86, 908.
6. Hixson, S. S.; Gere, J. A.; Franke, L. A. J. Am. Chem. Soc. 1979, 101, 3677.
7. Hixson, S. S. J. C. S. Chem. Comm., 1974, 681.
8. Hixson, S. S.; Factor, R. E. Tetrahedron Lett. 1975, 3111.
9. Hammond, G. S.; Wyatt, P.; deBoer, C. D.; Turro, N. J. J. Am. Chem. Soc. 1964, 86, 2532.
10. Kaupp, G. Angew. Chem. Int. Ed. Engl. 1971, 10, 340.
11. Shen, K. W. Tetrahedron Lett. 1973, 24.
12. Schmidt, W.; Wilkens, B. T.; Tetrahedron 1972, 28, 5649.
13. Gleiter, R.; Hailbronner, E.; Hekman, M.; Martin, H. D. Chem. Ber. 1973, 106, 28.
14. Bruckmann, P.; Klessinger, M. Chem. Ber. 1974, 107, 1108.
15. Bruckmann, P.; Klessinger, M. J. Electron Spectroscopy Relat. Phenom. 1973, 2, 341.
16. Pasto, D. J.; Fehlner, T. P.; Schwartz, M. E.; Baney, H. F. J. Am. Chem. Soc. 1976, 98, 530.
17. Prins, I.; Verhoeven, J. W.; deBoer, T. J.; Worrell, C. Tetrahedron 1977, 33, 127.



18. Shudo, K.; Kobayashi, J; Utsunomiya, C. Tetrahedron 1977, 33, 1721.
19. Kobayashi, T.; Nagakura, S. Bull. Chem. Soc. Japan 1974, 47, 2563.
20. Baker, A. D., May, D. P.; Turner, D. W. J. Chem. Soc. (B) 1968, 22.
21. Turner, D. W.; Baker, C.; Baker, A. D.; Brundle, C. R. Molecular Photoelectron Spectroscopy Wiley, London, 1970.
22. Fleming, I. Frontier Orbitals and Organic Chemical Reactions Wiley, New York, 1976 and references therein.

## CHAPTER VII. EXPERIMENTAL

The photoelectron spectra were recorded on a Perkin-Elmer PS-18 photoelectron spectrometer using a He(I) source. Xenon and Argon were used as internal calibrants. The resolution was 20-30 meV in all cases, as measured at FWHM (full-width at half-maximum intensity) on the Argon  $2P_{3/2}$  signal at 15.76eV. Vertical and adiabatic IPs are reported as the average of at least five determinations.

The following research groups supplied the samples:

- a) the piperidines were obtained from the laboratories of Professor J. D. Roberts of the California Institute of Technology, Pasadena, California.
- b) the oxanes and 1,3-dioxanes were obtained from the laboratories of Professor E. L. Eliel of the University of North Carolina, Chapel Hill, North Carolina.
- c) the 4-tert-butylcyclohexanones were obtained from the laboratories of Professor R. R. Fraser of the University of Ottawa, Ottawa, Ontario, Canada.
- d) the N-arylazacycloalkanes were obtained from the laboratories of Professor S. Searles, Jr. of the University of Missouri, Columbia, Missouri.
- e) phencyclidine and its analogs were obtained from the National Institute on Drug Abuse.
- f) the exocyclic alkenes were obtained from the laboratories of Professor S. P. McManus of the University of Alabama, Huntsville, Alabama.

g) the cumenes and cyclopropylbenzenes were obtained from Professor S. S. Hixson of the University of Massachusetts, Amherst, Massachusetts.

Commercially available samples were also recorded for completeness and reference to previous work.

## PART II. THEORETICAL STUDIES OF QUINONES

## CHAPTER VIII. QUINONES

## INTRODUCTION

Quinones represent a special type of  $\alpha, \beta$ -unsaturated ketones. As a class of compounds, they are among the oldest known and most interesting.<sup>1</sup> Quinones came to man's attention in two ways-- as pigments and as drugs.<sup>2</sup>

The quinone pigments are probably the largest class of natural coloring matters, but they make relatively little contribution to natural coloring. They are found mainly in the bark or underground portions of plants and if found elsewhere, are usually masked by other pigments. Two pigments which stand out are henna and madder. Henna is a paste made from powdered leaves and has been used since ancient Egypt as a cosmetic to dye fingernails, hair and beards, hands, feet, and the manes of horses. Madder is prepared from the roots of certain plants and contains the anthraquinone, alizarin. It has been used as a cloth dye, a foodstuff, a drug, and as a preventative against witchcraft. The synthesis of alizarin and the development of a commercial process in the mid-1800s are milestones of organic chemistry.<sup>3</sup>

Quinones were exploited by the Chinese as early as 2700 B.C. for drug purposes.<sup>2</sup> More recently, many have been found to exhibit significant antifungal, antibiotic, antimalarial, or antitumor activity. Adriamycin and daunomycin are two anthracycline antibiotics effective in cancer chemotherapy which have been the

targets of synthesis using quinone cycloadditions.<sup>4-8</sup> Cycloadditions to para-benzoquinones have been the cornerstones of syntheses of steroids,<sup>9</sup> cortisone,<sup>10</sup> reserpine, yohimbine, estrone, terramycin,<sup>11</sup> and gibberellic acid,<sup>12-13</sup> among others. One of the most characteristic reactions of quinones is their ease of reduction and re-oxidation.<sup>1</sup> Quinones are known to play key roles in photosynthesis<sup>14</sup> and in the respiratory electron transport chain,<sup>15</sup> in the biosynthesis of tetracycline antibiotics<sup>16</sup> and of aflatoxins,<sup>17</sup> in the mechanism of blood clotting,<sup>18</sup> in the defense mechanisms of various insects,<sup>19</sup> and possibly in the aging process.<sup>20</sup> The ease with which quinones undergo reversible reduction to semiquinones and hydroquinones is thought to account for their special abilities in many of these roles.<sup>2,21</sup>

This work is a report on two theoretical investigations. Non-benzenoid aromatics have been studied intensively in the last 25 years.<sup>22-26</sup> In view of the abundance of quinone chemistry, it is ironic that the first quinone of azulene was not prepared and characterized until 1980.<sup>27</sup> We have investigated the possible quinones of azulene, via the MINDO/3 method, to assess their relative stabilities and reactivities.<sup>28</sup> We have also systematically examined the influence of substituents upon the shapes of the frontier molecular orbitals of benzoquinones and naphthoquinones,<sup>29</sup> in order to rationalize the sites of reaction of these species with nucleophiles.



### THE QUINONES OF AZULENE

The quinones of azulene, or azuloquinones, lie at the cross-roads of several different avenues of interest and intense research. The last 25 years have witnessed a tremendous growth in the amount of information concerning non-benzenoid hydrocarbons,<sup>22-26</sup> i.e. compounds which display aromatic character despite the absence of benzene rings. The parent hydrocarbon of the azuloquinones, azulene, was an early member of this group of compounds.<sup>22</sup> Azulene also represents a special class of fused bicyclic compounds in which both rings comprise a non-benzenoid cycle of p orbitals. The fact that azuloquinones would be isomeric with the naphthoquinones increases the interest in these compounds. While no azuloquinones have been isolated as natural products,<sup>1</sup> it is surprising that not a single member of this group of compounds had been prepared and characterized prior to 1980.<sup>27</sup>

Compared to the ten possible naphthoquinone structures, there are sixteen potential azuloquinones, each of which we have given abbreviated names for easier reference, e.g. 12-AQ for 1,2-azuloquinone, Figures 1 and 2. There are some naphthoquinones and azuloquinones for which no bicyclic Kekulé structure can be drawn, i.e. "non-classical quinones" (cf. meta-benzoquinone). While calculations on some of the classical benzoquinones (BQs) and naphthoquinones (NQs) have been carried out using an SCF-LCAO program,<sup>30-32</sup> we are unaware of any systematic, comprehensive

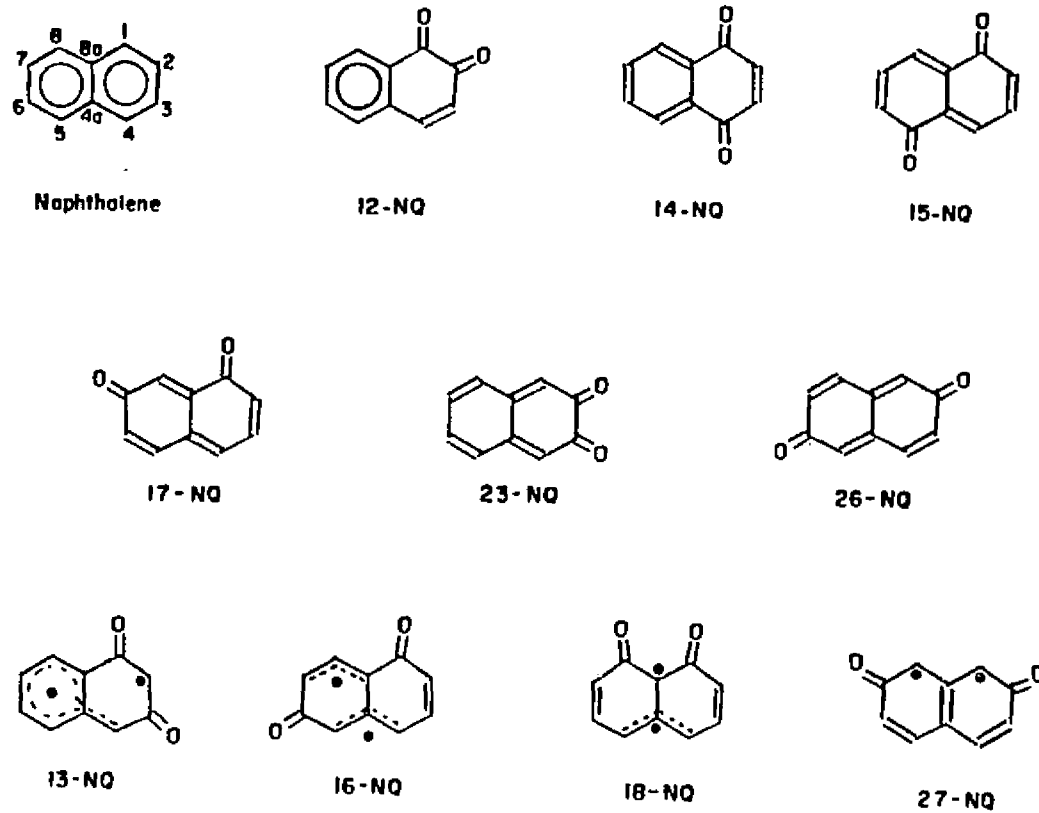


Figure 1. Naphthalene and the Naphthoquinones (NQs). Geometries shown are those obtained by MINDO/3 optimizations.

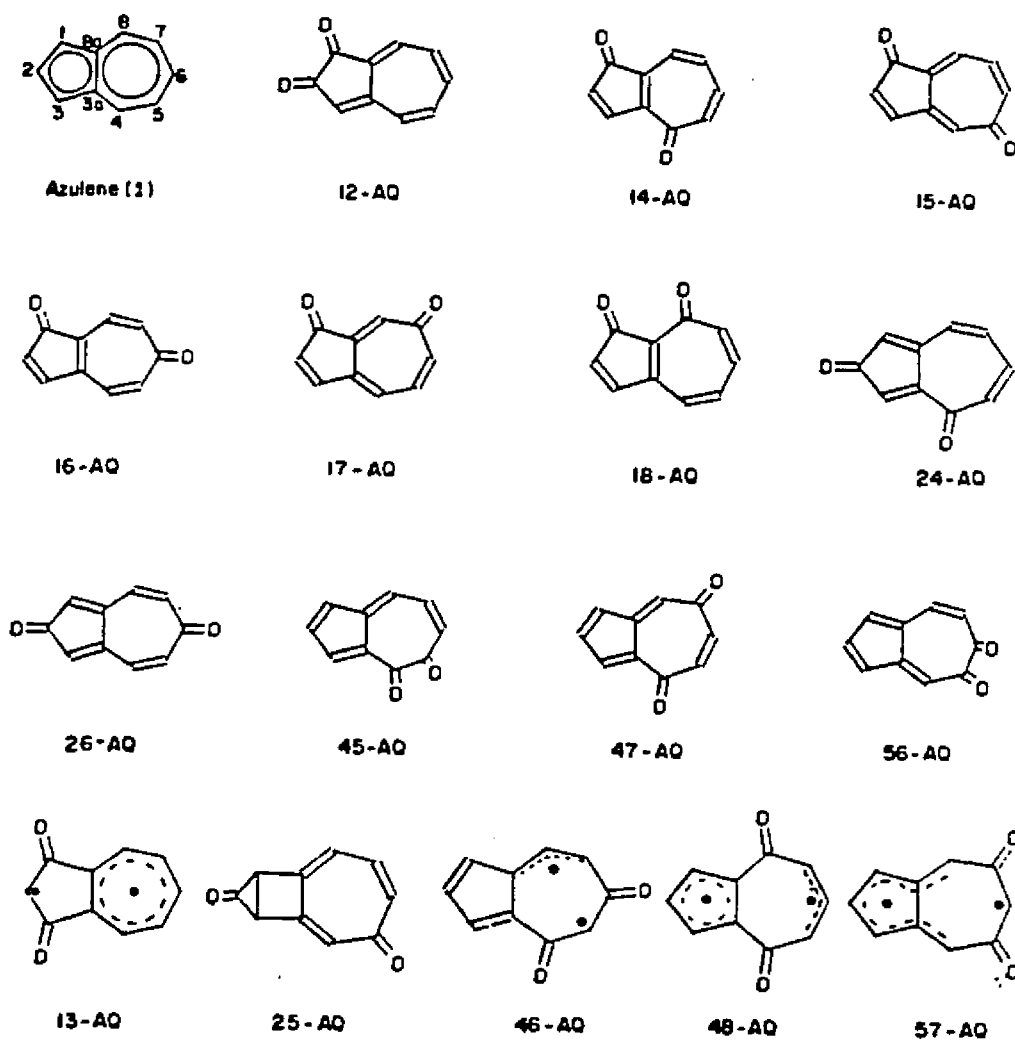


Figure 2. Azulene and the Azuloquinones (AQs). Geometries shown are those obtained by MINDO/3 optimizations.

calculations on these two groups which would provide a basis for direct comparison to the azuloquinones. Therefore, we have calculated, using the MINDO/3 program, the energies and optimized geometries of all the benzoquinones, naphthoquinones, and azuloquinones, including the non-classical structures.

The MINDO/3 program has been shown to provide reasonably reliable heats of formation of C,H,N,O molecules.<sup>33-34</sup> Despite its tendency to provide CH and CC bond lengths which are 0.01-0.015 Å too long, the program has a fairly accurate, rapid method for geometry optimization. The benzoquinone and naphthoquinone and results provide an immediate link to experimental data and serve as a guide in determining the validity of the azuloquinone calculations. STO-3G calculations<sup>35</sup> using the MINDO/3 optimized geometries were also carried out on selected species to test the MINDO/3 trends.

The azuloquinones are an attractive testing ground for theories of structure, bonding, and reactivity. The abundance of isomers will permit extensive comparisons to be made. It is well-known that calculations generally prove to be more successful in predicting differences between similar compounds, rather than absolute quantities. It is quite probable that some members will exhibit similar properties, thus presenting a demanding challenge to the theoretical model.

In several of the quinones, the optimized geometries were significantly non-planar. These structures are shown in Figure 3.

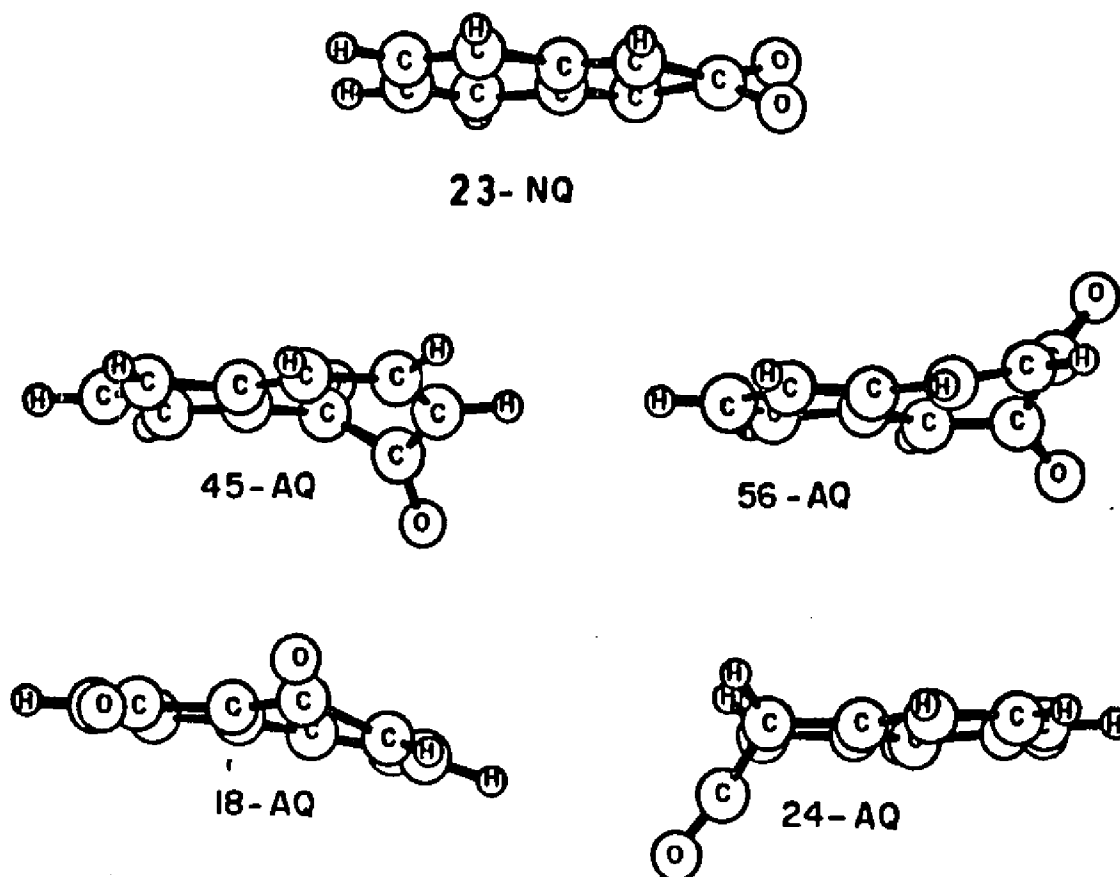
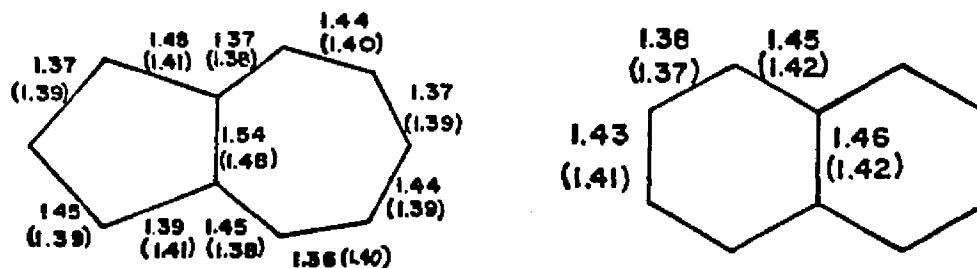


Figure 3. ORTEP Plots of the Quinones Predicted to be Nonplanar.

A major source of non-planarity is the relief of eclipsing that can occur with 1,2-diketones. Thus, 23-NQ, 45-AQ, and 56-AQ are significantly non-planar. A slight non-planarity in 18-AQ also relieves peri interactions between the two oxygen atoms. Finally, the non-classical 25-AQ is not an energy minimum, but collapses to a highly strained cyclopropanone. This species is partly stabilized due to formation of an aromatic (tropone) ring upon cyclization, a course not available to the other non-classical quinones.

MINDO/3 has a tendency to produce bond alternation in aromatic systems, based on the results for naphthalene and azulene, as shown below.



The naphthoquinones and azuloquinones are all predicted to show strong bond alternation, in agreement with experimental data on known quinones.<sup>36</sup> The formal double bonds all have lengths of 1.35–1.40 Å, except when the double bond forms the bridge, i.e. C-4a to C-8a in 12-NQ and 14-NQ or C-3a to C-8a in the azuloquinones. The C-C single bond lengths are all 1.45–1.55 Å, the C-C(O) bonds are 1.48–1.54 Å, the C(O)-C(O) bonds are 1.53–1.55 Å, and the CO double bonds are 1.20–1.21 Å. In every case, for both

sets of quinones, the bond shared by the two rings is longer than normal, whether it is a single bond or a double bond. We interpret these data to imply that  $\pi, \pi$  interaction along the central bond is not particularly favorable (cf. azulene<sup>37</sup>). As stated before, MINDO/3 does have a tendency to overestimate such bond lengths.

The heats of formation and MINDO/3 orbital energies for all the quinones are given in Tables 1, 2, and 3. From these data, relative trends for physical and chemical properties can be predicted. The MINDO/3 heats of formation ( $\Delta H_f$ ) allow the azuloquinones to be ranked from the lowest (most stable) to the highest (least stable) as follows:

$$15 < 17 < [14, 16, 18, 12] < [24, 26] < [45, 47] < 56$$

The azuloquinones which contain a tropone ring (15-AQ and 17-AQ) are more stable than those which contain a cyclopentadienone ring (24-AQ and 26-AQ). Those which contain both types of annulenone rings (14-AQ, 16-AQ, and 18-AQ) have intermediate stabilities. The non-classical azuloquinones are predicted to be much less stable. The range of stabilities is rather large and it is interesting to note that all the 1,n-AQs have  $\Delta H_f < 0$ , whereas all the m,n-AQs ( $m \neq 1$ ) have  $\Delta H_f > 0$ .

Calculated MINDO/3 heats of formation are in adequate agreement with experimental results for 14-BQ<sup>38</sup> ( $\Delta H_f^{\text{exptl}} = -29.3$

Table 1. Results of Calculations on the Benzoquinones.

Compound	$\Delta H_f$ MINDO/3 (kcal/mole)	LUMO MINDO/3 (eV)	HOMO MINDO/3 (eV)	HOMO/ LUMO gap MINDO/3 (eV)
"Classical"				
12-BQ	-35.5	-9.83	-0.94	8.89
14-BQ	-40.8	-10.91	-1.03	9.88
"Nonclassical"				
13-BQ	+10.4	-8.59	-2.79	5.80
=====				



Table 2. Results of Calculations on the Naphthoquinones.

Compound	$\Delta H_f$ MINDO/3 (kcal/mole)	LUMO MINDO/3 (eV)	HOMO MINDO/3 (eV)	HOMO/ LUMO gap MINDO/3 (eV)
"Classical"				
12-NQ	-16.9	-8.93	-0.77	8.16
14-NQ	-22.7	-9.26	-0.80	8.46
15-NQ	-9.4	-8.93	-1.26	7.67
17-NQ	-7.3	-8.96	-1.32	7.64
23-NQ	-0.4	-8.55	-1.26	7.29
26-NQ	-7.1	-9.42	-1.41	8.01

Table 2. (continued)

Compound	$\Delta H_f$ MINDO/3 (kcal/mole)	LUMO MINDO/3 (eV)	HOMO MINDO/3 (eV)	HOMO/ LUMO gap MINDO/3 (eV)
"Nonclassical"				
13-NQ	+27.0	-8.11	-2.56	5.55
16-NQ	+29.5	-7.75	-2.76	4.99
18-NQ	+25.3	-7.84	-2.49	5.35
27-NQ <sup>a</sup>	---	---	---	---

=====

a) This quinone is not an energy minimum.

Table 3. Results of Calculations on the Azuloquinones.

Compound	$\Delta H_f$ MINDO/3 (kcal/mole)	LUMO MINDO/3 (eV)	HOMO MINDO/3 (eV)	HOMO/ LUMO gap MINDO/3 (eV)
"Classical"				
12-AQ	-0.4	-8.41	-0.70	7.72
14-AQ	-0.8	-8.80	-1.03	7.77
15-AQ	-6.4	-9.27	-0.63	8.64
16-AQ	-0.6	-8.87	-1.17	7.70
17-AQ	-5.3	-9.01	-0.66	8.35
18-AQ <sup>a</sup>	+8.9	-9.01	-0.94	8.06
24-AQ	+4.7	-8.94	-1.16	7.78
26-AQ	+4.7	-9.18	-1.28	7.91
45-AQ <sup>a</sup>	+7.0	-8.82	-0.95	7.86
47-AQ	+7.2	-9.40	-1.16	8.23
56-AQ <sup>a</sup>	+9.5	-8.74	-0.96	7.78

Table 3. (continued)

Compound	$\Delta H_f$ MINDO/3 (kcal/mole)	LUMO MINDO/3 (eV)	HOMO MINDO/3 (eV)	HOMO/ LUMO gap MINDO/3 (eV)
"Nonclassical"				
13-AQ	+14.2	-7.91	-1.75	6.16
25-AQ <sup>b</sup>	---	---	---	---
46-AQ	+56.8	-8.02	-2.82	5.20
48-AQ	+54.1	-7.93	-2.94	4.99
57-AQ	+50.5	-7.88	-2.60	5.28

=====

a) Non-planar geometry after optimization; some orbitals out of plane by 0.1-0.3Å.

b) This quinone is not an energy minimum, but collapses to tricyclo[5.3.0.0<sup>8,10</sup>]-deca-1,4,6-trien-3,9-dione on optimization.

kcal/mole, cf. Table 1) and 14-NQ<sup>38</sup> ( $\Delta H_f^{\text{exptl}} = -26.5$  kcal/mole, cf. Table 2). The large negative  $\Delta H_f$  for 14-NQ (and 12-NQ) undoubtedly reflects the stability derived from the intact benzene ring present in the quinone. Of the "extended" naphthoquinones, 26-NQ has been known for many years.<sup>39</sup> The parent 15-NQ has resisted characterization, although the 3,7-di-tert-butyl derivative has been reported.<sup>40</sup> The reactivities of the known naphthoquinones correlate roughly with their MINDO/3 heats of formation, which range from -22.7 to -7.1 kcal/mole. The azuloquinones predicted to be most stable lie just below this range (cf. Table 3), although direct comparisons of  $\Delta H_f$  values may be misleading. Hückel calculations on these naphthoquinones and azuloquinones are consistent with the MINDO/3 results.

Ab initio STO-3G calculations were performed on three of the quinones using the MINDO/3 optimized geometries as an additional check on the validity of the MINDO/3 results. Relative energies by STO-3G for 26-NQ, 15-AQ, and 26-AQ are 0, +9.7, and +20.8 kcal/mole, respectively. MINDO/3 predicts the same order, although a smaller range, with  $\Delta H_f = 0$ , +0.7, and +11.8 kcal/mole.

According to frontier molecular orbital theory,<sup>41-42</sup> the two important quantities used in the rationalization of reactivity are the HOMO and LUMO energies. Using Koopmans' theorem,<sup>43</sup> the negative of the HOMO energy is equal to the ionization potential, which provides a measure of reactivity towards electrophiles. The first IP (HOMO) for all the azuloquinones is calculated to arise

from a  $\pi$  orbital, which lies higher than the non-bonding orbitals of the oxygen atoms. The first IPs fall in the range of 8.41 eV to 9.40 eV for the azuloquinones and a nearly identical range for the naphthoquinones. For comparison, the  $\pi$  IP of 14-BQ is calculated to occur at 10.91 eV, in excellent agreement with the observed IP at 10.93 eV,<sup>44</sup> by photoelectron spectroscopy. The azuloquinones can be ranked according to their HOMO energies (Table III), with the highest HOMO energy corresponding to the least reactivity toward electrophiles, as follows:

$$47 > 15 > [17,18] > 24 > [16,45,14,56] > 12$$

With the exception of 47-AQ, the thermodynamically most stable azuloquinones (15-AQ and 17-AQ) have the highest HOMO energies, and should be least reactive with electrophiles. The reactions of diazonium salts with benzoquinones and naphthoquinones have been studied, generally with poor to moderate yields.

The negative of the LUMO energy is equal to the electron affinity,<sup>43</sup> which provides a measure of reactivity towards nucleophiles. MINDO/3 indicates that the most stable azuloquinones (15-AQ, 17-AQ, and 12-AQ) have the highest LUMO energies (Table 3), i.e. they should be the least reactive toward nucleophiles. The complete ranking is as follows:

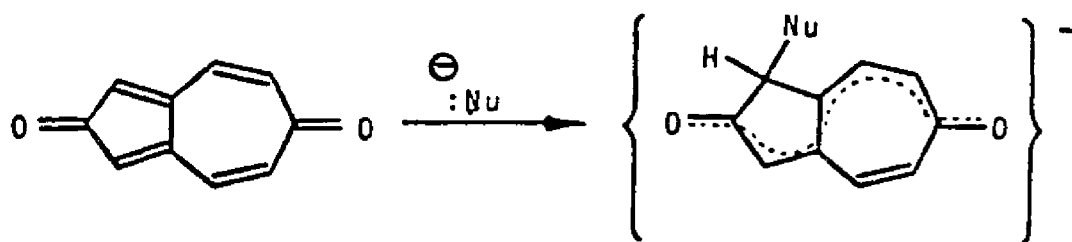
$$[15,17,12] > [18,45,56] > 14 > [47,24,16] > 26.$$

The STO-3G calculations on selected quinones referred to earlier give the same order of LUMO energies as MINDO/3. Prior theoretical work on quinones<sup>45-47</sup> has shown that electrochemical reduction potentials and the ability to form charge-transfer complexes both correlate with the electron affinities. The quinones with the highest LUMO are the hardest to reduce and form the least stable charge-transfer complexes. On an absolute scale, the azuloquinones ( $E_{\text{LUMO}} = -0.63$  to  $-1.28$  eV) are predicted to be harder to reduce than the extended naphthoquinones ( $E_{\text{LUMO}} = -1.26$  to  $-1.41$  eV). 12-BQ and 14-BQ<sup>45</sup> ( $E_{\text{LUMO}} = -1.0$  eV) fall in the middle of the azuloquinone range. From the reported reduction potentials for 14-BQ and 26-NQ, we predict that all the azuloquinones should have reduction potentials below 0.8 V. [The sole azuloquinone which has been characterized (12-AQ) has a reduction potential of  $-0.55$  V (vs. SCE) in acetonitrile.<sup>27</sup>]

Nucleophilic additions comprise the major known reactions of quinones.<sup>48</sup> As with many other electron-deficient  $\pi$  systems, quinones are susceptible to Michael additions. In molecular orbital terminology, this involves an interaction between the HOMO of the nucleophile and the LUMO of the acceptor (quinone). In the absence of other factors, the closer these two orbitals lie in energy, the faster the reaction should be. It follows that the reactivity of the azuloquinones should correlate with their LUMO energies, with those having the highest LUMO energy being least susceptible to Michael additions. Thus, 15-AQ and 17-AQ are again expected to be

least reactive. The azuloquinones should all be less reactive than the extended naphthoquinones.

Nucleophilic attack on a quinone, or any electron-deficient molecule, should be favored at the atom which has the largest LUMO coefficient.<sup>33-34</sup> We have shown that LUMO coefficients correctly predict the sites of reaction by nucleophiles with substituted benzoquinones and naphthoquinones.<sup>29</sup> The LUMO coefficients for the the azuloquinones, as obtained from the MINDO/3 calculations, are given in Table 4. For 26-AQ, attack should occur in the 1 position, as shown below.



This exemplifies a feature of the azuloquinones not shared by benzenoid quinones, viz., nucleophilic addition can lead to an anionic intermediate in which the charge is delocalized over both oxygen atoms. For the 1,n-azuloquinones (containing a tropone unit), MINDO/3 predicts a preferential attack at the ring junction.

Electron-donating substituents on the electron-deficient azuloquinones should raise the LUMO energy, being most effective when added to the site(s) with the largest coefficient.<sup>41-42</sup> Since these positions are also the locations predicted for nucleophilic attack, the substituents could impede Michael additions, both sterically and by raising the LUMO energy. For example, MINDO/3



Table 4. Calculated LUMO Coefficients of the Azuloquinones in Figure 3 (MINDO/3).

Compound	C-1	C-2	C-3	C-3a	C-4	C-5	C-6	C-7	C-8	C-8a	O-1	O-2
"Classical"												
12-AQ	0.28	0.22	0.15	-0.25	-0.38	0.33	0.34	-0.36	-0.22	0.33	-0.27	-0.21
14-AQ	0.29	0.29	-0.28	-0.48	-0.12	-0.25	-0.02	-0.36	0.17	0.44	-0.28	-0.11
15-AQ	0.33	0.25	-0.33	-0.23	0.08	0.28	0.34	-0.35	-0.28	0.36	-0.29	-0.24
16-AQ	0.29	0.31	-0.28	-0.47	0.13	-0.34	0.01	-0.32	0.11	0.44	-0.29	-0.01
17-AQ	0.25	0.37	-0.34	-0.41	0.34	0.34	-0.37	-0.22	0.03	0.12	-0.22	0.19
18-AQ <sup>a</sup>	0.28	0.31	-0.25	-0.45	-0.19	0.37	0.38	-0.23	0.08	0.46	-0.28	-0.08
24-AQ	0.37	0.30	0.37	-0.27	-0.23	-0.24	0.24	0.28	-0.26	-0.32	-0.30	-0.24
26-AQ	0.38	0.30	0.38	-0.31	-0.23	0.25	0.23	0.25	-0.23	-0.31	-0.30	-0.23
45-AQ <sup>a</sup>	0.33	-0.27	-0.39	0.27	0.16	-0.12	0.33	-0.24	-0.43	0.33	-0.11	-0.05
47-AQ	0.33	-0.25	-0.42	0.25	0.22	0.23	-0.20	-0.29	-0.38	0.32	-0.22	-0.28
56-AQ <sup>a</sup>	0.42	0.28	-0.34	-0.31	0.43	0.19	0.12	0.24	-0.21	-0.31	-0.13	-0.05

Table 4. (continued)

Compound	C-1	C-2	C-3	C-3a	C-4	C-5	C-6	C-7	C-8	C-8a	O-1	O-2
"Nonclassical"												
13-AQ	0.09	0.01	-0.09	-0.42	-0.23	0.50	-0.01	-0.50	0.24	0.41	-0.12	0.12
46-AQ	0.20	-0.29	-0.39	0.09	0.10	0.27	-0.02	-0.54	-0.10	0.55	-0.15	0.07
48-AQ	0.28	-0.04	-0.32	-0.11	0.10	0.58	-0.02	-0.61	0.08	0.21	-0.17	-0.14
57-AQ	0.57	0.00	-0.56	0.01	-0.39	-0.09	0.00	-0.09	-0.39	-0.01	-0.14	-0.14
=====												

a) Nonplanar geometry after optimization;  $p_z$  coefficient taken perpendicular to the approximate plane of the molecule.

predicts that donor substituents on the cyclopentadienone ring of 24-AQ and 26-AQ should be most effective in protecting these quinones from nucleophilic attack. The effect of donor substituents should also be evident in the rate of dimerization or polymerization, as discussed below. The substituents raise the LUMO energy, which increases the HOMO-LUMO gap, and retard the reaction. Electron-withdrawing substituents would be expected to lower the LUMO energy and accelerate the reaction. It is not surprising, therefore, that attempts to prepare a 2,6-azuloquinone bearing carbethoxy groups at the 1 and 3 positions yielded only the corresponding dimer.<sup>49</sup>

The tendency for dimerization and/or polymerization may be analyzed in terms of the interaction between the HOMO of one molecule with the LUMO of the other. As before, the rate of dimerization should be greatest for those azuloquinones with the smallest HOMO-LUMO gaps, other factors being equal. Consistent with the previous predictions of high stability for 15-AQ and 17-AQ, these quinones are indicated to have the largest HOMO-LUMO gaps. The other azuloquinones are not grouped in any obvious pattern, as follows:

$$15 > 17 > 47 > 18 > 26 > 45 > [24,56,14] > [12,16]$$

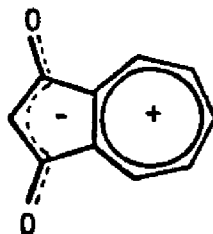
It is probably not accidental that the four known naphthoquinones are those with the largest HOMO-LUMO gaps. In fact, they were

prepared and characterized in order according to the magnitude of their HOMO-LUMO gaps: 14-NQ<sup>50</sup> (1873, 8.46 eV), 12-NQ<sup>51</sup> (1877, 8.16 eV), 26-NQ<sup>52</sup> (1907, 8.01 eV), and 3,7-di-tert-butyl-15-NQ<sup>40</sup> (1975, 7.67 eV).

The magnitude of the HOMO-LUMO gap is related to the energy of the  $\pi \rightarrow \pi^*$  transition,<sup>53</sup> and therefore to the color of these quinones. The naphthoquinones range in color from canary yellow for 14-NQ to orange for 12-NQ to red for the extended 26-NQ and 15-NQ, in correct agreement with the order of their HOMO-LUMO gaps. A comparison of the calculated HOMO-LUMO gaps in the azuloquinones suggests that these compounds will also range in color from yellow to orange to red.

None of the non-classical quinones at the bottom of either Figure 1 or 2 have ever been isolated. No simple Kekulé structure can be drawn for any of these, and we expect these compounds to have less favorable heats of formation, and smaller HOMO-LUMO gaps due to higher lying HOMOs and lower lying LUMOs, compared to the classical quinones. The MINDO/3 results are consistent with these expectations. Thus, the non-classical quinones are all predicted to suffer easy dimerization, polymerization, nucleophilic reduction, and reduction. Two azuloquinones yield unusual results worthy of note. 25-AQ is not an energy minimum, but collapses to a tricyclic structure, as indicated in Figure 2. The results for 13-AQ are particularly intriguing. Examination of the MINDO/3 geometry and the Hückel charge density pattern<sup>28</sup> suggests that

13-AQ can best be pictured as shown:



It is difficult to conceive of any non-classical quinone with a more stabilized zwitterionic form than this one in which both rings have aromatic character. 13-AQ is predicted to have the most favorable heat of formation, the largest HOMO-LUMO gap, and the highest lying LUMO of the non-classical quinones. Of them all, this one has the best chance for being observed.

#### AZULOQUINONE SUMMARY

Which of the azuliquinones will be the most stable? MINDO/3 has clearly predicted 15-AQ to have the most favorable heat of formation, the least susceptible to dimerization or polymerization, resistant to Michael addition, and difficult to reduce. The closely related 17-AQ probably ranks second overall. In general, the 1,n-azuliquinones are more stable, with more favorable heats of formation, higher reduction potentials, and higher lying LUMOs than the m,n-azuliquinones ( $m \neq 1$ ). Their susceptibility to dimerization varies considerably. The difficulties in making a final, complete ranking are exemplified by the following two

isomers: 12-AQ has a low heat of formation, should be resistant to reduction and nucleophilic attack, but has a small HOMO-LUMO gap which predicts rapid dimerization. Precisely the opposite predictions are made for 47-AQ. It should not dimerize, but is easier to reduce and is susceptible toward nucleophiles.

The presence of a tropone ring seems to favor stability. The azuloquinones with a tropone ring only are more stable than those which have both a tropone ring and a cyclopentadienone ring. Those quinones which contain only a cyclopentadienone ring are even less stable. A pentafulvene subunit seems even less favorable. Only 12-AQ possesses none of these systems.

These quinones could easily find practical applications. A large number of quinones have been tested and exhibit significant antitumor activity.<sup>54-55</sup> The wide range of predicted reduction potentials and alkylating abilities for the azuloquinones and their derivatives makes them promising candidates worthy of testing. The preparation of tetracyanoquinodimethide analogues would greatly expand the range of  $\pi$  acceptors available in the search for better solid state organic conductors.

#### SUBSTITUENT EFFECTS ON BENZOQUINONE MOLECULAR ORBITALS

A large quantity of information is available which details the preferred site(s) of attack by nucleophiles on benzoquinones and naphthoquinones. A number of Diels-Alder cycloadditions have also

been investigated to determine the regioselectivities of various substituents in these reactions, including methoxy-substituted benzoquinones and naphthoquinones. This is a study on the effect of substituents on the frontier molecular orbitals of these quinones to explain and make predictions about future reactions involving these quinones.

Finley<sup>48</sup> has provided an excellent survey of additions and cycloadditions to quinones. The results of kinetic additions have been summarized in Figures 4 and 5, although examples of thermodynamic control of cycloadditions through adduct rearrangement have been observed. Finley's review may be consulted for specific examples and greater detail.

Because the majority of additions and cycloadditions to quinones involve electron-rich nucleophiles, we will concentrate our attention on the low lying vacant molecular orbitals of the quinones. The LUMOs can be used in the context of frontier molecular orbital theory to explain the orientation of nucleophilic additions. According to frontier molecular orbital theory,<sup>41-42,56-60</sup> the rate and regioselectivity of a molecule with a nucleophile is dominated by the interaction of the LUMO of the molecule in question with the HOMO of the nucleophile. The closer these two orbitals are in energy, the more strongly they will interact and the faster the reaction will be. The orbital overlap will be greatest when the nucleophile interacts at the site of the largest LUMO coefficient. The most nucleophilic

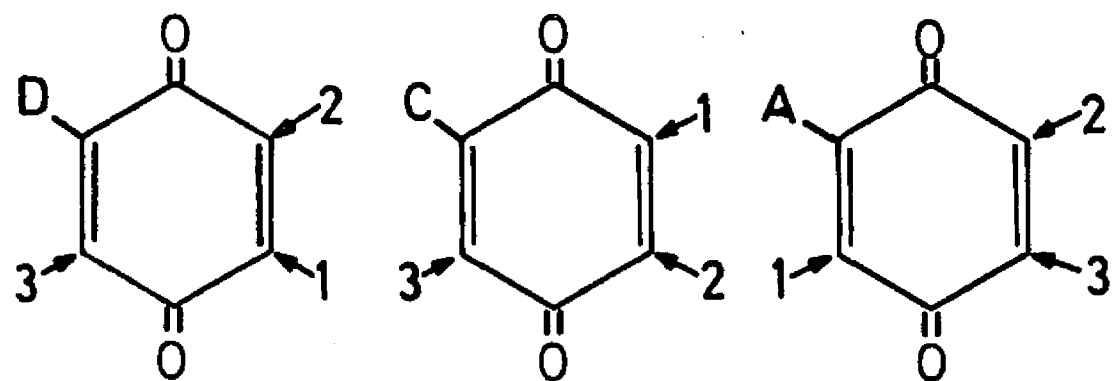


Figure 4. Summary of Sites of Attack by Nucleophiles on Substituted Benzoquinones. (D = donor, A = acceptor, C = conjugating substituent; position 1 is the most reactive, followed by 2, etc.)



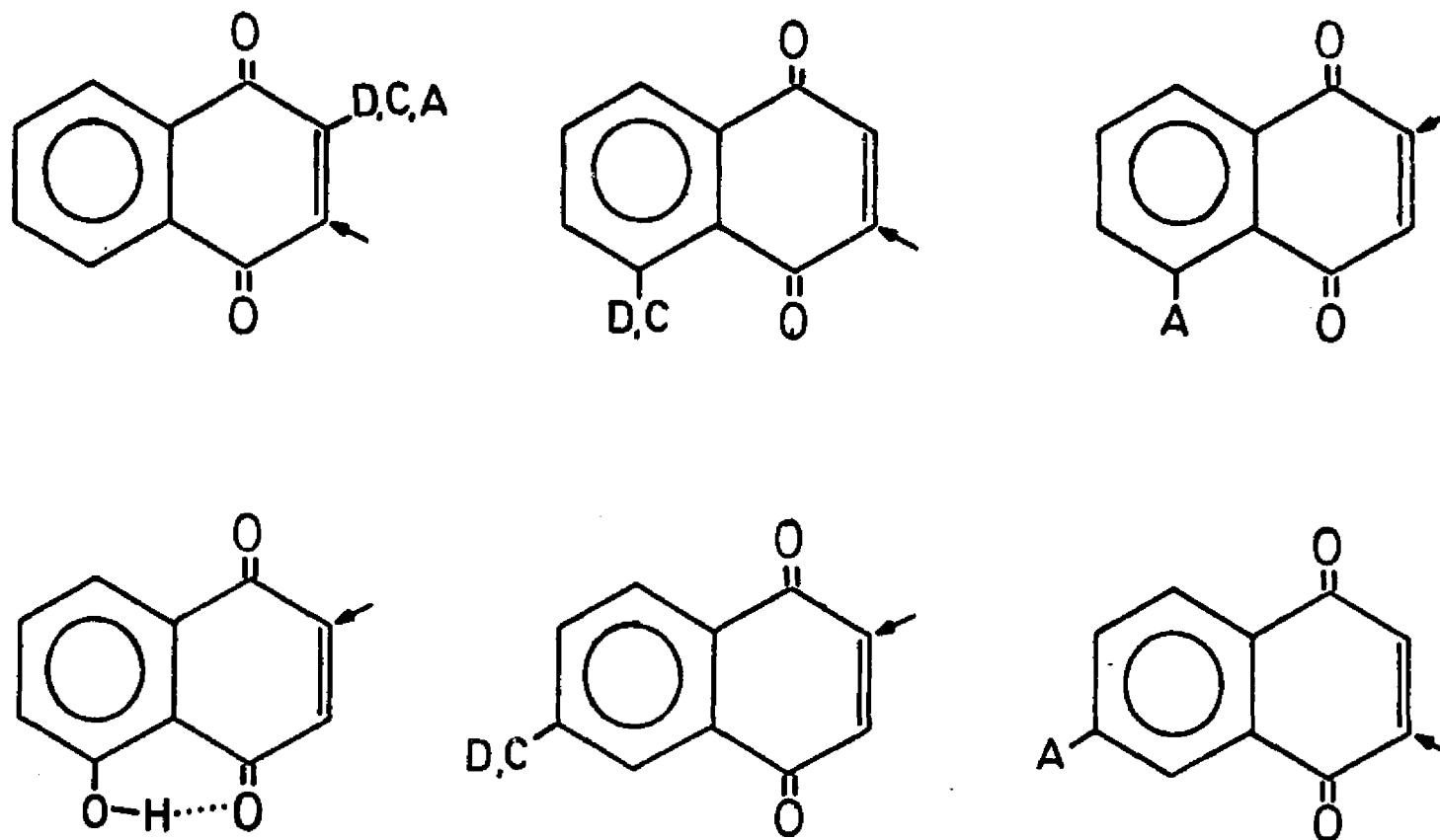


Figure 5. Summary of Sites of Attack by Nucleophiles on Substituted Naphthoquinones. (D = donor, A = acceptor, C = conjugating substituent)

terminus of a diene has the largest HOMO coefficient and should become attached to the largest LUMO coefficient site, even if the cycloaddition process is concerted.<sup>42</sup>

The previous section reported the results of semi-empirical (MINDO/3) calculations on benzoquinones,<sup>28</sup> supplemented by ab initio STO-3G calculations on a few select cases. Only STO-3G results are reported here.<sup>29</sup> Both methods generally give the same ordering of the high-lying filled and low-lying vacant orbitals of quinones. Furthermore, the substituent effects on the LUMO coefficients which are studied here are sufficiently large so that all the computational methods give qualitatively similar results. For economic reasons, the calculations utilized a benzoquinone geometry based on the crystal structure,<sup>61</sup> with substituents comprised of standard geometries<sup>62</sup> used to replace one of the hydrogens.

The two highest occupied and two lowest vacant orbitals of benzoquinone are shown in Figure 6. These  $\pi$  orbitals are heavily concentrated on the CC double bonds. Both filled orbitals are  $\pi_{CC}$  bonding orbitals while both vacant orbitals are  $\pi_{CC}$  antibonding orbitals. Negatives of the experimental ionization potentials<sup>63-64</sup> are shown in parentheses to compare with the calculated orbital energies of the occupied orbitals. The first electron affinity (EA) of benzoquinone<sup>65</sup> has also been indicated for comparison. The electron affinity which corresponds to placing the electron in the second lowest unoccupied molecular orbital (SLUMO) has been

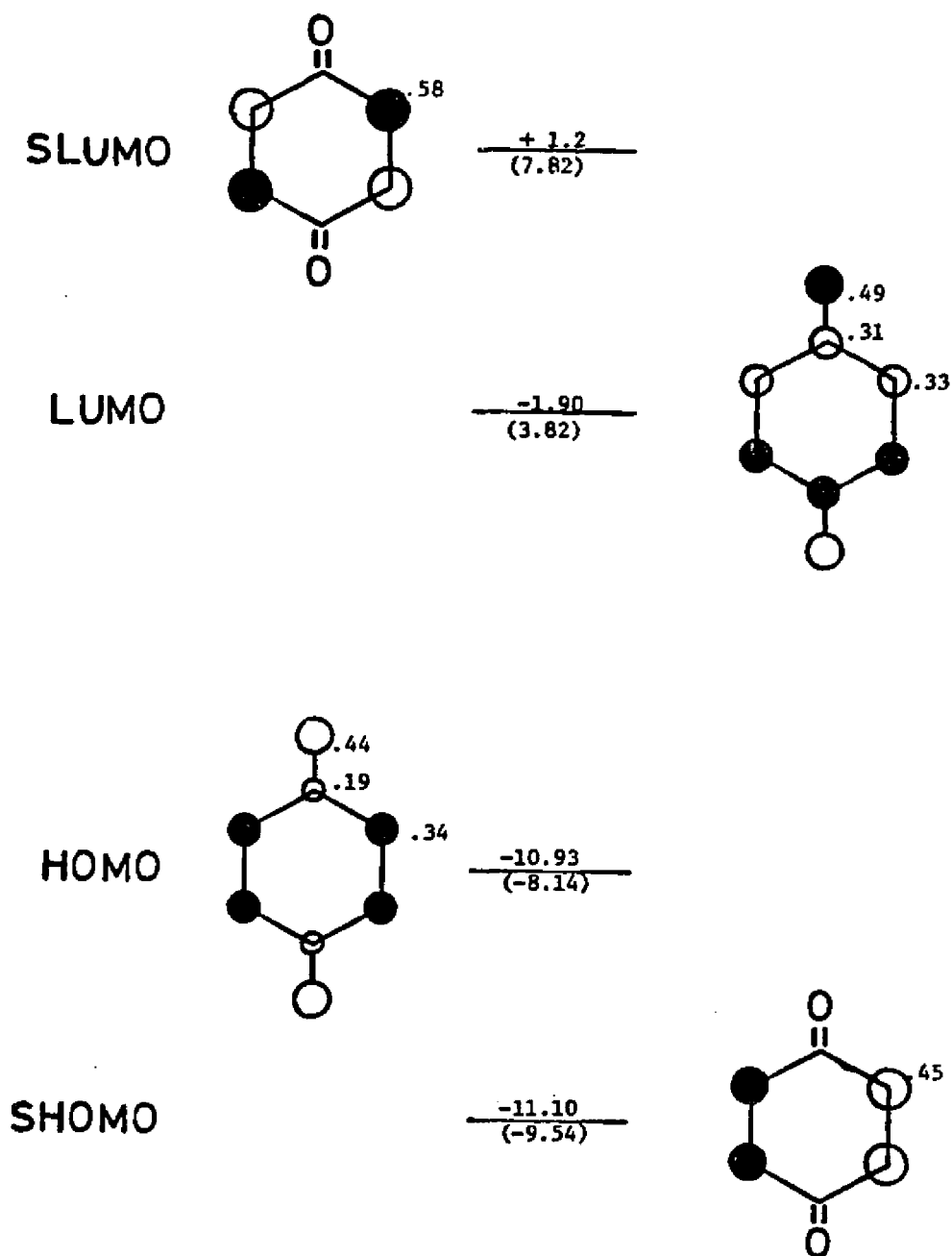


Figure 6. Some STO-3G  $\pi$  Molecular Orbitals and Energies of Benzoquinone.

estimated in the following manner: ethylene (experimental EA = -1.78 eV<sup>66</sup>) has a calculated LUMO energy of 8.68 eV, according to STO-3G. This is less than 1 eV above the energy of the SLUMO of benzoquinone. Therefore, the second EA of benzoquinone should be only slightly less negative than the EA of ethylene. We estimate (crudely) the second EA of benzoquinone to be 0.6 eV higher than that of ethylene.

The LUMO of benzoquinone is lowered in energy to a large extent because it is of the correct symmetry to interact with the carbonyl  $\pi^*$  orbitals. The SLUMO and the SHOMO have a nodal plane through the carbonyl orbitals, and are thus inductively lowered in energy. The HOMO is lowered both by induction and by admixture with the carbonyl  $\pi^*$  orbitals. However, these energy lowering effects are partially counteracted due to interaction with lower lying  $\pi$  orbitals of the carbonyl groups. As a point of reference, benzoquinone is a more electron-deficient species than fumaronitrile (IP = 11.15 eV, EA = 0.7 eV<sup>67</sup>) as assessed by the EA.

Upon the addition of a substituent, the symmetry of benzoquinone is reduced, and mixing occurs among the four  $\pi$  orbitals and the orbitals of the substituent. The STO-3G orbital energies and coefficients for several monosubstituted benzoquinones are given in Table 5. Standard substituent geometries were used, except for the methoxy group, where the normal aromatic methoxy group bond angles were used. (The aromatic C-C-O bond angle is 124° and the C-O-C bond angle is 118°). When several substituent

Table 5. Frontier  $\pi$  Molecular Orbitals (STO-3G) of Benzoquinone and 2-Substituted Benzoquinones.<sup>a</sup>

Benzoquinone	HOMO					LUMO				
	$\epsilon$	C-2	C-3	C-5	C-6	$\epsilon$	C-2	(-)C-3	(-)C-5	C-6
parent	-8.14	0.34	0.34	0.34	0.34	3.82	0.33	0.33	0.33	0.33
2-methyl	-7.97	0.38	0.40	0.29	0.29	3.91	0.33	0.32	0.34	0.33
2-hydroxy	-7.71	0.40	0.52	0.12	0.14	3.69	0.31	0.30	0.36	0.33
2-methoxy	-7.44	0.36	0.54	0.12	0.13	3.96	0.32	0.28	0.36	0.34
2-formyl	-8.24	0.37	0.38	0.29	0.29	3.38	0.34	0.41	0.27	0.29
2-vinyl	-7.32	0.37	0.48	0.09	0.10	3.72	0.34	0.37	0.30	0.30

a) Geometries were the same as for benzoquinone (reference 61), except that substituents in standard geometries (reference 62) were substituted for one hydrogen. Additional fixed parameters: methyl dihedral angle C=C-C-H = 0°; hydroxy dihedral angle C=C-O-H = 180°; methoxy bond angles C=C-O = 124°, C-O-C = 118°; methoxy dihedral angle C=C-O-C = 0°; formyl dihedral angle C=C-C=O = 0°; vinyl dihedral angle C=C-C=C = 0°.  $\epsilon$ 's are orbital energies (eV) and C's are the coefficients at the indicated atom.

conformations were possible, calculations were performed to determine the most stable conformation. Additional fixed parameters include: methyl dihedral angle ( $\text{C}=\text{C}-\text{C}-\text{H}$ ) =  $180^\circ$ ; methoxy dihedral angle ( $\text{C}=\text{C}-\text{O}-\text{C}$ ) =  $0^\circ$ ; hydroxy dihedral angle ( $\text{C}=\text{C}-\text{O}-\text{H}$ ) =  $0^\circ$ . The preferred dihedral angles for vinyl and formyl substituents ( $\text{C}=\text{C}-\text{C}=\text{C}$ , and  $\text{C}=\text{C}-\text{C}=\text{O}$ ) were also equal to  $0^\circ$ .

For the three donor substituents, methyl, hydroxy, and methoxy, the HOMO coefficients are polarized in the order  $\text{C}_3 > \text{C}_6 \geq \text{C}_5$  and are increased in the order expected according to the electron donating ability of the substituent:  $\text{H} < \text{methyl} < \text{hydroxy} < \text{methoxy}$ . The coefficients of the LUMO are polarized in the opposite direction ( $\text{C}_5 > \text{C}_6 \geq \text{C}_3$ ). The differences in the polarization magnitudes are small, but of the same order of magnitude as those which produce high regioselectivity in less complex examples.<sup>42</sup> According to perturbation theory, the selectivity for attack at various positions is proportional to the difference in the square of the coefficients at different positions.

Both the HOMO and LUMO are lowered in energy by the formyl substituent which is an electron acceptor. The coefficients of the LUMO are polarized in the order  $\text{C}_3 > \text{C}_6 > \text{C}_5$ , exactly opposite compared to the polarization caused by donors. The HOMO is polarized in the same direction for both donors and acceptors, and also in the same direction as the LUMO in this species. This latter effect is a result of some  $\pi$  donation by the carbonyl

orbitals.<sup>42</sup>

A vinyl substituent causes some mixed behavior. The HOMO is polarized in the same direction as caused by donors and formyl group, i.e.  $C_3 > C_6 > C_5$ . The HOMO is raised in energy, while the LUMO is lowered in energy. The polarization of the LUMO resembles that observed for acceptors:  $C_5 > C_6 > C_3$ .

The origin of these polarizations can be understood by applications of perturbation theory,<sup>68-69</sup> as shown in an unavoidably complex fashion in Figure 7. Substituents will cause the greatest mixing of those orbitals which are closest in energy and have the largest coefficients at the site of perturbation. A donor causes higher energy orbitals to mix into lower energy orbitals in a negative fashion at the site of substitution. Lower energy orbitals mix into higher energy orbitals in a positive fashion. For a donating substituent, the SLUMO will be mixed into the LUMO in a negative fashion, resulting in an uneven distribution over the two double bonds in the LUMO. The LUMO is polarized toward the unsubstituted double bond. The SHOMO mixes into the HOMO in a positive fashion (for a donor), resulting in a polarization of the substituted double bond. These vacant-vacant and filled-filled mixings cause a "side-to-side" polarization, but do not alter the ratio of C-2 to C-3 or C-5 to C-6.

Secondly, the donor causes the HOMO and SHOMO to be mixed into the LUMO in a positive fashion. This causes the LUMO coefficient at C-2 to be increased at the expense of the C-3

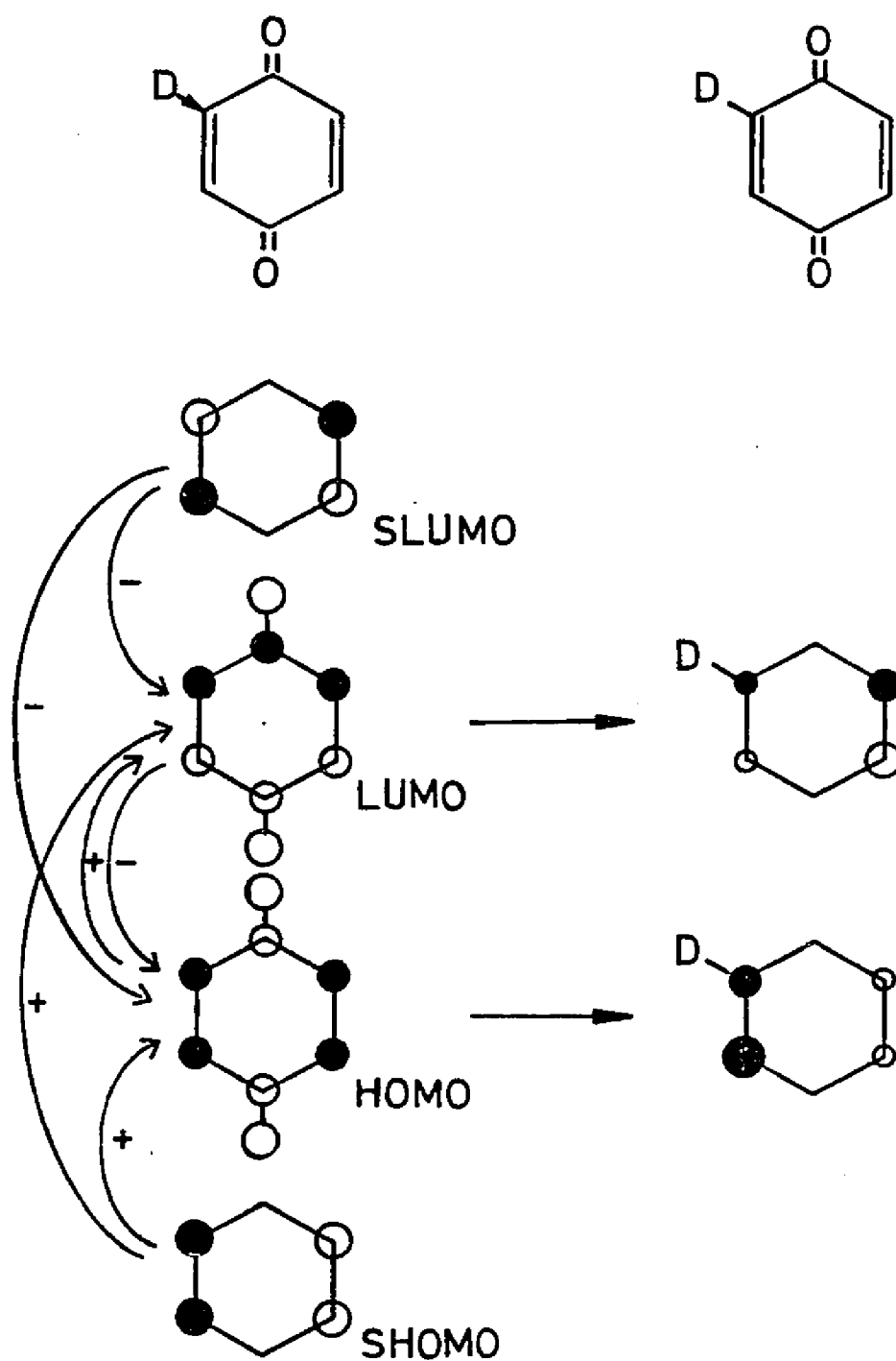


Figure 7. Orbital Mixing in Benzoquinone Caused by a Donor Substituent.



coefficient. Since the HOMO and SHOMO are nearly equal in energy, the SHOMO dominates the polarization at the unsubstituted double bond, because the SHOMO has the larger coefficients on the carbon atoms. The coefficient at C-5 increases at the expense of the C-6 coefficient. Both the SLUMO and LUMO are mixed into the HOMO in a negative fashion, causing a polarization toward the substituted double bond and larger coefficients at C-3, relative to C-2, and at C-6, relative to C-5.

An acceptor causes higher energy orbitals to mix into lower energy orbitals in a positive fashion at the site of substitution, and lower energy orbitals mix into higher energy orbitals in a negative fashion. These mixing rules result in a reversal of the trends in the LUMO coefficients for an acceptor, compared to a donor. The LUMO becomes concentrated on the substituted double bond, the coefficient at C-3 increases, and the C-5 coefficient becomes larger than that at C-6. The HOMO of 2-formylbenzoquinone is very much like that of a donor-substituted benzoquinone because the formyl group can act as a donor through its carbonyl  $\pi$  orbital.

The vinyl group exhibits its usual dual behavior. The LUMO is polarized as expected for an acceptor, but the coefficients at C-5 and C-6 are identical. The HOMO is polarized as expected for a donor substituent.

# SUBSTITUENT EFFECTS ON NAPHTHOQUINONE MOLECULAR ORBITALS

The geometry used for naphthoquinone and its derivatives in the calculations was essentially that of benzoquinone to which a standard hexagonal benzene was fused (all  $r_{CC} = 1.40 \text{ \AA}$ ).<sup>29,70</sup> The substituent geometries and dihedral angles for the substituents at the 2-position were the same as those noted earlier for the benzoquinones: methyl dihedral angle  $C=C-C-H = 0^\circ$ , hydroxy dihedral angle  $C=C-O-H = 180^\circ$ , methoxy dihedral angle  $C=C-O-C = 0^\circ$ , methoxy bond angles  $C=C-O = 124^\circ$  and  $C-O-C = 118^\circ$ , formyl dihedral angle  $C=C-C=O = 0^\circ$ , vinyl dihedral angle  $C=C-C=C = 0^\circ$ . For substituents at the 5-position, the following geometric conformations were indicated to be the most stable: methyl  $C_{10}-C_5-C-H$  dihedral angle  $= 180^\circ$ , methoxy  $C_{10}-C_5-O-C$  dihedral angle  $= 180^\circ$ , the formyl and vinyl  $C_{10}-C_5-C=O$  and  $C_{10}-C_5-C=C$  dihedral angles  $= 90^\circ$ . For substituents at the 6-position, the methyl group showed essentially no barrier to rotation, the hydroxy and vinyl dihedral angles ( $C_5-C_6-O-H$  and  $C_5-C_6-C=C$ )  $= 0^\circ$ , and the formyl dihedral angle  $C_5-C_6-C=O = 180^\circ$ .

Six of the  $\pi$  orbitals of naphthoquinone are shown in Figure 8. The HOMO and THOMO both resemble the HOMO of benzoquinone, since the benzo fusion splits the latter into two orbitals. The SHOMO is essentially a pure benzene orbital which is of the wrong symmetry to interact with the high-lying occupied orbital of benzoquinone. (In some of the substituted derivatives, the

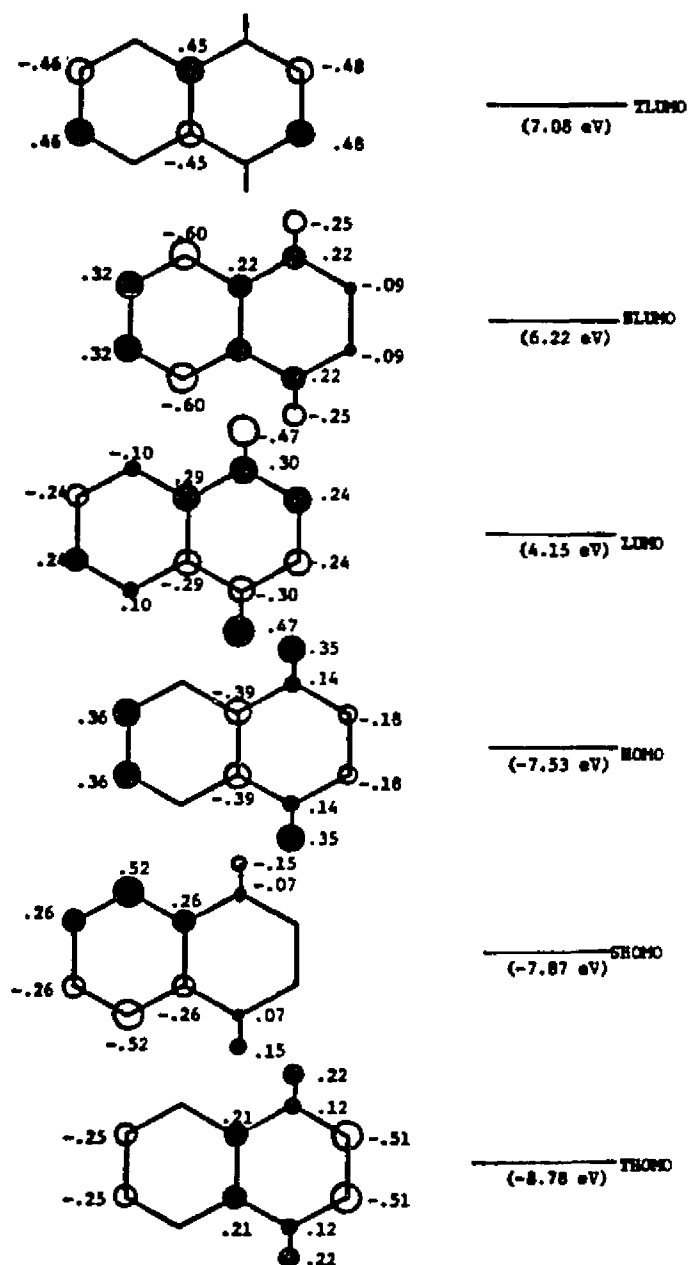


Figure 8. Some STO-3G  $\pi$  Molecular Orbitals and Energies of 1,4-Naphthoquinone.

positions of the HOMO and SHOMO are reversed. In these examples, we will be concerned with the orbital which resembles the HOMO of benzoquinone.) The same pattern is observed in the three lowest vacant orbitals. Because the THOMO and TLUMO have the greatest density on the reactive  $C_2-C_3$  bond, we have considered the effects of substituents on these orbitals, as well as on the HOMO and LUMO. In general, the HOMO and THOMO are polarized in the same direction, as are the LUMO and TLUMO. In the following discussion, we will refer to the "HOMO" and "LUMO" when, in fact, we are also considering both relevant filled or vacant orbitals. The calculations are summarized in Table 6. The orbital coefficients given are for the most stable rotamer, except for 5-hydroxynaphthoquinone, where results have been indicated for both a syn and anti conformation. The syn conformer is more stable by 6.6 kcal/mole than the anti conformer, and the orbital energies reflect the intramolecular hydrogen bonding which can occur in the syn conformation.

The polarization observed in the substituted double bond coefficients for the benzoquinones is also observed for the 2-substituted naphthoquinones. Donor substituents (methyl, hydroxy, and methoxy) raise the orbital energies in the expected order of electron donating ability and polarize the HOMO and THOMO toward the unsubstituted position, except for hydroxy which lowers the LUMO and TLUMO energies, similar to the benzoquinones. The LUMO

Table 6. Frontier  $\pi$  Molecular Orbitals (STO-3G) of Naphthoquinone and Substituted Naphthoquinones<sup>a</sup>

		THOMO		HOMO (or SHOMO)			LUMO			TLUMO		
1,4-Naphtho- quinone	$\epsilon$	C-2	C-3	$\epsilon$	C-2	C-3	$\epsilon$	C-2	(-)C-3	$\epsilon$	C-2	(-)C-3
parent	-8.78	0.51	0.51	-7.53	0.18	0.18	4.15	0.33	0.33	7.08	0.48	0.48
2-methyl	-8.46	0.48	0.51	-7.46	0.21	0.22	4.23	0.33	0.32	7.17	0.48	0.47
2-hydroxy	-8.09	0.29	0.40	-7.44	0.33	0.41	4.03	0.30	0.30	7.10	0.48	0.45
2-methoxy	-7.90	0.21	0.35	-7.22	0.32	0.46	4.28	0.31	0.28	7.26	0.49	0.45
2-formyl	-8.66	0.46	0.48	-7.67	0.19	0.19	3.70	0.35	0.42	6.18	0.14	0.35
2-vinyl	-7.76	0.16	0.22	-7.16	0.34	0.44	4.03	0.35	0.38	6.45	0.26	0.42
5-methyl	-8.75	0.51	0.51	-7.47	0.16	0.17	4.19	0.33	0.33	7.13	0.49	0.48
5-hydroxy <sup>b</sup>	-8.78	0.49	0.49	-7.59 <sup>e</sup>	0.22	0.22	4.19	0.31	0.33	7.01	0.48	0.48
5-methoxy	-8.70	0.49	0.49	-7.49 <sup>e</sup>	0.21	0.21	4.28	0.31	0.33	7.12	0.49	0.48
5-formyl <sup>c</sup>	-9.03	0.51	0.51	-7.83 <sup>e</sup>	0.14	0.13	3.81	0.34	0.31	6.86	0.48	0.48
5-vinyl <sup>c</sup>	-8.77	0.50	0.50	-7.51	0.18	0.18	4.17	0.33	0.33	7.09	0.48	0.48
5-hydroxy <sup>d</sup>	-9.04	0.51	0.52	-7.82 <sup>e</sup>	0.14	0.15	3.80	0.35	0.32	6.89	0.49	0.48

Table 6. (continued)

	THOMO			HOMO (or SHOMO)			LUMO			TLUMO		
	$\epsilon$	C-2	C-3	$\epsilon$	C-2	C-3	$\epsilon$	C-2	(-)C-3	$\epsilon$	C-2	(-)C-3
1,4-Naphtho-quinone												
6-methyl	-8.66	0.51	0.51	-7.31	0.13	0.14	4.21	0.34	0.33	7.13	0.48	0.48
6-hydroxy	-8.68	0.49	0.50	-7.97 <sup>e</sup>	0.15	0.12	4.12	0.34	0.33	7.11	0.49	0.47
6-methoxy	-8.55	0.48	0.50	-7.86 <sup>e</sup>	0.15	0.11	4.21	0.35	0.33	7.23	0.49	0.47
6-formyl	-8.86	0.50	0.50	-7.59	0.15	0.15	3.82	0.28	0.29	6.41	0.29	0.40
6-vinyl	-8.52	0.46	0.48	-7.75 <sup>e</sup>	0.15	0.12	4.10	0.31	0.31	6.72	0.33	0.43

=====

a) Substituent geometries and dihedral angles for the 2-substituents were the same as those described in the footnote to Table 5. 5-Methylnaphthoquinone (dihedral angle C(10)-C(5)-C-H = 180°) is 5.9 kcal/mole more stable than the dihedral angle = 0°; the 5-methoxy is anti; the 6-methyl group has essentially no barrier to rotation; the 6-hydroxy and 6-vinyl are anti; and the 6-formyl is syn.

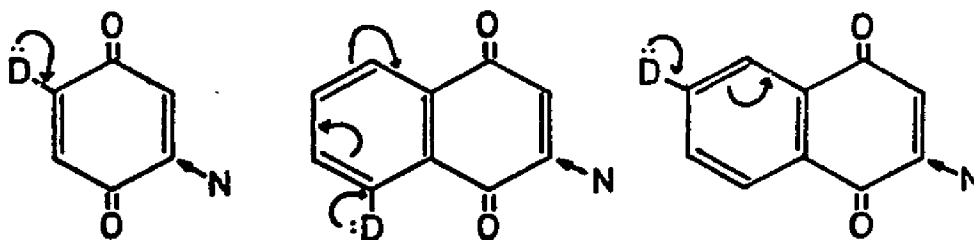
Table 6. (continued)

- b) The 5-hydroxy substituent is anti (dihedral angle C(10)-C(5)-O-H = 180°).
- c) The 5-formyl and 5-vinyl substituents are perpendicular and are 1.2 and 3.1 kcal/mole, respectively, more stable than the anti conformers.
- d) The 5-hydroxy substituent is syn (dihedral angle = 0°).
- e) This is the SHOMO, but corresponds in shape to the benzoquinone HOMO. The SHOMO is nearly degenerate.

and TLUMO coefficients indicate a polarization toward the substituted position.

The formyl group lowers the HOMO and LUMO energies and polarizes both the HOMO and LUMO in the same direction, toward the unsubstituted position, consistent with the benzoquinone results. The vinyl group also exhibits the dual behavior observed earlier. The HOMO energy is raised, the LUMO energy is lowered, and the coefficients are both polarized away from the site of attachment.

Temporarily excepting the syn-5-hydroxynaphthoquinone conformer which has an intramolecular hydrogen bond, substituents at the 5-position have the same effect as substituents attached directly to the benzoquinone nucleus at what would be considered the 9-position of naphthoquinone (i.e. meta to the 5-position). Similarly, a substituent at the 6-position is equivalent to a substituent attached to the benzoquinone nucleus at the 10-position of naphthoquinone. The structures show the analogy between a resonance donor at the 2-position of benzoquinone and the 5- and 6-positions of naphthoquinone.





Donors at C-5 cause a small increase in the C-3 coefficients in the LUMO, except for 5-methyl which shows no polarization in the coefficients. 5-Formyl increases the C-2 coefficient in the LUMO. The influence of 5-vinyl is too small to be noted here, which is consistent with the LUMO results for 2-vinylbenzoquinone. (The LUMO of anti-5-vinylnaphthoquinone is slightly polarized toward C-2.)

Donors at C-6 increase the C-2 coefficients in the vacant orbitals, and the effect is slightly larger than the effect caused by donors at C-5. The 6-formyl and 6-vinyl groups increase the C-3 coefficients in the LUMO. These results are consistent with the earlier results, using the resonance picture above.

Juglone (5-hydroxynaphthoquinone) is a special case in nucleophilic additions and cycloadditions,<sup>71-74</sup> because of intramolecular hydrogen bonding. Constraining the hydroxy group to the anti conformation, where hydrogen bonding to the peri carbonyl is impossible, the hydroxy group behaves as a donor, which is reflected in the orbital coefficients and energies, particularly for the vacant orbitals. However, the syn conformation is 6.6 kcal/mole more stable, due to the hydrogen bonding, and the hydroxy group acts as an acceptor, due to electrostatic attraction between the partially positive proton and the carbonyl oxygen. All the orbitals are stabilized, and the LUMO coefficients are polarized toward C-2.

### MOLECULAR ORBITALS AND REGIOSELECTIVITY

Having described the frontier molecular orbitals of substituted benzoquinones and naphthoquinones, we now turn to applications of these generalizations for understanding and predicting regioselectivities of nucleophilic additions and cycloadditions to quinones.

The LUMO polarizations of benzoquinones and naphthoquinones parallel nucleophilic reactivity: the site with the largest LUMO coefficient is the position most rapidly attacked by nucleophiles or by the more nucleophilic terminus of electron-rich dienes,<sup>48</sup> cf. Figures 4 and 5. The sole exception to this involves the site of donor substitution, which is always less reactive than predicted, based on the LUMO coefficients. It has been suggested previously that these sites are deactivated due to secondary orbital interactions (direct repulsive interactions) which occur between the donor substituent and the attacking nucleophile.<sup>75-76</sup>

For economic reasons, standard quinone geometries were used in these calculations. We have investigated 2-methoxybenzoquinone more thoroughly to explore the significance of substituents on geometries and coefficients. Figure 9A shows the standard geometry of 2-methoxybenzoquinone, along with the corresponding LUMO coefficients and  $\pi$  and total charges. This structure was fully optimized by MINDO/3. Using this geometry, the carbonyl bond lengths were optimized by STO-3G, since these lengths are

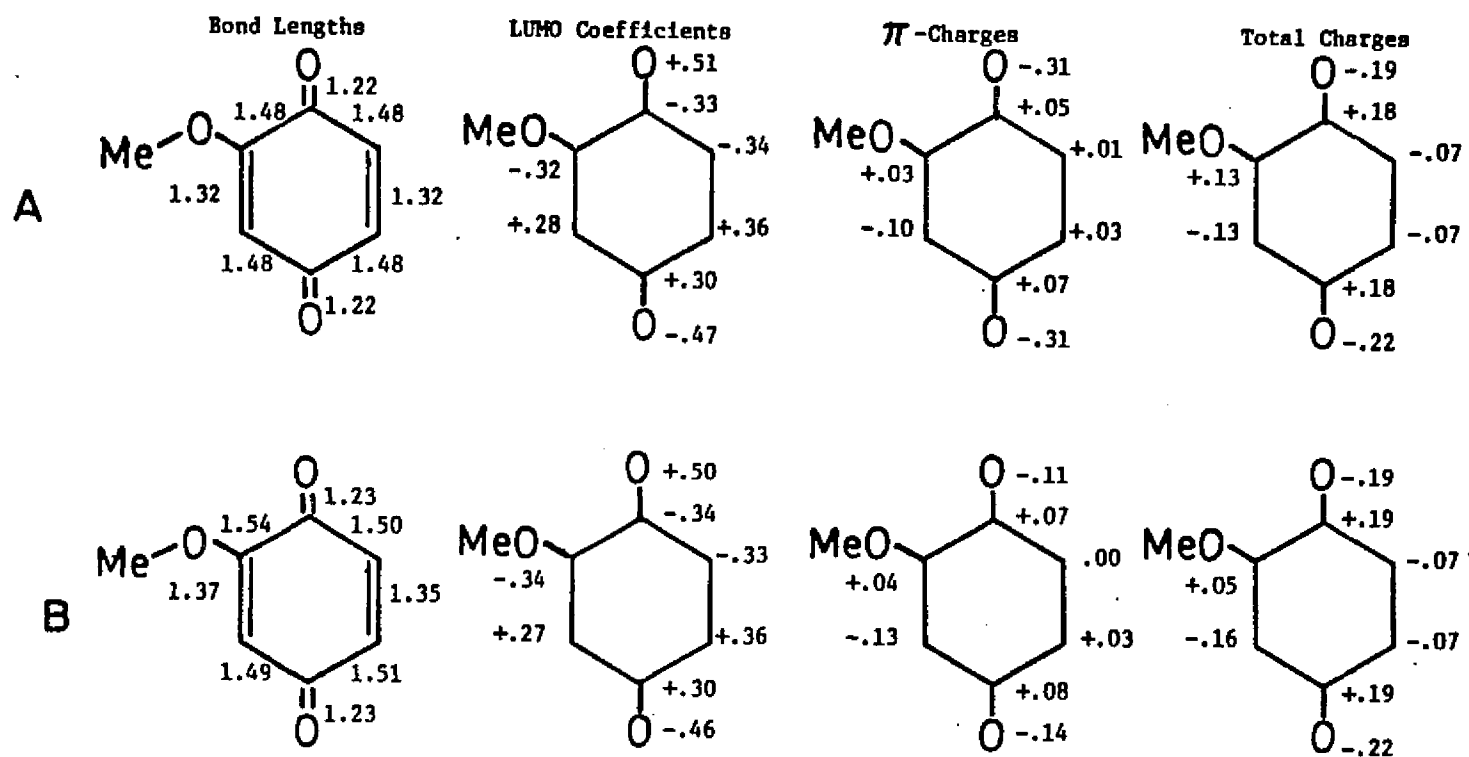


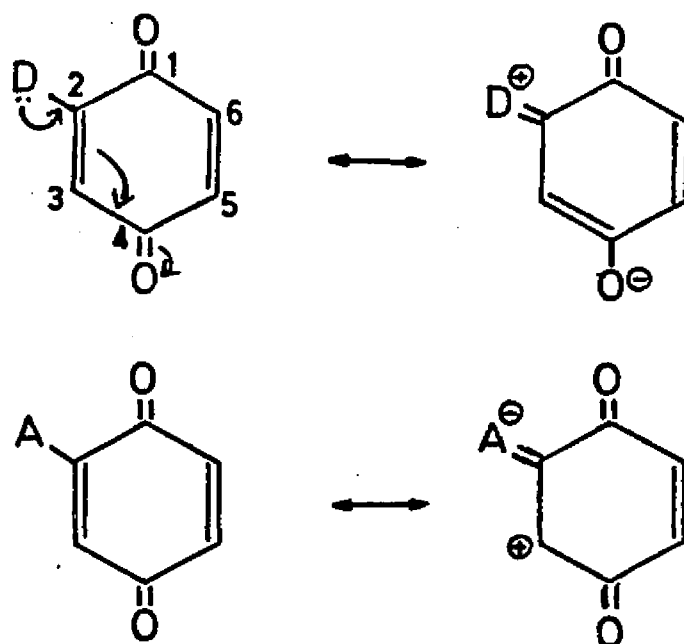
Figure 9. Geometries, LUMO Coefficients, and  $\pi$  and Total Charges of 2-Methoxybenzoquinone.

systematically different by the two methods. This optimization lengthens the C-2, C-3 bond, and shortens the C-3, C-4 bond lengths, Figure 9B, in agreement with expectation based on resonance delocalization by the methoxy group. There is an increase in the polarization of the LUMO and in the separation of  $\pi$  charges, with donation toward the C-4 carbonyl, as suggested by resonance theory.

As described earlier, the extent of charge-transfer stabilization upon interaction of a nucleophile HOMO with the quinone LUMO at any position is proportional to the square of the coefficient at that position. At the 5-, 6-, and 3-positions, the LUMO coefficients squared are 0.13, 0.11, and 0.08, in the same order as the order of attack by nucleophiles (cf. Figures 4 and 5). Upon interaction with a nucleophile, the geometrical distortions and coefficient polarizations will further increase to maximize bonding and minimize antibonding in the partially occupied LUMO.

Resonance theory arguments have been used previously to rationalize the site of attack by nucleophiles on quinones and the regioselectivity of Diels-Alder reactions of substituted quinones with unsymmetrical dienes.<sup>71-74</sup> Donor substituents selectively the electron-withdrawing ability of one of the carbonyl groups through resonance, so that attack occurs  $\beta$  to the other, more electron-deficient carbonyl, i.e. a Michael addition. Electron-withdrawing groups activate the adjacent position by resonance, as

shown below.



This same type of reasoning may also be applied to explain the effects of either a donor or an acceptor at the 5- or 6-position of naphthoquinone. This resonance theory argument works very successfully for donor or acceptor substituents, but encounters difficulty trying to predict and/or rationalize the site of reaction in the presence of a conjugating substituent, since the conjugating substituent can enter into both acceptor and donor resonance structures.

Resonance theory gives predictions of  $\pi$  charges in the reactants, and postulates that nucleophilic attack occurs at the site of highest partial positive charge. As Figure 9 shows, the sites of highest positive charge also correspond to the sites in the LUMO with the largest coefficients. The sites of largest

partial negative charge also correspond to sites with small LUMO coefficients. This is no accident, since the substituent reduces the symmetry and causes charge polarization in part by inducing mixing of the quinone filled and vacant orbitals. For example, the methoxy substituent causes the LUMO to mix into the HOMO in a negative fashion at C-2, thus increasing both the HOMO coefficients and  $\pi$  charges at both C-3 and C-5, at the expense of C-2 and C-6. SLUMO mixing into the HOMO (also in a negative fashion at C-2) increases the HOMO coefficients and  $\pi$  charges at C-3 and C-6, at the expense of C-2 and C-5. The latter effect dominates and leads to the HOMO coefficients and  $\pi$  charges shown in Figure 9. Although the  $\pi$  and total charges are a sum of all filled orbital charges, there remains a qualitative correspondence between a large HOMO coefficient, a small LUMO coefficient, and a large  $\pi$  charge, and vice versa. In these molecules, there is a definite parallel between resonance theory and frontier molecular orbital theory, such that either may be used reliably to explain or predict the site of reaction in these quinones with a nucleophile.

# REFERENCES

1. Thomson, R. H. Naturally Occurring Quinones Butterworths, London, 1957.
2. Bentley, R.; Campbell, I. M. "Biological Reactions of Quinones", in The Chemistry of The Quinonoid Compounds Patai, S., Ed., Wiley, London, 1974, ch. 13 and references therein.
3. For a historical review, see Fieser, L. J. Chem. Educ. 1930, 7, 2609.
4. Boeckman, R. K., Jr.; Dolak, T. M.; Culos, K. O. J. Amer. Chem. Soc. 1978, 100, 7098.
5. Kelly, T. R.; Montury, J. Tetrahedron Lett. 1978, 4311, and references therein.
6. Furina, F.; Prados, P. Tetrahedron Lett. 1979, 477, and references therein.
7. Krohn, K.; Tolkiehn, K. Tetrahedron Lett. 1978, 4023.
8. Wiseman, J. R.; French, N. I.; Hallmark, R. K.; Chiong K. G. Tetrahedron Lett. 1978, 3765.
9. Woodward, R. B.; Sondheimer, F.; Taub, D.; Heusler, K.; McLamore, W. M. J. Am. Chem. Soc. 1951, 73, 2403, 3546, 3548; 1952, 74, 4223.
10. Sarett, L. H.; Arth, G. E.; Lukes, R. M.; Beyler, B. M.; Poos, G. I.; Johns, W. F.; Constantin, J. M. J. Am. Chem. Soc. 1952, 74, 4974.
11. For a summary of these and others, see: Anand, N.; Bindra, J. S.; Ranganathan, S. Art in Organic Synthesis Holden-Day, San Francisco, 1970.
12. Corey, E. J.; Danheiser, R. L.; Chandrasekan, S.; Siret, P.; Keck, G. E.; Gras, J. L. J. Am. Chem. Soc. 1978, 100, 8031.
13. Corey, E. J.; Danheiser, R. L.; Chandrasekan, S.; Keck, G. E.; Gopalan, B.; Larsen, S. D.; Siret, P.; Gras, J. L. J. Am. Chem. Soc. 1978, 100, 8034.
14. Morton, R. A.; Biol. Rev. 1971, 46, 47.

15. Wainis, W. W. The Mammalian Mitochondrial Respiratory Chain Academic Press, New York, 1970.
16. McCormick, J. R. D.; Jensen, E. R. J. Am. Chem. Soc. 1968, 90, 7126.
17. Cox, R. H.; Churchill, F.; Cole, R. J.; Dorner, J. W. J. Am. Chem. Soc. 1977, 99, 3159.
18. De Luca, H. F.; Suttie, J. W., Eds. The Fat Soluble Vitamins University of Wisconsin Press, Madison, Wis., 1969.
19. Thomson, R. H. Naturally Occurring Quinones Academic Press, New York, 1971.
20. Pryor, W. A. Chem. Eng. News 1971, 49, 34.
21. Morton, R. A. Biochemistry of Quinones Academic Press, New York, 1965.
22. Ginsburg, D., ed. Nonbenzenoid Aromatic Hydrocarbons Interscience, New York, 1959.
23. Lloyd, D. Carbocyclic Nonbenzenoid Aromatic Compounds American Elsevier, New York, 1966.
24. Snyder, J. P., Ed. Nonbenzenoid Aromatics Academic Press, New York, 1969.
25. Nozoe, T., Ed. Topics in Nonbenzenoid Aromatic Chemistry Wiley, New York, 1973.
26. Morita, T.; Karasawa, M.; Takase, K. Chem. Lett. 1980, 197.
27. Turney, T. A. "Nonbenzenoid Quinones" in The Chemistry of the Quinoid Compounds S. Patai, Ed., Wiley, London, Ch. 16.
28. Scott, L. T.; Rozeboom, M. D.; Houk, K. N.; Fukunaga, T.; Linder, H. J.; Hafner, K. J. Am. Chem. Soc. 1980, 102, 5169.
29. Rozeboom, M. D.; Tegmo-Larsson, I. M.; Houk, K. N. J. Org. Chem. 1981, 102, 5169.
30. Dewar, M. J. S.; deLlano, C. J. Am. Chem. Soc. 1969, 91, 789.



31. Dewar, M. J. S.; Morita, T. J. Am. Chem. Soc. 1969, 91, 796.
32. Gleicher, G. J.; Church, D. F.; Arnold, J. C. J. Am. Chem. Soc. 1974, 96, 2403, and references cited therein.
33. Bingham, R. C.; Dewar, M. J. S.; Lo, D. H. J. Am. Chem. Soc. 1975, 97, 1285.
34. Dewar, M. J. S.; Loc, D. H.; Ramsden, C. A. J. Am. Chem. Soc. 1975, 97, 1311.
35. Hehre, W. J.; Stewart, R. F.; Pople, J. A. J. Chem. Phys. 1969, 51, 2657.
36. Bernstein, J.; Cohen, M. D.; Leiserowitz, L. "The Structural Chemistry of Quinones", in The Chemistry of the Quinone Compounds S. Patai, ed., Wiley, London, Ch 2.
37. Dewar, M. J. S. The Molecular Orbital Theory of Organic Chemistry McGraw-Hill, New York, 1969.
38. Cox, J. D.; Pilcher, G. Thermochemistry of Organic and Organometallic Compounds Academic Press, New York, 1970.
39. Willstatter, R.; Parnas, J. Chem. Ber. 1907, 40, 1406.
40. Schmand, H. L. K.; Boldt, P. J. Am. Chem. Soc. 1975, 97, 447.
41. Fleming, I. Frontier Orbitals and Organic Chemical Reactions, Wiley, New York, 1976.
42. Houk, K. N. Acc. Chem. Res. 1975, 8, 361.
43. Koopmans, T. Physica (Utrecht) 1934, 1, 104.
44. Dougherty, D.; McGlynn, S. P. J. Am. Chem. Soc. 1977, 99, 3234.
45. Briegleb, G. Angew. Chem. Int. Ed. Engl. 1964, 3, 617.
46. Davis, K. N. C.; Hammond, P. R.; Peover, M. E. Trans. Faraday Soc. 1965, 61, 1516.
47. Chen, E. C. M.; Wentworth, W. E. J. Chem. Phys. 1975, 63, 3183.

48. Finley, K. T. "The Addition and Substitution Chemistry of Quinones," in The Chemistry of The Quinonoid Compounds S. Patai, ed., Wiley, London, ch. 17.
49. Morita, T.; Takase, K. Chem. Lett. 1977, 513.
50. Groves, C. E. J. Chem. Soc. 1873, 26, 209.
51. Stenhouse, J.; Groves, C. E. J. Chem. Soc. 1877, 32, 47.
52. Willstatter, R.; Parnas, J. Chem. Ber. 1907, 40, 1406.
53. Laszlo, P.; Stang, P. J. Organic Spectroscopy Harper and Row, New York, 1971, p. 80.
54. Driscoll, J. S.; Hazard, G. F., Jr.; Wood, H. B., Jr.; Goldin, A. Cancer Chemother. Rep., Part 2 1974, 4, 1.
55. Driscoll, J. S., Ed. "Proceedings of the Symposium on Quinones as Anticancer Agents", Cancer Chemother. Rep., Part 2, 1974, 4, 1.
56. Fukui, K. Fortschr. Chem. Forsch. 1970, 15, 1, and references therein.
58. Epiotis, W. D. Theory of Organic Reactions Springer-Verlag, West Berlin, 1978.
59. Klopman, G., Ed. Chemical Reactivity and Reaction Paths Wiley-Interscience, New York, 1974, Ch. 4.
60. Hudson, R. F. Chemical Reactivity and Reaction Paths Wiley-Interscience, New York, 1974, Ch. 5.
61. Trotter, J. Acta Crystallogr. 1960, 13, 86.
62. Pople, J. A.; Gordon, M. J. Am. Chem. Soc. 1967, 89, 4253.
63. Dougherty, D.; McGlynn, S. P. J. Am. Chem. Soc. 1977, 99, 3234.
64. Bigelow, R. W. J. Chem. Phys. 1978, 68, 5086.
65. Chen, E. M.; Wentworth, W. E. J. Chem. Phys. 1975, 63, 3183.
66. Jordan, K. D.; Burrow, P. D. Acc. Chem. Res. 1978, 11, 341.

67. Houk, K. N.; Munchausen, L. L. J. Am. Chem. Soc. 1976, 98, 937.
68. Libit, L.; Hoffmann, R. J. Am. Chem. Soc. 1974, 96, 1370.
69. Santiago, C.; McAlduff, E. J.; Houk, K. N.; Snow, R. A.; Paquette, L. A. J. Am. Chem. Soc. 1978, 100, 6149 and references therein.
70. Gaultier, J.; Hauw, C. Acta Crystallogr. 1965, 18, 179.
71. Kelly, T. R.; Goerner, R. N., Jr.; Gillard, J. W.; Prazak, B. K. Tetrahedron Lett. 1976, 3869.
72. Kelly, T. R.; Gillard, J. W.; Goerner, R. N., Jr. Tetrahedron Lett. 1976, 3873.
73. Kelly, T. R. Tetrahedron Lett. 1978, 1387.
74. Kelly, T. R.; Montury, M. Tetrahedron Lett. 1978, 4309, 4311.
75. Tegmo-Larsson, I.-M.; Rozeboom, M. D.; Rondan, N. G.; Houk, K. N. Tetrahedron Lett. 1981, 2047.
76. Houk, K. N.; Domelsmith, L. N.; Strozler, R. W.; Patterson, R. T. J. Am. Chem. Soc. 1978, 100, 6531.
77. Thomson, R. H. J. Org. Chem. 1951, 16, 1082.

## VITA

Melvin D. Rozeboom was born November 13, 1951, in Roak Rapids, Iowa. He attended public schools in Steen and Hills, Minnesota, and graduated from Hills-Beaver Creek High School in 1969. He entered Central College in Pella, Iowa that same year. He married Caryn Caster on March 3, 1973, and was awarded a B.A. in May of the same year. After two years spent laboring for a construction company, he began graduate studies at South Dakota State University in 1975. He was employed as a teaching assistant until his graduation in 1977 with an M.S. in Chemistry. He entered Louisiana State University in 1977, and was employed as a teaching assistant until 1979. He has held an appointment as a research assistant since 1979, and is currently a candidate for the Doctor of Philosophy degree in Organic Chemistry. He will be accepting a post-doctoral research assistantship with Dr. John E. Bartmess, at Indiana University in the Fall of 1981.

## EXAMINATION AND THESIS REPORT

Candidate: Melvin Dale Rozeboom

Major Field: Organic Chemistry

Title of Thesis: Part I. Photoelectron Spectroscopic Studies Of Amines, Alkenes, and Substituted Benzenes Part II. Theoretical Studies Of Quinones

Approved:

H. N. Houk  
Major Professor and Chairman

Seán P. Mc Glynn  
Dean of the Graduate School

### EXAMINING COMMITTEE:

George F. J. Jones

Seán P. Mc Glynn

Robert J. Gale

Buddhadhar Sen

William H. Fisher

Date of Examination:

October 9, 1981